



Warsaw University of Life Sciences

Department of Hydrology, Meteorology and Water Management

Institute of Environmental Engineering

MSc. Nelson Venegas Cordero

Detection of changes in river floods and flood generating mechanisms in Poland

Wykrywanie zmian we wskaźnikach powodziowych i
mechanizmach powodziotwórczych w Polsce

Doctoral thesis

Praca doktorska

Doctoral thesis prepared under the supervision of

dr hab. Mikołaj Piniewski, prof. WULS

Department of Hydrology, Meteorology and Water Management

Warsaw, 2024

Statement of the supervisor of the doctoral thesis

I represent that this thesis has been prepared under my supervision and I represent that it fulfils the requirements for submission thereof in the proceedings for the award of the scientific doctoral degree.

Date:

22.04.2024

Signature of the supervisor:



Statement of the author of the doctoral thesis

Aware of legal liability, including criminal liability for making a false statement, I hereby represent that the present doctoral thesis has been written by myself and does not contain any content obtained in a manner inconsistent with the applicable laws, in particular the Act of 4 February 1994 on Copyright and Related Rights (consolidated text of 28 October 2022, Polish Journal of Laws of 2022, item 2509, as amended).

I represent that the thesis presented herein has not previously been the basis of any procedure related to the award of the doctoral degree.

I further represent that this version of the thesis is identical to the attached electronic version.

I acknowledge that the doctoral thesis will be subjected to the anti-plagiarism procedure.

Date:

22-04-2024

Signature of the author of the thesis:



Acknowledgements

I would like to express my gratitude to my parents, Fernando Venegas and Flor Cordero, for their unwavering support and love. I also thank my brothers, Fernando, Adrián, and Alonso, for their companionship.

Additionally, I am grateful to my soulmate Priscilla Gallo for her loving support and inspiration to do my best.

I am thankful to my supervisor, Dr. Mikolaj Piniewski, for his invaluable guidance, advice and assistance at every stage of this work. Also, I would like to express my gratitude to all coauthors for their invaluable support and valuable feedback.

I am also grateful to the members of the Department of Hydrology, Meteorology and Water Management and the Doctoral School at Warsaw University of Life Sciences for their assistance throughout this process.

Lastly, I extend my thanks to my friends and colleagues for their support during this journey.

Table of Contents

Abstract.....	9
1. Introduction.....	11
2. Research objectives	13
3. Study area, data and methods	14
3.1 Study area	14
3.2 Data.....	15
3.3 Methods	17
4. Results and discussion	22
4.1 Trends in observed river floods in Poland.....	22
4.2 Assessment of flood generation mechanisms over Poland.....	26
4.3 The effect of urbanization on river floods in Poland.....	29
5. Conclusions.....	32
6. References.....	34
7. Other achievements	40
8. Articles (reprinted)	

Annex 1: Detection of trends in observed river floods in Poland

Co-author statements - Article 1

Annex 2: Model-based assessment of flood generation mechanisms over Poland: The roles of precipitation, snowmelt, and soil moisture excess

Co-author statements - Article 2

Annex 3: Urbanization vs climate drivers: investigating changes in fluvial floods in Poland

Co-author statements - Article 3

Abstract

River floods in Poland are influenced by a combination of climatic and anthropogenic factors. This thesis, consisting of three interrelated scientific articles, investigates the changes in various river flood indicators based on the annual maximum flow and peak-over-threshold concepts, as well as in flood generation mechanisms in Poland using extensive observed and simulation datasets. The research hypothesis is that climate-related drivers have a stronger influence on current trends in river flood indicators in Poland than urbanization.

The thesis indicates that flood magnitude has decreasing trends in the north-eastern part of Poland and an increasing trend in the southern, mountainous part. The statistical significance of most trends in other flood indicators, such as peak-over-threshold magnitude and frequency, and flood timing, has not been established. Snowmelt has been the primary cause of floods across the country, but its importance has decreased in recent decades, particularly in the northern part of the country, in favour of the soil moisture excess. Extreme precipitation has been identified as the primary mechanism only in the southern, mountainous region. The thesis also examines the impact of urbanization on flood dynamics using the paired catchment approach. The analysis of changes in imperviousness based on high-resolution GIS products showed a consistent upward trend in urbanization in selected catchments. The evidence for the effect of urbanization on floods has been assessed as moderate.

This thesis highlights the importance of understanding river flood dynamics in Poland by integrating climatic and anthropogenic factors. It demonstrates methodological advancements by integrating process-based model outputs into statistical analyses of floods and their changes. It contributes to the broader understanding of floods in Poland and emphasizes the importance of considering both natural variability and human intervention in the development of effective flood risk management strategies.

Streszczenie

Na powódzie rzeczne w Polsce wpływa kombinacja czynników klimatycznych i antropogenicznych. W niniejszej rozprawie, składającej się z trzech powiązanych ze sobą artykułów naukowych, badane są zmiany w różnych wskaźnikach powodzi rzecznych opartych na przepływach maksymalnych oraz metodzie przewyższeń (ang. POT – *peak over threshold*), jak i zmiany czynników powodziotwórczych w Polsce przy użyciu obszernych zbiorów danych obserwacyjnych i symulacyjnych. Hipoteza badawcza mówi, że wpływ czynników klimatycznych na obserwowane zmiany wskaźników powodziowych w Polsce jest silniejszy niż wpływ urbanizacji.

W rozprawie wykazano, że wskaźnik wielkości powodzi wykazuje tendencję spadkową w północno-wschodniej części Polski i tendencję wzrostową w południowej, górzystej części kraju. W przypadku większości trendów w innych wskaźnikach, takich jak wielkość i częstotliwość powodzi wyznaczone metodą POT oraz czas występowania powodzi, nie stwierdzono statystycznej istotności zmian. Topnienie śniegu było główną przyczyną występowania powodzi w większości kraju, ale jego znaczenie zmniejszyło się w ostatnich dziesięcioleciach, szczególnie w północnej części kraju, na korzyść wskaźnika nadmiaru wilgoci w glebie (ang. *soil moisture excess*). Ekstremalne opady zostały zidentyfikowane jako główny mechanizm tylko w południowej, górzystej części Polski. W pracy przeanalizowano również wpływ urbanizacji na dynamikę powodzi przy użyciu tzw. metody par zlewni (ang. *paired-catchment approach*). Analiza zmian nieprzepuszczalności terenu w oparciu o produkty GIS o wysokiej rozdzielczości wykazała stały trend wzrostowy urbanizacji w wybranych zlewniach. W drodze analiz statystycznych ustalono, że dowody na wpływ urbanizacji na występowanie powodzi w wybranych zlewniach były umiarkowane.

Niniejsza rozprawa podkreśla znaczenie zrozumienia dynamiki powodzi rzecznych w Polsce poprzez integrację czynników klimatycznych i antropogenicznych. Demonstruje postęp metodologiczny poprzez włączenie wyników symulacji pochodzących z modeli opartych na procesach z analizami statystycznymi powodzi i ich zmian. Przyczynia się to do szerszego zrozumienia powodzi w Polsce i podkreśla znaczenie uwzględnienia zarówno naturalnej zmienności klimatycznej, jak i interwencji człowieka w opracowywaniu skutecznych strategii zarządzania ryzykiem powodziowym.

1. Introduction

Floods are a global hazard that can have significant impacts on communities and economies. In recent decades, there has been an increase in the number of flood events, resulting in significant human and financial losses in various countries (Kundzewicz et al., 2019). Floods have occurred on every continent except Antarctica (Blöschl et al., 2017; Fang et al., 2022; Kundzewicz et al., 2014a; Kundzewicz et al., 2019). Between 1994 and 2013, floods accounted for approximately 43% of global disasters, affecting an estimated 2.5 billion people and resulting in around 0.16 million deaths (CRED, 2015; Hu et al., 2018). Central Europe has experienced devastating floods, such as the flood in Germany, the Netherlands, and Belgium in July 2021, which claimed over two hundred lives and caused widespread infrastructure damage worth billions of euros (Koks et al., 2021; Kreienkamp et al., 2021). These events highlight the urgent need to understand the underlying dynamics that lead to such extreme occurrences.

River floods can be caused by various factors, such as extreme precipitation, excess soil moisture, snowmelt, ice jam, and rain-on-snow events. These factors intensify the hydrological cycle (Berghuijs et al., 2019; Blöschl et al., 2017; Kundzewicz and Pińskwar, 2022). Research has increasingly focused on understanding the dynamics and causes of floods. However, flood-generating mechanisms are complex and spatially heterogeneous, particularly in a changing climate (Kundzewicz et al., 2014a; Berghuijs et al., 2019). Moreover, anthropogenic activities, such as urbanization or deforestation, can significantly alter catchment characteristics, resulting in faster runoff and a higher risk of flood, due to decreased infiltration and increased soil moisture levels (Bian et al., 2020; Blöschl, 2022; Szeląg et al., 2021).

In this thesis, the term ‘flood’ is understood in hydrological terms, i.e. either as the annual maximum flow (AMF) or peaks-over-threshold (POT) flow, as used in several scientific articles on flood detection (Berghuijs et al., 2019; Bertola et al., 2021; Blöschl et al., 2019; Mediero et al., 2014; Singh et al., 2021). In recent years, flood studies at the global and European level have either partially or completely excluded Poland from their analyses (e.g. Mangini et al., 2018; Villarini et al., 2011; Wasko et al., 2020) or have not used the most

recent data, rarely going beyond 2010 (e.g. Blöschl et al., 2017, 2019; Berghuijs et al., 2019; Bertola et al., 2020; Stein et al., 2020).

The research on flood trends in Poland has been mainly region-specific. For instance, studies conducted in the Tatra Mountains have shown that floods in the southern region are mainly caused by heavy and prolonged rainfall (Kundzewicz et al., 2014b; Ruiz-Villanueva et al., 2016). Jokiel (2007) analysed the monthly extreme flows of three rivers in central Poland (Warta, Bzura and Pilica) from 1951-2000. The study revealed a reduction in maximum flows during the cold half-year for the Pilica and Bzura rivers. Similarly, Górník (2018) observed a decrease in the annual runoff for the Vistula river, particularly for the maximum flow from 1951-2015. Finally, Strupczewski et al. (2001) found that between 1921 and 1990, the annual maximum flow discharges in Poland exhibited a predominant decreasing trend during this period.

Recent studies worldwide have analysed potential flood mechanisms (e.g. Berghuijs et al., 2019; Bertola et al., 2020, 2021; Fang et al., 2022; Jiang et al., 2022a, Jiang et al., 2022b; Singh et al., 2021) and the impact of urbanization on floods (e.g. Prosdocimi et al., 2015; Requena et al., 2017; Szeląg et al., 2021). These studies indicate that floods can be caused by a range of climate and anthropogenic factors, including precipitation, temperature, snow, soil moisture, urbanization, or catchment conditions (Prosdocimi et al., 2015; Tarasova et al., 2019; Trambly et al., 2022). For instance, Berghuijs et al. (2019) conducted a pan-European study on flood mechanisms and found that snowmelt was a significant contributor to floods in most of Poland. While, Szeląg et al. (2021) investigated the relationship between precipitation changes and impervious surfaces in Poland. Their findings demonstrate that urbanization has a significant impact on flood frequency.

It has been observed that flood analyses conducted in Poland tend to be region-focused, and often exclude post-2010 data when carried out at a country scale (e.g. Blöschl et al., 2017, 2019; Mangini et al., 2018). However, Raczyński and Dyer (2023) conducted a country-wide study using recent observed data until 2020. Their study indicates a decrease in flooding across the country, except for mountainous areas in southeastern Poland. Thus, further research is required in Poland due to the ongoing changes in flood drivers across the country.

2. Research objectives

This thesis aims to evaluate flood trends (magnitude, frequency and timing) for a large sample of Polish rivers and determine the influence of climate-related drivers such as extreme precipitation, soil moisture excess and snowmelt as well as anthropogenic factors (urbanization) on river floods. Three principal research questions are:

- What is the evidence for changes in river floods in near-natural catchments in Poland?
- Which climatic factors (precipitation, snowmelt, soil moisture excess) contribute most to river floods in Poland?
- What is the impact of urbanization on river floods in comparison to climatic drivers in Poland?

The main research hypothesis is:

Climate-related drivers have a stronger influence on current trends in river flood indicators in Poland than urbanization.

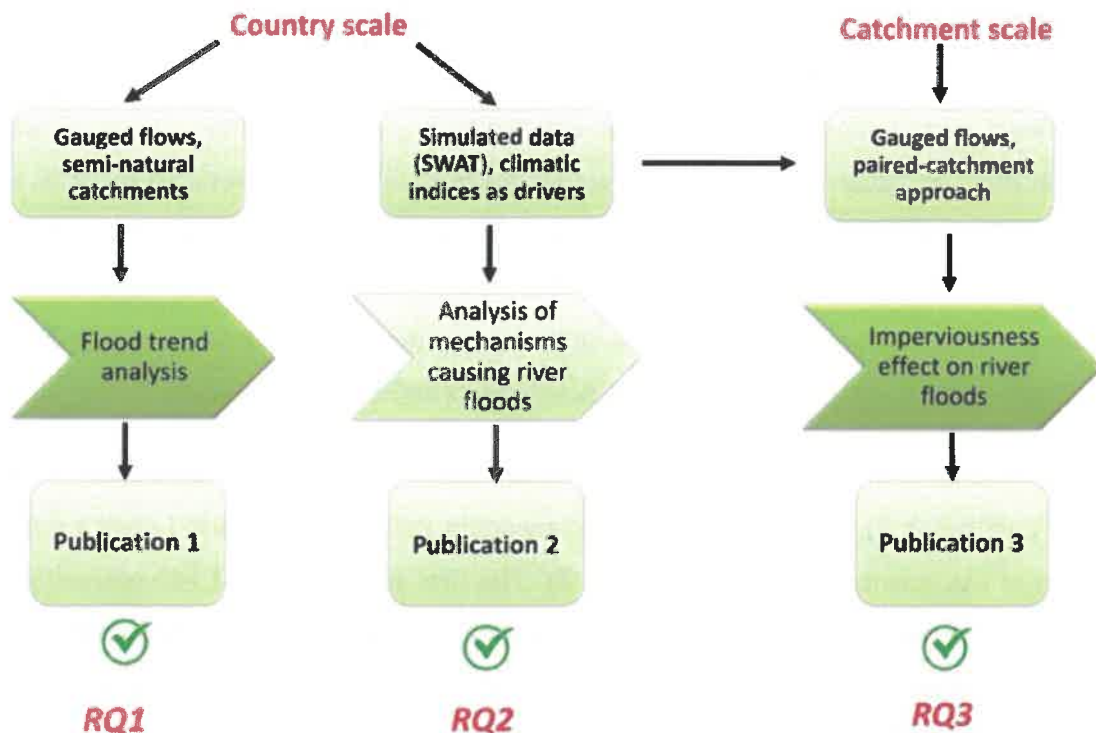


Fig. 1: Research work-flow chart.

The thesis was based on the following list of research articles, which are inter-connected, as shown in the flow chart in Fig. 1:

1. **Venegas-Cordero, N., Kundzewicz, Z. W., Jamro, S., & Piniewski, M. (2022).** Detection of trends in observed river floods in Poland. *Journal of Hydrology: Regional Studies*, 41, 101098 (IF = 4.7). <https://doi.org/10.1016/j.ejrh.2022.101098>
2. **Venegas-Cordero, N., Cherrat, C., Kundzewicz, Z. W., Singh, J., and Piniewski, M. (2023).** Model-based assessment of flood generation mechanisms over Poland: The roles of precipitation, snowmelt, and soil moisture excess. *Science of the Total Environment*, 891, 164626 (IF = 9.8). <https://doi.org/10.1016/j.scitotenv.2023.164626>
3. **Venegas-Cordero, N., Mediero, L., and Piniewski, M. (2024).** Urbanization vs climate drivers: investigating changes in fluvial floods in Poland. *Stochastic Environmental Research and Risk Assessment* (IF = 4.2). <https://doi.org/10.1007/s00477-024-02717-z>

3. Study area, data and methods

3.1 Study area

The research conducted in this thesis concerned the area of Poland, a country located in a transitional warm temperate climatic zone, affected by air masses from the Atlantic Ocean and the Eurasian landmass. The temperature ranges from 6 °C in the northeast to 10 °C in the southwest, and drops below 0 °C in the highest mountain regions. Precipitation exhibits spatial variability, with the northern and central regions receiving approximately 500-700 mm/year, while the southern and mountainous areas experience totals of around 780 and 1100 mm, respectively (Błażejczyk, 2006; Kundzewicz and Matczak, 2012).

The study areas in all three articles were the entire Polish territory with some neighbouring areas (Publication 2), a large sample of catchments in Poland (Publication 1) and a small sample of catchments (Publication 3) (Fig. 2). The first article analysed 146 near-natural catchments covering all major geographic regions. The study area in the second article was larger, covering 4381 sub-basins across Poland and neighbouring countries, such as the Czech Republic, Germany, Slovakia, Russia, Ukraine, and Belarus, which amounts to

approximately 350,000 km², as reported by Marcinkowski et al. (2021). The third paper considers the selection of four pairs of gauges from an initial assemble that covered the entire country. The selection was based on specific criteria, which are detailed in Table 3. The first pair is located in the northern part of Poland, while the remaining three are grouped together in the southern part of the country.

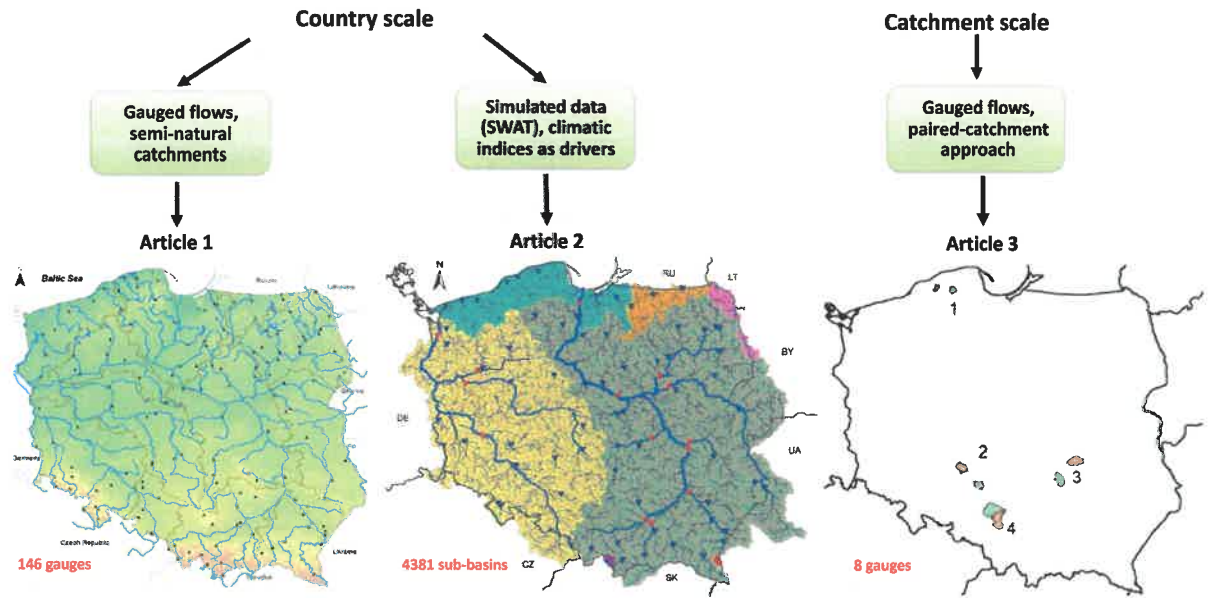


Fig. 2: Study sites included in Article 1, 2 and 3.

3.2 Data

Daily discharge data from the Institute of Meteorology and Water Management-National Research Institute (IMGW-PIB) was extracted to assess trend detection in Poland (Table 1). This data was used in articles 1 and 3. A total of 146 gauging stations were selected, divided into two subsets: A, consisting of 56 gauges for the period 1956-2019, and subset B, consisting of all 146 gauges from 1981 to 2019. The gauges (near-natural catchments) were carefully selected to ensure that they were not influenced by human factors, such as large dams, urbanization or any water abstractions. Furthermore, it is important to note that the near-natural catchments should have a minimum record length of 20 years and ideally should be those that are pristine or have stable land-use conditions, as noted by Hodgkins et al. (2017) and Whitfield et al. (2012). The selection process also considered the length of available data and the number of gauges in a given region, as described in Piniewski et al. (2018).

Table 1: Main data applied in this thesis.

Data	Source	Article	Description
Discharge [mm/day]	IMGW-PIB	I, III	Observed daily discharge data. The record length ranges from 30 to 70 years.
SWAT model outputs	PL-SWAT- 51_20 (Marcinkowski et al., 2021)	II, III	Long-term simulated water balance and streamflow daily data for Poland. The spatial structure includes 4,381 sub-basins. Four variables used: precipitation [mm/day], snowmelt [mm/day], soil moisture content [mm] and water yield [mm/day].
Map of hydrographic division of Poland (MPHP)	IMGW-PIB	I, II, III	The MPHP provides the general boundaries of river basin districts in Poland.
Global Human Settlement (GHS)	Copernicus Services	III	The distribution of built-up surfaces, ranging from 0 to 10,000 m ² , was estimated for each grid cell at a 100 m resolution for the period 1975-2020.
High Resolution Layer (HRL) Imperviousness Degree	Copernicus Services	III	The sealing density ranging from 0% to 100% at a 20 m resolution for the period between 2006 and 2018.

In the process of assessing flood generating mechanisms over Poland, we used the outputs from the process-based hydrological model Soil & Water Assessment Tool (SWAT, Arnold et al., 1998) assembled in an open dataset PL-SWAT. This dataset covers a period of 70 years (1951-2020) and includes 4381 sub-basins with an average size of 80 km² (Marcinkowski et al., 2021). It contains simulated daily discharge and water balance time series from the SWAT model, forced with the G2DC-PL+ gridded daily climate dataset (Piniewski et al., 2021). In this thesis, the water yield (mm/day) was used as the proxy for discharge at sub-basin level and three variables used for estimation of indices representing different flood

generation mechanisms: precipitation (mm/day), snowmelt (mm/day), and soil moisture (mm) in articles 2 and 3 (Table 1).

Finally, to assess the impact of urbanization on floods, high-resolution imperviousness raster layers derived from two Copernicus products were used: the Global Human Settlement (GHS) layer, which provides built-up data from 1975-2020 at 100 m resolution, and the High Resolution Layer (HRL) Imperviousness Degree dataset from 2006-2018, at 20 m resolution.

The Map of the Hydrographic Division of Poland (MPHP) is the official source of hydrographic network information for Poland (Janczewska et al., 2023). It contains catchment boundaries, river network, and flow gauges operated by IMGW-PIB, which were used in Articles 1 and 3 (see Table 1).

3.3 Methods

This thesis applied different methods to assess changes in trends and flood generating mechanisms in Poland, as shown in Table 2.

Table 2: Main methods use in this thesis.

Method	Article	Description
Hydrological methods for flow data analysis	I, II, III	<p>Peak-over-threshold [POT]: It detects all high flows exceeding a specific threshold, not just one high flow event per year such as in annual maximum flow. POT series were identified from a predefined quantile.</p> <p>Flood seasonality (circular statistics): The dates of flood timing were converted into an angular value to evaluate trend on timing and its seasonality.</p>
Statistical tests for trend detection	I, II, III	<p>Mann Kendall (MK) and Sen Slope: To identify the presence of monotonic upward or downward. Multi-temporal MK applied for all possible combinations of starting and ending years.</p> <p>Chi-square test on parametric Poisson: Trends in POT frequency, it can fit the series of count, assuming that such count has a Poisson distribution.</p> <p>The Pettitt test: a non-parametric method designed to detect change points in the mean or median of a time series of flood and drivers.</p>
Soil moisture excess calculation	II, III	The concurrence of heavy precipitation with high antecedent soil moisture.
Correlation analysis (multi-temporal)	II, III	The correlation and multi-temporal correlation allows to detect which climate drivers better explain the floods.
Estimation of relative importance of flood drivers	II	The importance of different factors driving flood events by analysing their seasonal pattern (Berghuijs et al., 2019).
Spatio-temporal analysis of imperviousness	III	Zonal statistics functions in ArcGIS to calculate catchment-averaged imperviousness over Poland.
Paired-catchment approach	III	This method involves comparing the response of two catchments with similar physical characteristics. One of the catchments as a treatment ('urban') and the other as a control ("non-urban").

The identification of flood events in the time series was carried out using two methods: annual maximum flow (QMAX) and peak-over-threshold (POT). QMAX was used in three of the articles, while POT was used in articles 2 and 3 (see Table 2). QMAX represents the maximum discharge recorded in a year, while POT (Fig. 3) is determined by selecting peaks above a defined threshold level (Cunnane, 1973; Madsen et al., 1997; Mangini et al., 2018). According to Mediero et al. (2014), POT series are often considered as an improvement over the QMAX series as they consider a larger number of floods and provide more information about their magnitude, timing, and frequency.

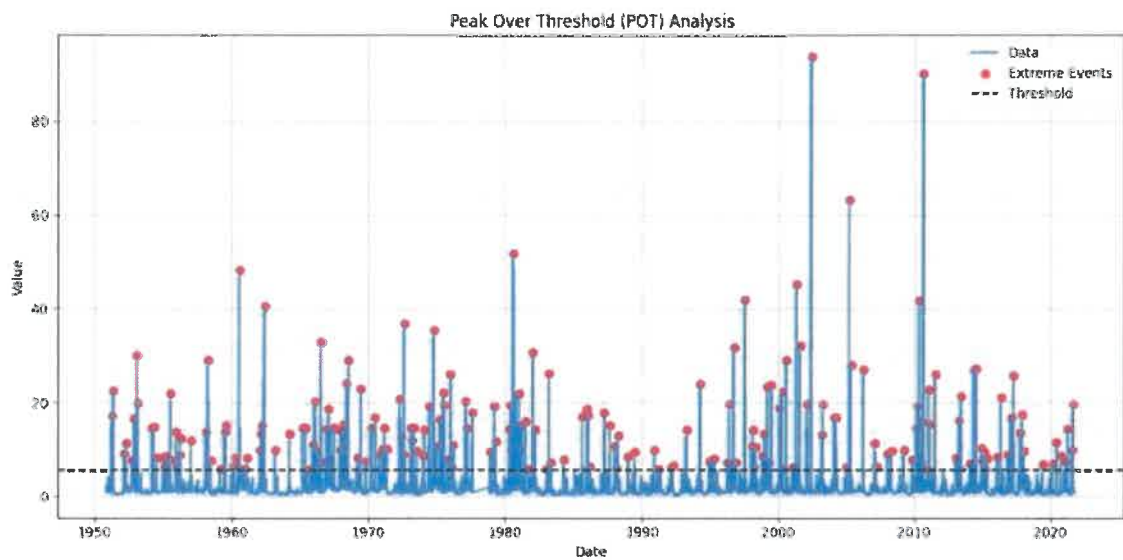


Fig. 3: POT time series. The blue line represents the daily discharge data, the black hash-line shows the threshold, and the red dots represent the flood events.

The study also considered potential mechanisms of flood changes, such as extreme precipitation, snowmelt, and soil moisture excess. These flood mechanisms were specifically applied in articles 2 and 3 (Table 2). In addition, flood seasonality was detected by converting flood timing dates into angular values, as described in Mediero et al. (2014), Blöschl et al. (2017), and Wasko et al. (2020). Please refer to the Annex (articles 1 and 2) for further details.

Statistical tests were used to detect trends. The non-parametric Mann-Kendall (MK) test with Sen's slope approach (Kendall, 1975; Mann, 1945; Sen, 1968) was applied to flood indices (articles 1, 2 and 3) and variables representing flood generation mechanisms (articles 2 and 3). The MK test is a widely used method for detecting monotonic trends in hydro-

meteorological data, as commonly employed in trend detection studies worldwide (Blöschl et al., 2017; Blöschl et al., 2019; Mangini et al., 2018; Mediero et al., 2014; Piniewski et al., 2018). The Sen method calculates the median slope of all possible ordered pairs of the time series. This method is preferred because it is more robust to outliers compared to parametric analysis (Piniewski et al., 2018). Flood trends were assessed for significance using a 10% (0.1) significance level, consistent with other flood trend studies (Blöschl et al., 2017, 2019; Do et al., 2020; Trambly et al., 2019; Vormoor et al., 2016). The chi-square test was used to analyse flood frequency trends in articles 1 and 3 (Table 2). This test assumes that the frequency of floods follows a Poisson distribution that varies linearly over time (Mangini et al., 2018; Vormoor et al., 2016). The Pettitt test, a non-parametric test designed to detect change points in the mean or median of a time series (Pettitt, 1979), was applied in article 3.

The MK, Sen's slope, and Poisson regression tests were also applied in their multi-temporal modification, including a sensitivity analysis for the period considered (article 3). This analysis identifies trends for all possible combinations of starting and ending years in the time series (Hannaford et al., 2013, 2021; Mediero et al., 2014; Ruiz-Villanueva et al., 2016).

The concept of soil moisture excess as a mechanism of floods was calculated using the following equation (Berghuijs et al., 2019):

$$SME = P - (SM_{MAX} - SM) \quad (1)$$

where P represents the daily precipitation, SM_{MAX} is the soil moisture storage capacity (fixed at 125 mm as Berghuijs et al., 2019), and SM is the daily soil moisture. Both P and SM were extracted from the SWAT model outputs.

A correlation analysis was applied in article 2 to determine which climate mechanism best explains the floods. Additionally, the sensitivity of the period was evaluated by applying multi-temporal correlation in article 3 for all possible combinations of starting and ending years (minimum 20 years). For more information, please refer to the Annex section that covers articles 2 and 3.

The relative importance of individual flood drivers (article 2), namely precipitation, snowmelt, and soil moisture excess, was assessed by examining circular statistics for annual

flood occurrences as explained above. To perform this assessment, the method established by Berghuijs et al. (2019) was applied, which is based on the following linear equations:

$$\bar{x}_f = \alpha_{pcp}\bar{x}_{pcp} + \alpha_{sn}\bar{x}_{sn} + \alpha_{mo}\bar{x}_{mo} \quad (2)$$

$$\bar{y}_f = \alpha_{pcp}\bar{y}_{pcp} + \alpha_{sn}\bar{y}_{sn} + \alpha_{mo}\bar{y}_{mo} \quad (3)$$

$$1 = \alpha_{pcp} + \alpha_{sn} + \alpha_{mo} \quad (4)$$

where α is the relative importance of each flood driver (pcp = precipitation, sn = snowmelt, and mo = soil moisture excess), the average cosine and sine components of the dates of occurrence of the drivers are represented by \bar{x}_f and \bar{y}_f . Therefore, the driver's influence on floods is measured on a scale of 0 to 1, where 0 indicates no influence and 1 indicates full explanation.

Additionally, two sub-periods (1952-1985 and 1986-2020) were analysed to investigate changes in flood mechanisms in recent decades based on the following equation:

$$\Delta\alpha = \alpha_{post1986} - \alpha_{pre1986} \quad (5)$$

where $\Delta\alpha$ represents the relative change, and $\alpha_{post1986}$ and $\alpha_{pre1986}$ represent the indices of relative importance of the given flood driver for each sub-period.

Finally, to investigate the effect of urbanization on river floods, the paired catchment approach was applied (article 3). This method involves comparing the response of two catchments with similar characteristics (Bosch and Hewlett, 1982; Kreibich et al., 2017; Prosdocimi et al., 2015; Van Loon et al., 2019). One of the catchments was chosen as a treatment (referred to as 'urban') and the other as a control (referred to as 'non-urban').

The selection of paired catchments was carried out in consecutive steps, as shown in Table 3:

Table 3: Procedure of paired catchment selection applied in this study (Table 2, in Annex 3)

Step	Description	Number
1	All gauged catchments	1073
2	Filtered by area ($A < 1000 \text{ km}^2$)	706
3	Filtered by record length (≥ 30 years)	394
4	Filtered by presence of gaps (less than 1 year)	318
5	Filtered by high Imperviousness characteristics (subset of potential urban catchments)	23
6	Removal of nested catchments	16
7	Final matching of catchment pairs	4*

* 4 pairs of urban and non-urban catchments

After the selection, a series of statistical methods were applied to the QMAX and POT time series that were previously extracted for the four paired catchments. In addition, a multiple linear regression was used to assess the impact of climatic variables on the QMAX time series. This regression model included maximum precipitation, soil moisture excess, and snowmelt as predictor variables for annual maximum flow (Vicente-Serrano et al., 2019), was performed using the following equation:

$$Q \sim PCP + SME + SMN \quad (6)$$

where Q, PCP, SME, and SMN represent the annual maximum flow, precipitation, soil moisture excess, and snowmelt, respectively.

4. Results and discussion

4.1 Trends in observed river floods in Poland

The first step of the research conducted in this thesis involved investigating trends in river flood indicators across Poland. Data from 146 flow gauges distributed throughout the country were used to focus on flood magnitude, frequency, and timing. Both annual maximum daily flow and peak-over threshold methodologies were employed. The analysis covered two distinct periods, 1956-2019 and 1981-2019, to ensure maximum temporal and spatial coverage.

The trend results for flood magnitude indicated spatial variability, with significant trends observed across Poland (Fig. 4 and Table 4). Specifically, a downward trend in flood magnitude is detected in the northeastern part of Poland, while an increasing trend is observed in the south. These trends are attributed to factors such as changing air temperatures, snowmelt patterns, and precipitation distribution (Blöschl et al., 2017, 2019; Ruiz-Villanueva et al., 2016). Furthermore, a recent study carried out by Raczyński and Dyer (2023) in Poland has revealed a positive trend in floods in specific coastal and southeastern regions. In addition, the QMAXM and POTM gauges generally display a decreasing trend, with 53% of the gauges showing a significant negative trend for the longer period, while only 17% presented a significant negative trend for the shorter period (Table 4).

In terms of flood frequency (Table 4, denoted as POTF), there is weaker evidence of trends compared to flood magnitude trends. Although a downward pattern is predominant (with a general decreasing of 71% and 66%) the statistical significance of these trends is lower than that of magnitude trends. For comprehensive information on flood magnitude and frequency, please refer to sections 3.1-4.1 and 3.2-4.2 of Annex 1, respectively.

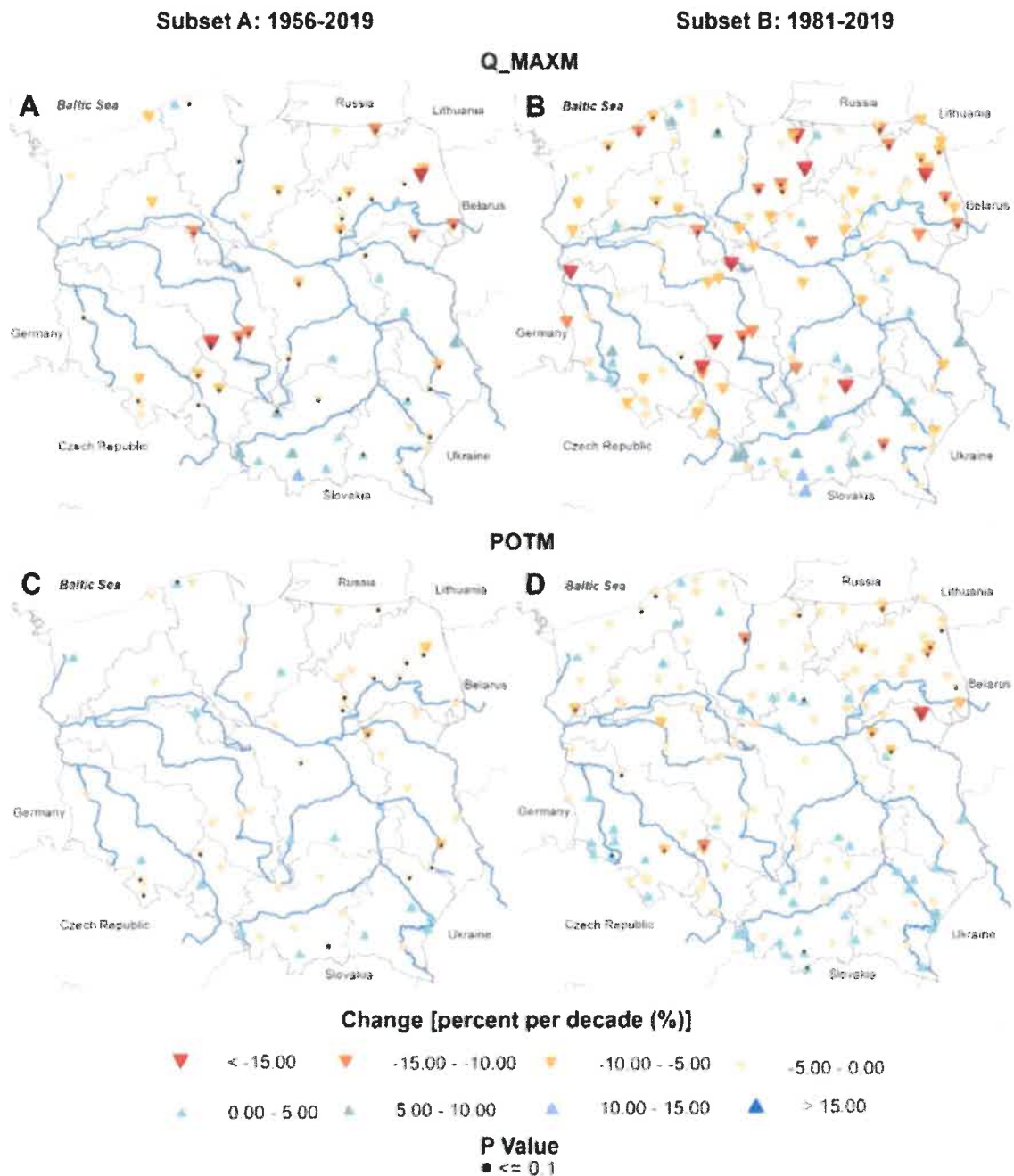


Fig. 4: Trends in QMAX and POT magnitude. Changes are denoted by triangle symbols, with blue indicating positive changes and red indicating negative changes, expressed as a percentage change per decade. Point symbols represent statistically significant changes with $P \leq 0.1$.

Table 4: Number and percentage of gauges with increasing or decreasing trends in flood indicators: QMAXM (magnitude), POTM (magnitude), POTF (frequency), QMAXTAn (annual timing), QMAXTWi (winter timing) and QMAXTSu (summer timing) for two analysis periods (1956-2019 and 1981-2019).

Indices	Gauges	1956-2019 (58 gauges)			1981-2019 (146 gauges)		
		Up	Down	All	Up	Down	All
QMAXM	All gauges	15 (26%)	43 (74%)	58 (100%)	37 (25%)	109 (75%)	146 (100%)
	Significant ≤ 0.1	3 (5%)	31 (53%)	34 (58%)	1 (1%)	25 (17%)	26 (18%)
POTM	All gauges	14 (24%)	44 (76%)	58 (100%)	51 (36%)	95 (64%)	146 (100%)
	Significant ≤ 0.1	1 (1%)	16 (28%)	17 (29%)	4 (3%)	16 (11%)	20 (14%)
POTF	All gauges	17 (29%)	41 (71%)	58 (100%)	49 (34%)	97 (66%)	146 (100%)
	Significant ≤ 0.1	0 (0%)	4 (7%)	4 (7%)	1 (1%)	4 (3%)	5 (4%)
		Later (↑)	Earlier (↓)	All	Later (↑)	Earlier (↓)	All
QMAXTAn	All gauges	30 (52%)	28 (48%)	58 (100%)	57 (39%)	89 (61%)	146 (100%)
	Significant ≤ 0.1	6 (10%)	1 (1%)	7 (11%)	7 (5%)	8 (5%)	15 (10%)
QMAXTSu	All gauges	14 (24%)	44 (76%)	58 (100%)	22 (17%)	124 (85%)	146 (100%)
	Significant ≤ 0.1	5 (9%)	6 (10%)	11 (19%)	2 (1%)	10 (7%)	12 (8%)
QMAXTWi	All gauges	32 (55%)	26 (45%)	58 (100%)	68 (47%)	78 (53%)	146 (100%)
	Significant ≤ 0.1	1 (2%)	0 (0%)	1 (2%)	6 (4%)	2 (1%)	8 (5%)

The analysis of flood timing was conducted for the annual maximum (Q_MAXTAn), winter half annual maximum (Q_MAXTWi), and summer half annual maximum (Q_MAXTSu) as presented in Table 4. Q_MAXTSu exhibited a strong decreasing trend for both subsets in almost all regions of Poland, with low statistical significance (10% of gauges for 1956-2019 and 7% for 1981-2019). However, only 5% of all streamflow gauges showed statistically significant changes for Q_MAXTWi. Flood timing varies across Poland, with southern regions experiencing earlier floods and northeastern and northwestern regions experiencing delayed floods (refer to Fig. 5 in the section 3.3 of Annex 1). These variations are linked to climate fluctuations, such as the North Atlantic Oscillation (NAO), snowmelt processes, and precipitation patterns (Kaczmarek, 2003; Kundzewicz et al., 2019). Finally, the comparison of the two data subsets indicates stronger trends in the more recent period (1981-2019), suggesting that a shorter time series may yield more pronounced changes. These findings highlight the complexity and variability of flood patterns in Poland, emphasizing the need for further research to understand the driving forces behind these trends.

4.2 Assessment of flood generation mechanisms over Poland

The previous section has highlighted the complexity and variability of flood trends in Poland, indicating the need for further research to understand the driving mechanisms behind river floods. Therefore, in the second step of research in this thesis, a model-based assessment of flood generation mechanisms was conducted (Publication 2).

In this study, it was assumed that three main potential flood drivers in Poland are extreme precipitation (PCPmax), snowmelt (SNmax), and soil moisture excess (SMEmax). A trend analysis of annual maximum discharge (Qmax), PCPmax, SNmax, and SMEmax reveals diverse patterns across Poland. Qmax shows a decreasing trend in central, southeast, and northeast Poland, but exhibits an increasing trend in the northwest and southern regions, in accordance with Blöschl et al. (2019). Similarly, PCPmax generally demonstrates an increasing magnitude, with notable variations in the northwest and southeast. In contrast, SNmax shows a widespread decreasing trend, particularly significant in the eastern region. The trends in SMEmax vary across the country, with positive and negative slopes concentrated in the southern and eastern regions (refer to Fig 3 and section 3.1 of Annex 2).

Understanding the seasonality of flood drivers is crucial for identifying patterns in flood timing. Qmax usually peaks between February and April, with variations in mountainous areas. Precipitation occurs in July inland and in August near the Baltic Sea coast (Fig. 5). Snowmelt primarily occurs in February, while excess soil moisture exhibits mixed occurrences throughout the study area, reflecting the diverse hydrological regimes across Poland (see Fig. 5 and section 3.2 in Annex 2).

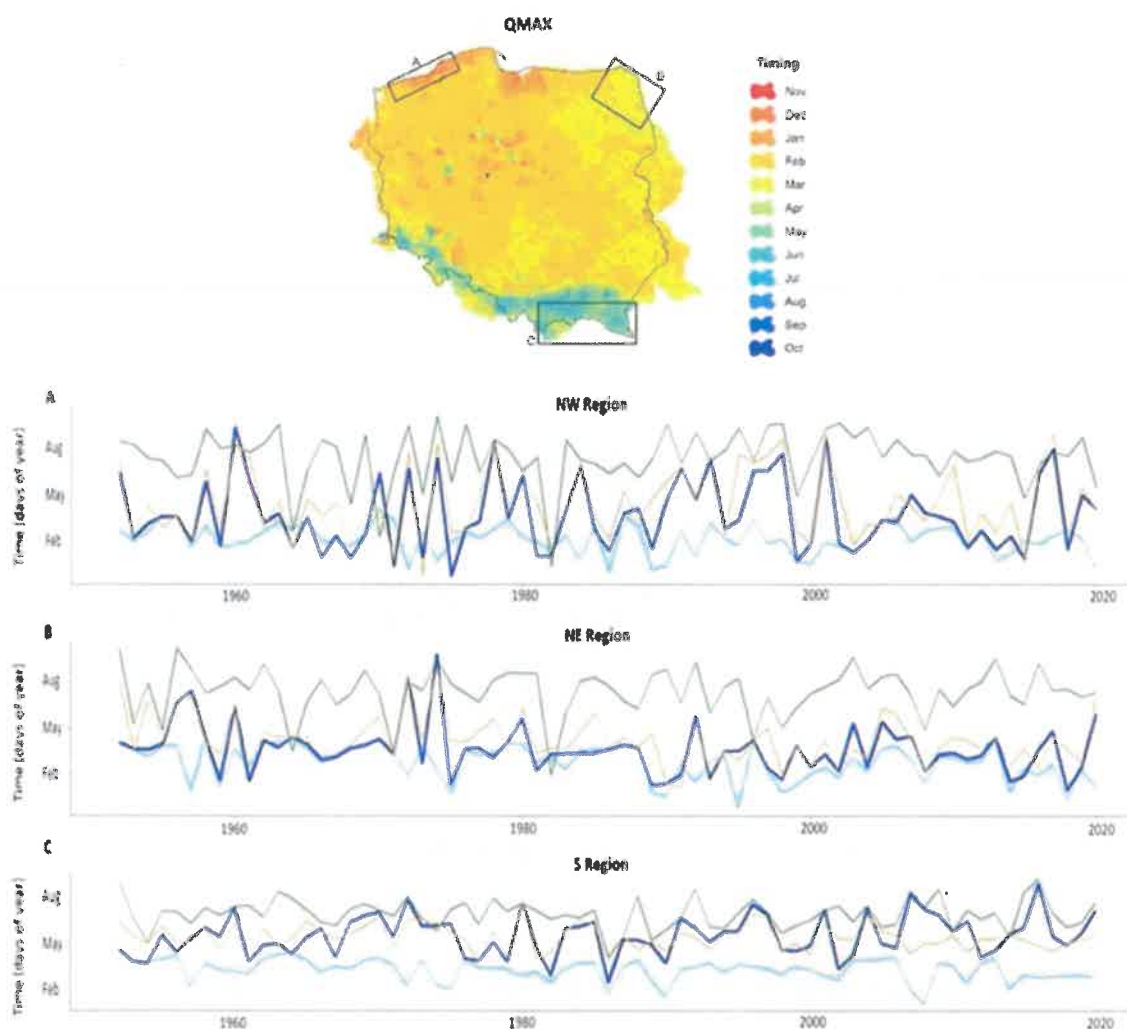


Fig. 5: Flood seasonality and long-term temporal evolution of flood timing in three focus regions (A-C). Blue: Annual maximum daily flood, Green: annual maximum 3-day precipitation, Cyan: annual maximum 3-day snowmelt and Orange: annual maximum daily soil moisture excess.

The Spearman correlation reveals that flood timing (0.83) and magnitude (0.72) in the Northwest strongly correlate with soil moisture excess, while precipitation and snowmelt show moderate to weak relationships. Similar trends were observed in the Northeast, with snowmelt having the highest correlation of 0.80 for flood magnitude (0.51 for timing), underscoring its pivotal role in shaping flood dynamics in this region. Precipitation has a significant impact on flood timing (0.43) and magnitude (0.75) in the southern region.

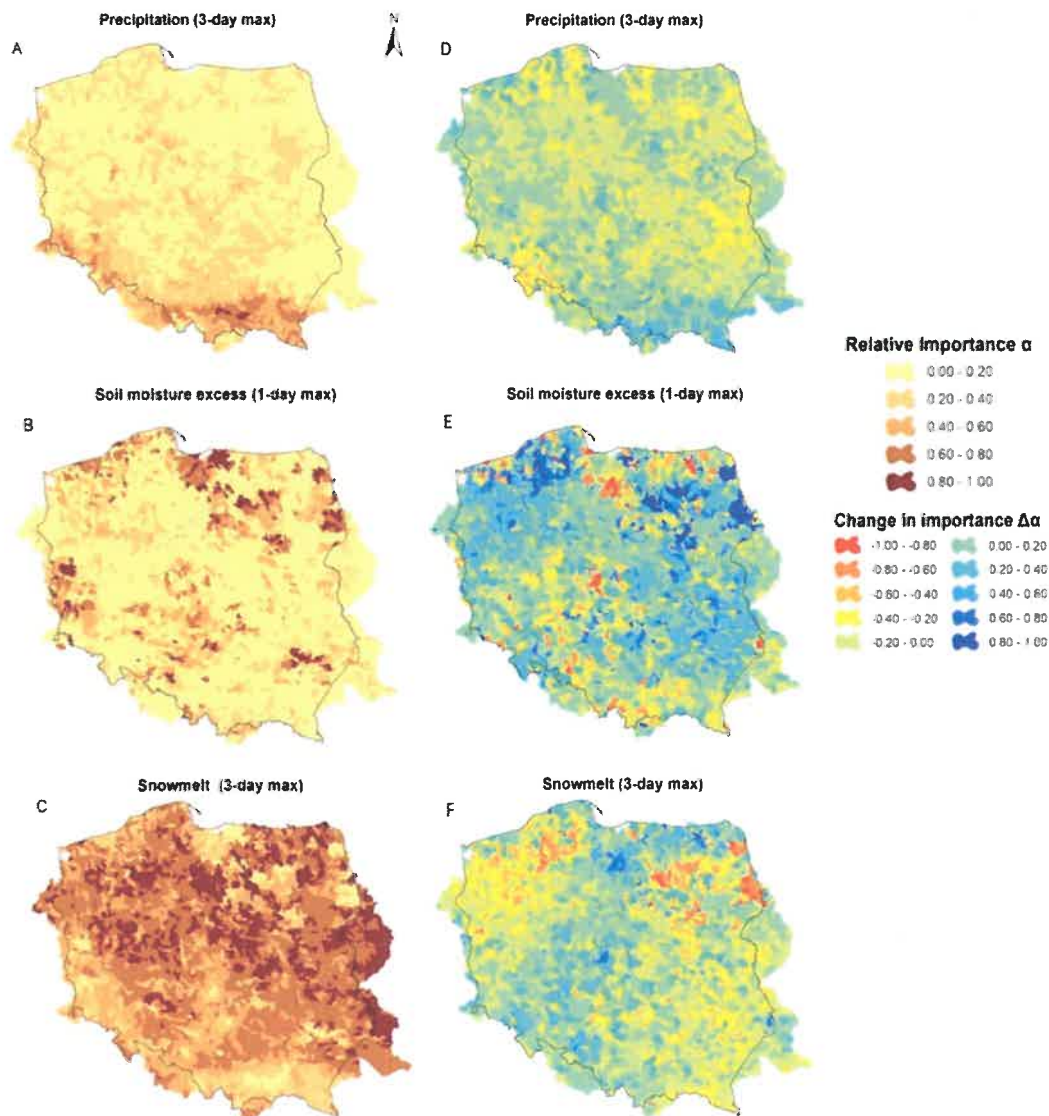


Fig. 6: Relative importance of annual maximum 3-day precipitation (A), annual maximum daily soil moisture excess (B), and annual maximum 3-day snowmelt (C) for 1952-2020. Changes in the relative importance of precipitation (D), soil moisture excess (E), and snowmelt (F) for the comparison of 1952-1985 and 1986-2020.

The dominant flood generation mechanisms over Poland are shown in the relative importance analysis. Snowmelt is identified as the main mechanism, particularly in the northern and central regions (Fig. 6-C), which is consistent with pan-European studies on flood mechanism (Berghuijs et al., 2019; Kemter et al., 2020). Brunner and Fischer (2022) also found that snowmelt floods were the most common type of floods in Central Europe. The importance of soil moisture excess is high in the north and west, while extreme precipitation is particularly significant in the southern region (Fig. 6-A). This is consistent with recent flood studies that have identified precipitation as a key causal factor in the south of Poland (Kemter et al., 2020; Bertola et al., 2021), where the floods are primarily characterized by heavy and prolonged rainfall (Kundzewicz et al., 2014b; Ruiz-Villanueva et al., 2016).

Finally, changes in precipitation, soil moisture excess, and snowmelt were detected by comparing two sub-periods (1952–1985 and 1986–2020). The results indicate increased precipitation intensity in mountainous regions, while changes in soil moisture excess and snowmelt exhibit mixed tendencies in Poland. Specifically, there are increasing trends in the northwest and east for soil moisture excess, while snowmelt shows a decreasing trend over much of the country. This statement indicates a shift towards soil moisture excess, which is consistent with Kemter et al. (2020). They noted that the significance of soil moisture excess has increased in the Central and Northern regions of Europe in recent decades.

4.3 The effect of urbanization on river floods in Poland

While the Publication 1 focused on flood trends in near-natural catchments, with minimum human impacts, and the Publication 2 on natural, climatic flood drivers, Publication 3 takes into consideration one major aspect of anthropogenic influence on floods: increasing imperviousness resulting from urbanization. In order to capture the effect of urbanization on floods, a paired-catchment analysis was conducted for four pairs of urban and non-urban catchments in Poland, using QMAX and POT time series data.

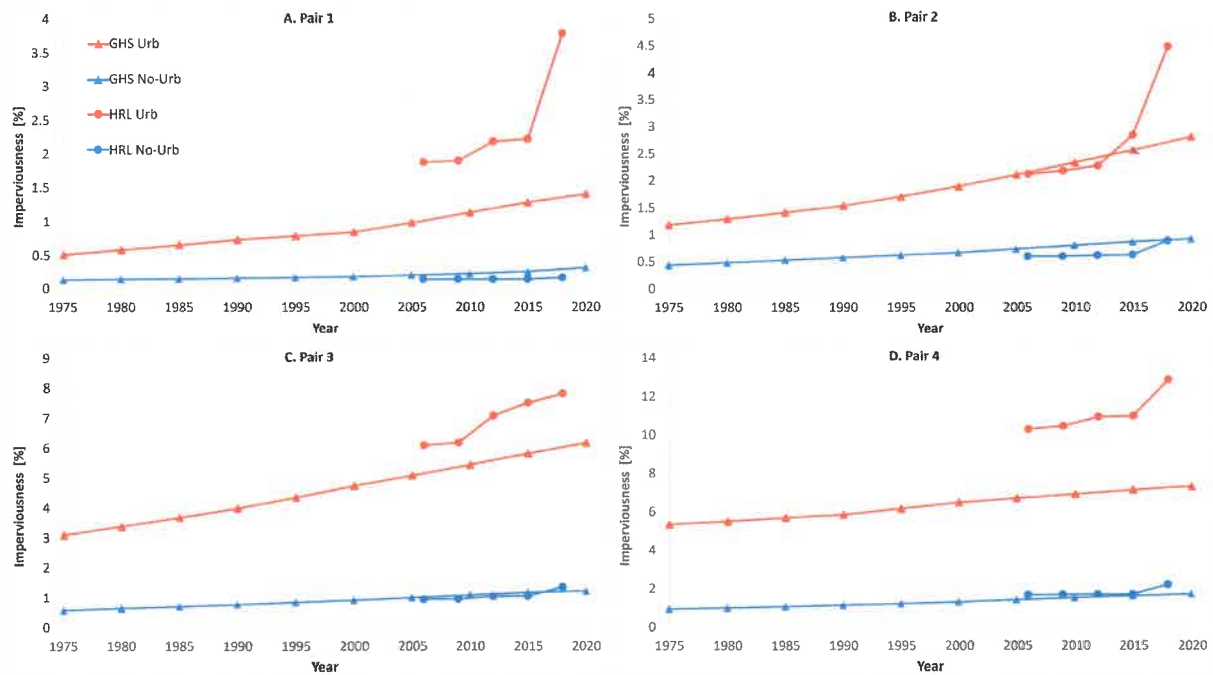


Fig. 7: Changes in imperviousness (%) for all catchment pairs for 1975-2020. Red color refers to urban catchments and blue color to non-urban. Circles represent HRL data and triangles GHS.

The results consistently show a rise in imperviousness across all pairs, with urban catchments experiencing significantly higher rates of imperviousness compared to non-urban catchments. This trend highlights the ongoing urbanization dynamics within the studied regions (Fig. 7). To identify temporal changes in flood dynamics, a change point detection analysis using the Pettitt test was conducted. This analysis revealed changes in the QMAX time series for only one catchment pair, indicating potential shifts in flood dynamics over time. This finding highlights the significance of considering temporal variability when assessing flood trends and attributing them to specific factors, such as urbanization (see Fig. 4; section 3.1 in Annex 3).

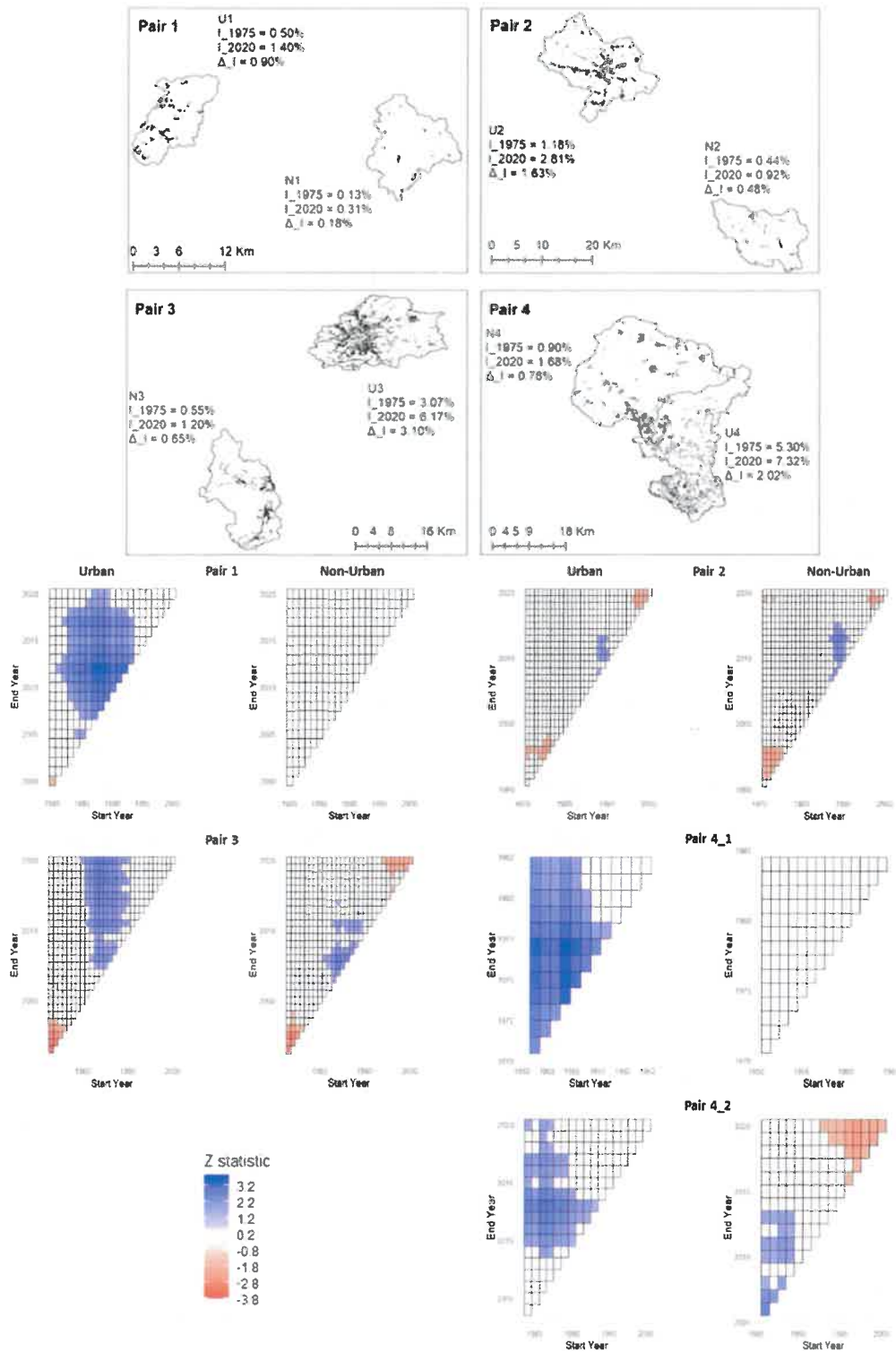


Fig. 8: Paired-catchment maps showing changes in imperviousness rates between 1975 (I_1975) and 2020 (I_2020) (top). Multi-temporal trend analysis using MK test for QMAX (bottom).

The examination of QMAX trends exposed differences between urban and non-urban catchments. Some pairs exhibited noteworthy rises in flood magnitude, particularly in urban catchments (Fig. 8). Additionally, the impact of impervious surfaces on flood magnitude was confirmed by the both, QMAX and POT approach, particularly in later periods. However, only one pair showed significant differences between urban and non-urban catchments in the analysis of flood frequency (refer to Fig. 6; section 3.4 in Annex 3), highlighting the complexity of flood dynamics and the varied impact of imperviousness across different regions.

The residual analysis did not reveal any statistically significant increasing trends for most urban catchments. However, the study indirectly supports the hypothesis that urbanization affects floods through differences in residuals. This highlights the need for further investigation into the mechanisms driving flood trends in urban environments. In summary, the evidence regarding the effect of urbanization on floods is, at best, moderate. The rate of imperviousness increase in the studied urban catchments may not have been as high as observed worldwide. Studies in the UK, for example, showed a 7% increase in imperviousness and a 10.1% rise in UK urban catchments over 30 and 40 years, respectively (Prosdocimi et al., 2015; Requena et al., 2017). In general, flood patterns are influenced by various factors, including antecedent catchment conditions, snowmelt or extreme precipitation, which also can vary across seasons (Kochanek et al., 2012; Sivapalan et al., 2005).

5. Conclusions

The thesis presented a detection and flood generating mechanisms analysis of river floods in Poland, with the objective of identifying the impact of climate variables and urbanization. The analysis addressed three principal questions: the evidence for changes in river floods in Poland, the main causative mechanism to river floods, and the impact of urbanization in selected catchments. The main research hypothesis suggests that in Poland, urbanization may contribute to localized flood hazard. However, the broader trends and dynamics of river floods are primarily shaped by climate-related drivers.

Here, we present the key insights found:

- The analysis shows the spatial variability of flood magnitude in different regions of Poland, with a general increase in flood magnitude in the southern region and a decreasing trend in magnitude in the central and northern regions.
- There is a relatively low fraction of gauges with statistically significant changes for studied indices, with exception of QMAX flood magnitude (around 60% of gauges with significance for 1956–2019).
- The evidence for changes in the frequency of river floods was weak. However, a clear trend of earlier river flood timing was observed in the southern, while a later trend was observed in northeastern and northwestern Poland.
- There is evidence of climate change in large parts of northern Poland for the last decades (1986-2020), where soil moisture excess becomes more important as flood mechanism, which can be explained by temperature warming and decreasing role of snow processes.
- While increasing fraction of impervious areas in urban catchments is naturally expected to lead to increased magnitude and frequency of floods, it remains challenging to find hard evidence for that. This challenge may be related to a small sample of suitable catchment pairs and on relatively low rate of imperviousness increase, compared to other countries.

On the methodological level, the following conclusions can be formulated:

- This thesis presents methodological advancements by integrating process-based model outputs into flood statistical analyses workflows to enhance the understanding of flood trends and mechanisms.
- The methodology developed in this thesis consisting of: i) flood trend detection, ii) examining different climate drivers of floods, and iii) analysing the impact of urbanization, is applicable at a range of scales from local to regional and country scale, making it important for advancing the knowledge about floods.
- It is clear from the findings of this thesis that there is an opportunity to explore new methodological directions. One is the integration of machine learning techniques to identify complex patterns in flood drivers across the country. Another is advanced process-based hydrological modelling to study the effect of dynamic land use changes

on floods. Additionally, further exploration of the connection between soil moisture excess and floods is recommended. This study highlights the growing importance of this relationship across the country.

Finally, the extensive research on flood dynamics in Poland provides valuable insights into the complexity of flood patterns. The complexities observed in this study, which do not always align with previous research, emphasize the necessity for further investigation to develop more effective flood management strategies. This thesis enhances the understanding of flood mechanisms, both climatic and anthropogenic, and provides a basis for informed flood risk management strategies and the development of proactive flood protection measures..

6. References

- Berghuijs, W. R., Harrigan, S., Molnar, P., Slater, L. J., and Kirchner, J. W. (2019). The relative importance of different flood-generating mechanisms across Europe. *Water Resources Research*, 55(6), 4582-4593.
- Bertola, M., Viglione, A., Vorogushyn, S., Lun, D., Merz, B., and Blöschl, G. (2021). Do small and large floods have the same drivers of change? A regional attribution analysis in Europe. *Hydrology and Earth System Sciences*, 25(3), 1347-1364.
- Bertola, M., Viglione, A., Lun, D., Hall, J., & Blöschl, G. (2020). Flood trends in Europe: are changes in small and big floods different?. *Hydrology and Earth System Sciences*, 24(4), 1805-1822.
- Bian, G., Du, J., Song, M., Zhang, X., Zhang, X., Li, R. and Xu, C. Y. (2020). Detection and attribution of flood responses to precipitation change and urbanization: a case study in Qinhuai River Basin, Southeast China. *Hydrology Research*, 51(2), 351-365.
- Blazejczyk, K. (2006). Climate and bioclimate of Poland. Natural and human environment of Poland. A geographical overview, 31-48.
- Blöschl, G. (2022). Three hypotheses on changing river flood hazards. *Hydrology and Earth System Sciences*, 26(19), 5015-5033.
- Blöschl, G., Hall, J., Parajka, J., Perdigão, R. A., Merz, B., Arheimer, B., ... and Živković, N. (2017). Changing climate shifts timing of European floods. *Science*, 357(6351), 588-590.

- Blöschl, G., Hall, J., Viglione, A., Perdigão, R. A., Parajka, J., Merz, B., ... and Živković, N. (2019). Changing climate both increases and decreases European river floods. *Nature*, 573(7772), 108-111.
- Brunner, M. I., and Fischer, S. (2022). Snow-influenced floods are more strongly connected in space than purely rainfall-driven floods. *Environmental Research Letters*, 17(10), 104038.
- Bosch, J.M. and Hewlett, J. (1982). A review of catchment experiments to determine the effect of vegetation changes on water yield and evapotranspiration. *Journal of hydrology*, 55(1-4): 3-23.
- CRED (Centre for Research on the Epidemiology of Disasters), 2015. The human cost of natural disasters: A global perspective. Université Catholique de Louvain. Brussels: Centre for Research on the Epidemiology of Disasters.
- Cunnane, C. (1973). A particular comparison of annual maxima and partial duration series methods of flood frequency prediction. *Journal of hydrology*, 18(3-4), 257-271.
- Do, H. X., Mei, Y., and Gronewold, A. D. (2020). To what extent are changes in flood magnitude related to changes in precipitation extremes?. *Geophysical Research Letters*, 47(18), e2020GL088684.
- Fang, G., Yang, J., Li, Z., Chen, Y., Duan, W., Amory, C., and De Maeyer, P. (2022). Shifting in the global flood timing. *Scientific Reports*, 12(1), 18853.
- Górník, M. (2018). Wieloletnie zmiany przepływów Wisły i Bugu (1951–2015). Long-term (1951–2015) changes in runoff along Poland's Rivers Vistula and Bug. *Przegląd Geograficzny*, 90(3), 479-494.
- Hannaford, J., Buys, G., Stahl, K. and Tallaksen, L. (2013). The influence of decadal-scale variability on trends in long European streamflow records. *Hydrology and Earth System Sciences*, 17(7): 2717-2733.
- Hannaford, J., Mastrantonas, N., Vesuviano, G. and Turner, S. (2021). An updated national-scale assessment of trends in UK peak river flow data: how robust are observed increases in flooding? *Hydrology Research*, 52(3): 699-718.
- Hodgkins, G. A., Whitfield, P. H., Burn, D. H., Hannaford, J., Renard, B., Stahl, K., and Wilson, D. (2017). Climate-driven variability in the occurrence of major floods across North America and Europe. *Journal of Hydrology*, 552, 704-717.

- Hu, P., Zhang, Q., Shi, P., Chen, B., and Fang, J. (2018). Flood-induced mortality across the globe: Spatiotemporal pattern and influencing factors. *Science of the Total Environment*, 643, 171-182.
- Janczewska, N., Matysik, M., and Absalon, D. (2023). Verification of the consistency of surface water spatial databases and their importance for water management in Poland. *Journal of Hydrology: Regional Studies*, 49, 101486.
- Jiang, S., Bevacqua, E., and Zscheischler, J. (2022a). River flooding mechanisms and their changes in Europe revealed by explainable machine learning. *Hydrol. Earth Syst. Sci.* 26, 6339-6359.
- Jiang, S., Zheng, Y., Wang, C., and Babovic, V. (2022b). Uncovering flooding mechanisms across the contiguous United States through interpretive deep learning on representative catchments. *Water Resources Research* 58(1), e2021WR030185.
- Jokiel, P. (2007). Przepływy ekstremalne wybranych rzek środkowej Polski w latach 1951-2000. *Acta Universitatis Lodziensis. Folia Geographica Physica*, 8(8), 99-129.
- Kaczmarek, Z. (2003). The impact of climate variability on flood risk in Poland. *Risk Analysis: An International Journal*, 23(3), 559-566.
- Kendall, M. G. (1975). Rank correlation methods. Oxford University Press, USA, London.
- Kemter, M., Merz, B., Marwan, N., Vorogushyn, S., and Blöschl, G. (2020). Joint trends in flood magnitudes and spatial extents across Europe. *Geophysical Research Letters*, 47(7), e2020GL087464.
- Kochanek, K., Strupczewski, W. G., and Bogdanowicz, E. (2012). On seasonal approach to flood frequency modelling. Part II: flood frequency analysis of Polish rivers. *Hydrological Processes*, 26(5), 717-730.
- Koks, E., Van Ginkel, K., Van Marle, M., and Lemnitzer, A. (2021). Brief communication: Critical infrastructure impacts of the 2021 mid-July western European flood event. *Natural Hazards and Earth System Sciences Discussions*, 2021, 1-11.
- Kreibich, H., Di Baldassarre, G., Vorogushyn, S., Aerts, J. C., Apel, H., Aronica, G. T. and Merz, B. (2017). Adaptation to flood risk: Results of international paired flood event studies. *Earth's Future*, 5(10), 953-965.

- Kreienkamp, F., Philip, S. Y., Tradowsky, J. S., Kew, S. F., Lorenz, P., Arrighi, J., and Wanders, N. (2021). Rapid attribution of heavy rainfall events leading to the severe flooding in Western Europe during July 2021. *World Weather Attribution*.
- Kundzewicz, Z. W., and Matczak, P. (2012). Climate change regional review: Poland. *Wiley Interdisciplinary Reviews: Climate Change*, 3(4), 297-311.
- Kundzewicz, Z. W., Kanae, S., Seneviratne, S. I., Handmer, J., Nicholls, N., Peduzzi, P., and Sherstyukov, B. (2014a). Flood risk and climate change: global and regional perspectives. *Hydrological Sciences Journal*, 59(1), 1-28.
- Kundzewicz, Z. W., Stoffel, M., Kaczka, R. J., Wyżga, B., Niedźwiedź, T., Pińskwar, I., and Mikuś, P. (2014b). Floods at the northern foothills of the Tatra Mountains—a Polish-Swiss research project. *Acta Geophysica*, 62, 620-641.
- Kundzewicz, Z. W., Szwed, M., and Pińskwar, I. (2019). Climate variability and floods—A global review. *Water*, 11(7), 1399.
- Kundzewicz, Z. W., and Pińskwar, I. (2022). Are pluvial and fluvial floods on the rise?. *Water*, 14(17), 2612.
- Madsen, H., Rasmussen, P. F., and Rosbjerg, D. (1997). Comparison of annual maximum series and partial duration series methods for modeling extreme hydrologic events: 1. At-site modeling. *Water resources research*, 33(4), 747-757.
- Mann, H. B. (1945). Nonparametric tests against trend. *Econometrica: Journal of the econometric society*, 245-259.
- Mangini, W., Viglione, A., Hall, J., Hundecha, Y., Ceola, S., Montanari, A., and Parajka, J. (2018). Detection of trends in magnitude and frequency of flood peaks across Europe. *Hydrological Sciences Journal*, 63(4), 493-512.
- Marcinkowski, P., Kardel, I., Płaczowska, E., Giełczewski, M., Osuch, P., Okruszko, T., Venegas-Cordero, N., and Piniewski, M. (2021). High-resolution simulated water balance and streamflow data set for 1951–2020 for the territory of Poland. *Geoscience Data Journal*, 10(2), 195-207.
- Mediero, L., Santillán, D., Garrote, L., and Granados, A. (2014). Detection and attribution of trends in magnitude, frequency and timing of floods in Spain. *Journal of Hydrology*, 517, 1072-1088.

- Pettitt, A.N. (1979). A non-parametric approach to the change-point problem. *Journal of the Royal Statistical Society: Series C (Applied Statistics)*, 28(2): 126-135.
- Piniewski, M., Szcześniak, M., Kardel, I., Chattopadhyay, S., and Berezowski, T. (2021). G2DC-PL+: a gridded 2 km daily climate dataset for the union of the Polish territory and the Vistula and Odra basins. *Earth System Science Data*, 13(3), 1273-1288.
- Piniewski, M., Marcinkowski, P., and Kundzewicz, Z. W. (2018). Trend detection in river flow indices in Poland. *Acta Geophysica*, 66, 347-360.
- Prosdocimi, I., Kjeldsen, T.R. and Miller, J.D. (2015). Detection and attribution of urbanization effect on flood extremes using nonstationary flood-frequency models. *Water Resources Research*, 51(6): 4244-4262.
- Raczyński, K., and Dyer, J. (2023). Changes in streamflow drought and flood distribution over Poland using trend decomposition. *Acta Geophysica*, 1-22.
- Requena, A. I., Prosdocimi, I., Kjeldsen, T. R. and Mediero, L. (2017). A bivariate trend analysis to investigate the effect of increasing urbanisation on flood characteristics. *Hydrology Research*, 48(3), 802-821.
- Ruiz-Villanueva, V., Stoffel, M., Wyżga, B., Kundzewicz, Z. W., Czajka, B. and Niedźwiedź, T. (2016). Decadal variability of floods in the northern foreland of the Tatra Mountains. *Regional Environmental Change*, 16, 603-615.
- Sen, P. K. (1968). Estimates of the regression coefficient based on Kendall's tau. *Journal of the American statistical association*, 63(324), 1379-1389.
- Singh, J., Ghosh, S., Simonovic, S. P., and Karmakar, S. (2021). Identification of flood seasonality and drivers across Canada. *Hydrological Processes*, 35(10), e14398.
- Sivapalan, M., Blöschl, G., Merz, R., and Gutknecht, D. (2005). Linking flood frequency to long-term water balance: Incorporating effects of seasonality. *Water Resources Research*, 41(6).
- Strupczewski, W. G., Singh, V. P., and Mitosek, H. T. (2001). Non-stationary approach to at-site flood frequency modelling. III. Flood analysis of Polish rivers. *Journal of Hydrology*, 248(1-4), 152-167.
- Szeląg, B., Suligowski, R., Drewnowski, J., De Paola, F., Fernandez-Morales, F. J. and Bąk, Ł. (2021). Simulation of the number of storm overflows considering changes in

- precipitation dynamics and the urbanisation of the catchment area: A probabilistic approach. *Journal of Hydrology*, 598, 126275.
- Tarasova, L., Merz, R., Kiss, A., Basso, S., Blöschl, G., Merz, B., Viglione, A., Plötner, S., Guse, B., Schumann, A. and Fischer, S. (2019). Causative classification of river flood events. *Wiley Interdisciplinary Reviews: Water*, 6, p.e1353.
- Tramblay, Y., Mimeau, L., Neppel, L., Vinet, F., and Sauquet, E. (2019). Detection and attribution of flood trends in Mediterranean basins. *Hydrology and Earth System Sciences*, 23(11), 4419-4431.
- Tramblay, Y., Villarini, G., Saidi, M. E., Massari, C., and Stein, L. (2022). Classification of flood-generating processes in Africa. *Scientific reports*, 12, 18920.
- Van Loon, A. F., Rangelcroft, S., Coxon, G., Breña Naranjo, J. A., Van Ogtrop, F. and Van Lanen, H. A. (2019). Using paired catchments to quantify the human influence on hydrological droughts. *Hydrology and Earth System Sciences*, 23(3), 1725-1739.
- Vicente-Serrano, S. M., Peña-Gallardo, M., Hannaford, J., Murphy, C., Lorenzo-Lacruz, J., Dominguez-Castro, F., and Vidal, J. P. (2019). Climate, irrigation, and land cover change explain streamflow trends in countries bordering the northeast Atlantic. *Geophysical Research Letters*, 46(19), 10821-10833.
- Villarini, G., Smith, J. A., Serinaldi, F., and Ntelekos, A. (2011). Analyses of seasonal and annual maximum daily discharge records for central Europe. *Journal of Hydrology*, 399(3-4), 299-312.
- Vormoor, K., Lawrence, D., Schlichting, L., Wilson, D., and Wong, W. K. (2016). Evidence for changes in the magnitude and frequency of observed rainfall vs. snowmelt driven floods in Norway. *Journal of Hydrology*, 538, 33-48.
- Wasko, C., Nathan, R., and Peel, M. C. (2020). Trends in global flood and streamflow timing based on local water year. *Water Resources Research*, 56(8), e2020WR027233.
- Whitfield, P. H., Burn, D., Hannaford, J., Higgins, H., Hodgkins, G. A., Marsh, T. J., and Looser, U. (2012). Hydrologic reference networks I. The status of national reference hydrologic networks for detecting trends and future directions. *Hydrological Sciences Journal*, 57(8), 1562-1579.

7. Other achievements

Here, a list of other scientific articles, which the Author has contributed during preparation of this thesis:

- [2024] **Venegas-Cordero, N.**, Marcinkowski, P., Stachowicz, M and Grygoruk, M. Water balance as a prerequisite for river and wetland management: Biebrza catchment case study, Poland. *Ecohydrology & Hydrobiology*. Under Revision.
- [2024] Marcinkowski, P., Reza Eini, M., **Venegas-Cordero, N.**, Jefimow, M and Piniewski, M. Diverging projections of future droughts in high-end climate scenarios for different potential evapotranspiration methods: a national-scale assessment for Poland. *International Journal of Climatology*. Under Revision.
- [2023] Stachowicz, M., **Venegas-Cordero, N.**, and Ghezelayagh, P. Two centuries of changes-revision of the hydrography of the Biebrza Valley, its transformation and probable ecohydrological challenges. *Ecohydrology & Hydrobiology*. doi.org/10.1016/j.ecohyd.2023.08.008
- [2022] Marcinkowski, P., Kardel, I., Płaczkowska, E., Giełczewski, M., Osuch, P., Okruszko, T., **Venegas-Cordero, N.**, Ignar, S. and Piniewski, M. High-resolution simulated water balance and streamflow data set for 1951–2020 for the territory of Poland. *Geoscience Data Journal*. doi.org/10.1002/gdj3.152
- [2021] Birkel, C., Dehaspe, J., Chavarria-Palma, A., **Venegas-Cordero, N.**, Capell, R., & Durán-Quesada, A. M. Projected climate change impacts on tropical life zones in Costa Rica. *Progress in Physical Geography: Earth and Environment*. doi.org/10.1177/03091333211047046

List of grants and awards

Here, a list of grants and awards, which the Author has contributed during preparation of this thesis:

- Award of best doctoral students in the Project "Actions towards internationalization of the Doctoral School of the Warsaw University of Life Sciences - SGGW". DocSGGW - Doctoral School Goes Gladly Worldwide. (2023).
- Grant of the Helmholtz Visiting Researcher Grant at Helmholtz Centre for Environmental Research – UFZ, Leipzig, Germany (2023).

- Award of a doctoral scholarship within the framework of the DocSGGW - Doctoral School Goes Gladly Worldwide project (2022-2023).
- Grant of PRELUDIUM 21 call for scientists who do not hold a PhD degree. Principal Investigator, funding: 139 513 PLN (2022).

List of conference presentations and lectures

Here, a list of conferences and lectures, which the Author has contributed during preparation of this thesis:

- The 6th IAHR Europe Congress. Which took place from February 15-18, 2021. Participation in online e-conference on an e-learning platform.
- IAHS-AISH Scientific Assembly 2022, Montpellier (France) from 29 May to 3 June 2022: Detection of trends in observed river floods in Poland by Nelson Venegas Cordero et al. Oral presentation in S2 – Floods: Processes, Forecasts, Probabilities, Impact Assessments and Management.
- The EGU General Assembly 2023, Vienna, Austria, 23–28 April 2023. Model-based flood attribution over Poland: the roles of precipitation, snowmelt and soil moisture excess. Poster in Session HS2.4.3 – Space-time dynamics of floods: processes, controls, and risk.
- The AGU General Assembly 2023, San Francisco, USA, 11–15 December 2023. Model-based flood attribution over Poland: the roles of precipitation, snowmelt and soil moisture excess. Poster in Session H23R: Floods and Droughts in a Changing Climate: Characteristics, Mechanisms, Interactions, and Projections.
- Lecture invitation: Oral presentation in the 3rd edition of the River University 2022. Water Association and Coalition Clean Baltic, Estonia.

List of scientific projects and implementations

Here, a list of scientific projects and implementations, which the Author has contributed during preparation of this thesis:

- Project ATRIFLOP: ATtribution of changes in RIVER FLOODs in Poland. NCN: 2022/45/N/ST10/03551. Poland's National Science Centre (Preludium program). Author Role: PI.

- Project OPTAIN: OPTimal strategies to retAIN and re-use water and nutrients in small agricultural catchments across different soil-climatic regions in Europe. H2020 Research & Innovation project. Author Role: Researcher.
- Contribution to the Biebrza National Park Nature Protection Plan's Water Resources Statement (in Polish: Operat Zasobów Wodnych Planu Ochrony Biebrzańskiego Parku Narodowego). Chapter on Charakterystyka składników bilansu wodnego, surowy bilans wodny w zlewniach wodowskazowych oraz w granicach Biebrzańskiego Parku Narodowego i jego otuliny.
- Implementation report: Wykonanie obliczeń wielkości składowych bilansu wodnego przy założeniu różnych scenariuszy zmian klimatu dla obszaru całej Polski. Institute of Environmental PROtection (IOŚ-PIB).

List of internships and trainings

Here, a list of internships at research institutions and relevant trainings during preparation of this thesis:

- Internship at Helmholtz Centre for Environmental Research – UFZ; research group of Compound Environmental Risks. September 2023 to December 2023 and from April 2024 to July 2024.
- Internship at Universidad Politécnica de Madrid, Spain (Escuela de Ingenieros de Caminos, Canales y Puertos/ research group of Hydroinformatics and Water Resources). March 2022.
- Artificial Intelligence for Detection and Attribution of Climate Extremes; Summer School 2022. Cosponsor(s) European Union, eXtreme events: Artificial Intelligence for Detection and Attribution, International Year of Basic Sciences for Sustainable Development.
- Potsdam Summer School 2021. Water our global common good – the hydrosphere across land and sea (2021). Certificate of Potsdam Institute for Climate Impact.
- IS-ENES3 Summer School on Climate data use for impact assessments (2021). Certificate of the Infrastructure for the European Network for Earth System Modelling.

8. Articles (reprinted)

Annex 1: Detection of trends in observed river floods in Poland. *Journal of Hydrology: Regional Studies*, 41, 101098 (IF = 4.7). <https://doi.org/10.1016/j.ejrh.2022.101098>



Contents lists available at ScienceDirect

Journal of Hydrology: Regional Studies

journal homepage: www.elsevier.com/locate/ejrh



Detection of trends in observed river floods in Poland

Nelson Venegas-Cordero^a, Zbigniew W. Kundzewicz^b, Shoaib Jamro^a,
Mikołaj Piniewski^{a,*}

^a Department of Hydrology, Meteorology and Water Management, Warsaw University of Life Sciences, Nowoursynowska 166, 02-787 Warsaw, Poland

^b Meteorology Lab, Department of Construction and Geoengineering, Faculty of Environmental Engineering and Mechanical Engineering, Poznań University of Life Sciences, Poznań, Poland

ARTICLE INFO

Keywords:

Trend detection
Flood
Peak-over-threshold
Annual maximum flow, Poland

ABSTRACT

Study Region Poland (representative sample of 146 flow gauges free of major human modifications, located in 12 major river basins) Study Focus The objective was to present trends in selected river flood indicators (magnitude, frequency and timing) in Poland, using the annual maximum daily flow and peak-overthreshold approaches. Two periods (1956–2019 and 1981–2019) were analyzed. The first period maximized the temporal coverage and featured 58 gauges, while the second period maximized spatial coverage and featured 146 gauges. Trends were computed using the non-parametric Mann-Kendall test (MK) and Sen slope for changes in magnitude and timing, while flood frequency trend was detected by chisquare test on parametric Poisson regression. New Hydrological Insights for the Region We found a general decreasing trend in flood magnitude, with frequently occurring statistical significance, for the majority of river basins (particularly in north-eastern Poland). The strongest of these trends exceeded 15% per decade. A positive trend was detected in the southern part, particularly in the Upper Vistula Basin. No substantial and significant trends were detected in flood frequency, where identified changes mostly did not exceed values of ± 0.2 events per decade. Trend in flood timing showed a strong pattern of earlier flood occurrences in the southern half of the country for both periods, and an opposite behaviour in the north-eastern and northwestern regions.

1. Introduction

Flood is a catastrophic natural hazard that leads to human and economic losses each year in many countries. Floods account for 43% of the number of global disasters between 1994 and 2013, affecting approximately 2.5 billion people and causing 0.16 million deaths (CRED, 2015; Hu et al. 2018). In the last decade, large river floods occurred in many countries at all continents, except the Antarctic. The floods in 2010 in China set a damage record close to US \$70 billion in inflation-adjusted currency for 2015 (Kundzewicz et al., 2019). In addition, Kundzewicz et al. (2014a) demonstrated that the exposure of people and material assets is very high, in both absolute and relative terms in a few densely populated countries of South East Asia, such as Bangladesh, Cambodia and Vietnam. Absolute terms refer to the number of people as well as the value of assets and GDP (Gross Domestic Product) exposed to floods, while relative terms refer to share of population and percentage of economy exposed to floods. Jonkman (2005) demonstrated that floods have a major impact on people, ecosystems and historical-cultural aspects.

* Corresponding author.

E-mail address: mikolaj.piniewski@sggw.edu.pl (M. Piniewski).

<https://doi.org/10.1016/j.ejrh.2022.101098>

Received 6 December 2021; Received in revised form 28 February 2022; Accepted 23 April 2022

Available online 28 April 2022

2214-5818/© 2022 The Author(s). Published by Elsevier B.V. This is an open access article under the CC BY-NC-ND license (<http://creativecommons.org/licenses/by-nc-nd/4.0/>).

The Central European region is not free of major flood risk. Kundzewicz et al. (2005) mentioned major river floods in the region - on the Odra in 1997, on the Vistula in 2001 and on the Elbe in 2002. Also, recent events, such as floods in Germany in 2013 (Blöschl et al., 2013; Schröter et al., 2015) and, in particular, floods in Germany and Belgium in July of 2021 (Kreienkamp et al., 2021) caused huge losses in the region. The latter deluge killed over 210 people, that is far more than any other flood in the European Union (EU) in last 50 years and generated damages in infrastructure (houses, roads, bridges, etc.) reaching several tens of billions of Euros. There are a number of mechanisms influencing flood generation in Central Europe. Wyżga et al. (2016) explained that heavy precipitation and processes of snowmelt, snow cover, ice jam, soil freezing are factors of relevance for the flood occurrences in Poland. Furthermore, intense precipitation in Poland has caused urban flash floods in many cities (e.g., Poznań, Gdańsk and Warsaw) in the last decades (Kundzewicz and Kowalczak, 2014; Bryndal et al., 2017).

Climate change has a direct influence on river floods, due to the shifts in climatic parameters such as precipitation and temperature. Consequently, the increase of river flood hazard has become relevant due to the increase of the atmosphere water holding capacity (Field et al., 2012; Blöschl et al., 2019 and Seneviratne et al., 2021). Moreover, studies based on observations showed how the climate change has intensified the water cycle, resulting in changes of the magnitude, frequency and timing of river floods (Blöschl et al., 2017). Model-based studies aimed at assessment of future climate change impact on floods project a gradual increase in the magnitude and frequency of floods for a large part of the Central European region under the RCP8.5 scenario (Alfieri et al., 2015).

The usage of the term “flood” in the present paper follows neither the colloquial understanding of destructive abundance of water nor the meaning accepted in the EU Floods Directive (EU, 2007), where the term flood is defined as follows: “the temporary covering by water of land not normally covered by water”. In the present paper, we follow a stance taken in many scientific papers on flood trend change detection, tackling high river discharges, either via the notion of annual maximum flow (AMF) or peak-over-threshold (POT) discharge. There is a caveat, though, that - in the former case - the highest flow in a dry year may actually be in the zone of what is normally considered to be a medium discharge. In contrast, the latter approach deals only with really high discharges - higher than a selected threshold.

In recent years, several flood trend detection studies have been carried out at the national (Mediero et al., 2014; Petrow and Merz, 2009) and the European (Bertola et al., 2020; Blöschl et al., 2017; Blöschl et al., 2019; Kemter et al., 2020; Mangini et al., 2018) levels. Methodologically, such studies frequently use the non-parametric Mann-Kendall test (MK) and Sen slope (Sen, 1968) (e.g. Mediero et al., 2014; Mediero et al., 2015; Blöschl et al., 2017; Mangini et al., 2018 and Blöschl et al., 2019). The test is applicable for non-normal data distribution, that is also for flood time series (Kundzewicz and Robson, 2004; Stahl et al., 2010; Mediero et al., 2014). Moreover, detection of trends in frequency of floods has been typically assessed using the chi-square test (Frei and Schär, 2001; Vormoor et al., 2016 and Mangini et al., 2018).

At the national scale, Mediero et al. (2014) analyzed the trends in magnitude, frequency and timing of floods in Spain, finding a decreasing trend in annual maximum flow (AMF), while the results for the peak-over-threshold (POT) showed a general decrease of magnitude and frequency. Petrow and Merz (2009) detected positive trends in flood magnitude and frequency for a considerable number of studied basins in winter, especially in the western and the eastern region of Germany, while mixed changes were found for the summer season in the south and the east parts of the country. In a similar national study for Poland, Piniewski et al. (2018) found a general decreasing trend for the annual maximum flow, with only 21% of gauges with an upward tendency over the country, while Grygoruk et al. (2021) identified no trends in floods in the Lower Basin of the Biebrza Valley in north-east of Poland.

At the European level, Blöschl et al. (2017,2019) detected patterns in the magnitude and timing of floods with an earlier flood occurrence in the north-east of Europe and a flood magnitude decreasing in the eastern part due to an earlier snowmelt produced by a temperature rise. They also mentioned that the flood discharge would decline in the southern Poland from $0.1 \text{ m}^3 \text{ s}^{-1} \text{ km}^{-2}$ to approximately $0.075 \text{ m}^3 \text{ s}^{-1} \text{ km}^{-2}$ if a continuous decrease of discharge is present for the next years. Mangini et al. (2018) searched for trends in magnitude and frequency of floods using both the annual maximum flow and peak-over-threshold methods, reporting the highest positive trend in POT magnitude occurring in Central Europe. Also, Bertola et al. (2020), who studied the difference in changes in small and large floods over the European region, found an upward tendency in the northwestern Europe, similar to results of Blöschl et al. (2017,2019). Mangini et al. (2018) mentioned that trend with both approaches is not always consistent, which suggests that both methods should be used to capture uncertainty in flood trend detection. Moreover, global-scale and pan-European studies (e.g., Villarini et al., 2011b; Mangini et al., 2018; Do et al., 2020; Wařko et al., 2020) on annual maximum daily discharge and flood trends have partially or completely left Poland out of the analyses due to the lack of free access to Polish data that persisted until recently. Meanwhile, studies that included Poland in their analysis (e.g. Blöschl et al., 2017; Blöschl et al., 2019; Bertola et al., 2020) usually included the pre-2010 data.

Floods can be characterized in quantitative terms in a number of different ways, e.g. by magnitude, frequency and timing indicators, which belong, together with duration and rate of change, to the set of five components of flow regime which regulate the ecological processes in river systems (Duan and Cai, 2018; Poff et al., 1997; Richter et al., 1996). Poff et al. (1997); Zhang and Wei (2014) and Duan and Cai (2018) used these indicators to characterize high river discharges, including floods. In addition, studies have shown the importance of these indicators for an overall and accurate description that allows a better understanding of flood processes and characteristics (Burn and Whitfield, 2017; Mostofi Zadeh et al., 2020; Zhang et al., 2021).

In this study, detection of trends in a comprehensive set of indicators of floods in Poland is carried out to fill in the knowledge gaps identified above. The trend analysis focuses on observed daily discharge data processed using AMF and POT methods. The analyses are carried out for two different periods (1956–2019 and 1981–2019) characterized by different spatial coverage of flow gauge data.

2. Data and methodology

2.1. Study area

This study was carried out for a large set of catchments distributed across Poland (Fig. 1), located mainly in drainage basins of two large rivers, the Vistula and the Odra (VOB region).

For the sake of synthesizing results, we used the generalized boundaries of river basin districts, aligned with those assumed in the EU Floods Directive reports provided by the Polish water authorities to the European Commission. Since some of these so called “water regions” were very small, we merged them with their larger neighbors. In result, 12 water regions, hereafter called “river basins” were distinguished (Fig. 1). The median area of these river basins is equal to 26,761 km².

The climate of Poland is characterized by the influence of air masses from the Atlantic Ocean and the Eurasian land. The country is located in a transitional warm temperate climatic zone (Blażejczyk, 2006). The annual average temperature, 7.9 °C, (Kundzewicz and Matczak, 2012) is increasing with the global warming. Spatially, it ranges from 6 °C in the northeast to 10 °C in the southwest, and in the highest mountain it is below 0 °C. In addition, the annual total precipitation for the northern and central belt is approximately 500–700 mm/year, while in the southern and the mountain region the total precipitation attain values around 780 and 1100 mm, respectively, (Blażejczyk, 2006). Two dominant land-use and land-cover classes are agriculture and forests that occupy 63% and 32% of Polish territory, respectively. There is no strong spatial gradient in land use, but agricultural areas prevail mainly in the central part of the country. Southern, higher-elevated, part of Poland features more impermeable soils. Soil cover in the rest of the country that was shaped by numerous glaciations is highly variable in space. Soil permeability ranges from very low (e.g. in the Vistula River delta) to high (different clusters located mainly in central Poland).

2.2. River flow data

The data analyzed in this study were extracted from the Institute of Meteorology and Water Management-National Research Institute (IMGW-PIB) holdings. The selection took into account the balance between the number of gauges in particular regions and the available length of the time series, as described in Piniewski et al. (2018), who used 147 flow gauges in Poland. The selected gauges are also free of important human influences on the flow regime, such as presence of large dams located upstream.

Since flow gauges differed with respect to the start date of hydrologic measurements, it was decided to conduct the analyses separately for two scenarios: the subset “A” consisting of 58 gauges with data available from 1956 to 2019 (thus maximizing the temporal coverage), and the subset “B” including all 146 gauges (thus maximizing spatial coverage) with data from 1981 to 2019 (Fig. 1). The choice followed the database initially assembled by Piniewski et al. (2018) and updated here by adding data from three recent years, 2017–2019. The median of catchment areas is equal to 551 km², with a minimum and maximum catchment area of 6 and

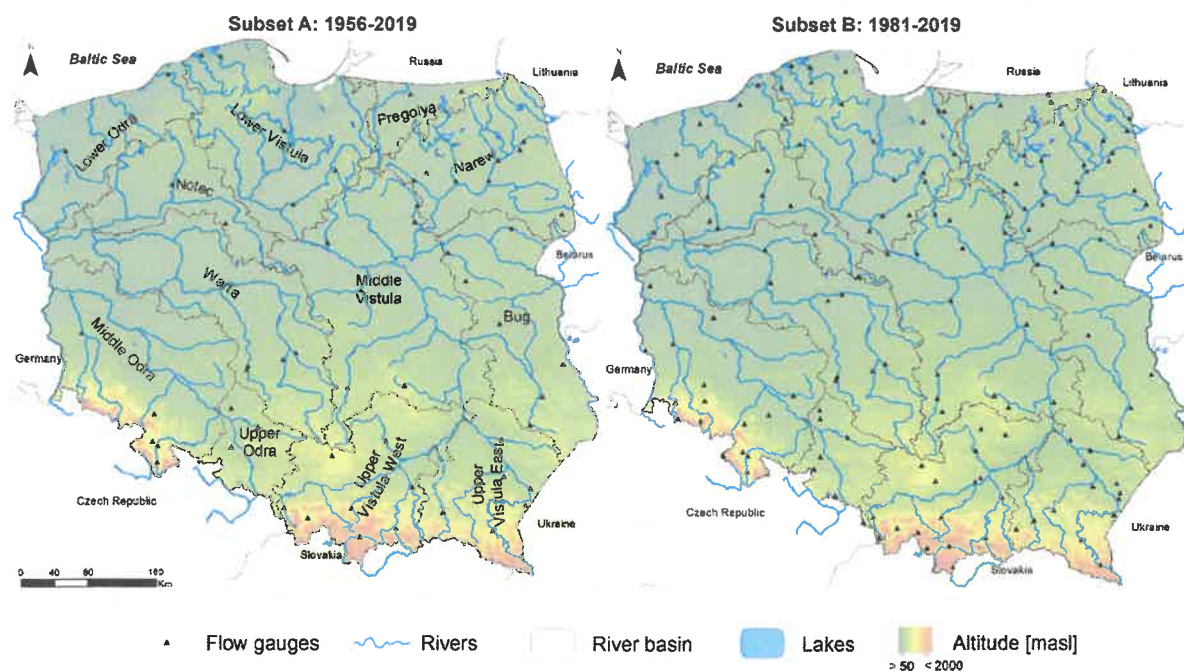


Fig. 1. Study area in Poland, with twelve river basins (labelled in the left panel map) and flow gauges (black triangles) with data from two time periods: 1956–2019 and 1981–2019.

6931 km², respectively, for the whole dataset.

2.3. Indices of floods

The indices to determine the changes in indicators of floods are compiled in Table 1. The annual maximum river flow (denoted as Q_MAX) is the maximum of the discharge recorded in a hydrological year (in Poland it is assumed as 1 November – 30 October), while the concept of peak-over-threshold (POT) is based on the peaks above a defined threshold level (Cunnane, 1973; Madsen et al., 1997; Mangini et al., 2018).

The Q_MAX series were extracted from the daily discharge data set, as the maximum value in a hydrological year for each of the gauges. For determination of the half-year indicators (denoted as Q_MAXT_{wi} and Q_MAXT_{su} for winter and summer, respectively), maximum flow values per half-year were extracted from the data set.

The POT approach detects all high flows exceeding a specific threshold, not just one high flow event per year such as in annual maximum flow (Davison and Smith, 1990; Villarini et al., 2011a). That is, the number of episodes in one year can be different from one, being zero or an integer number 1, 2, 3... Hence, the magnitude and the frequency of high flows, above a threshold, can be determined. In this case, POT series were identified from a predefined quantile (92.5th, 95th or 97.5th percentile) as a threshold. The percentiles were selected as a threshold depending on the variable study conditions (Villarini et al., 2011a; Ward et al., 2018; Kumar et al., 2020; Gupta and Dhanya, 2020), in order to obtain an appropriate number of events during the year (at least 30 and not more than 3 n for the whole POT time series, where n is the length of time series). The great majority of gauges (123 of the whole dataset) were assigned to the 97.5th threshold. However, for some gauges located mainly in the northern part of Poland (but not very close to the coast) this threshold had to be reduced in order to grasp a higher number of POT events. In our study, a dependence criterion of 30-day was arbitrarily selected to define independent peaks between two consecutive events (Mallakpour and Villarini, 2015).

For describing the changes in magnitude of floods, the analyses were processed with both POT magnitude and Q_MAX magnitude (denoted as POTM and Q_MAXM, respectively), while for flood frequency they were focused on POT approach and the frequency of exceedance was denoted as POTF. The changes in flood timing were assessed based on Q_MAX approach, separately for annual and sub-annual periods (summer and winter half-years, i.e., November–April and May–October, respectively) to detect the day of occurrence of the events.

The trends of Q_MAX timing is presented with an annual and a seasonal approach (summer and winter half-year) by the application of mean day of high flow (MDF), where the dates of flood timing were converted into an angular value (Macdonald et al., 2010; Mediero et al., 2014; Blöschl et al., 2017; Do et al., 2020; Wasko et al., 2020), as per the following equations:

$$\varnothing_{ij} = DF_{ij} \frac{2\pi}{J_d} \quad (1)$$

$$\varnothing_{ij} = \tan^{-1} \frac{\bar{y}}{\bar{x}}; \text{ when } \bar{x} > 0, \bar{y} \geq 0 \quad (2)$$

$$\varnothing_{ij} = \tan^{-1} \frac{\bar{y}}{\bar{x}} + \pi; \text{ when } \bar{x} \leq 0 \quad (2)$$

$$\varnothing_{ij} = \tan^{-1} \frac{\bar{y}}{\bar{x}} + 2\pi; \text{ when } \bar{x} > 0, \bar{y} < 0 \quad (2)$$

$$\bar{x} = \frac{1}{P} \sum_{i=1}^E \cos \varnothing_{ij} \quad (3)$$

$$\bar{y} = \frac{1}{P} \sum_{i=1}^E \sin \varnothing_{ij} \quad (4)$$

Table 1

List of river flood indices used in this study.

Index	Abbreviation	Description
Indicators of Magnitude		
Annual maximum daily flow magnitude (m ³ /s)	Q_MAXM	Maximum daily discharge in a hydrological year
Peak-over-threshold magnitude (m ³ /s)	POTM	Magnitude of discharge peaks exceeding a selected threshold
Indicators of Frequency		
Peak-over-threshold frequency	POTF	Annual number of discharge peaks exceeding a selected threshold
Indicators of Timing		
Annual maximum daily flow timing (days)	Q_MAXT _{An}	Day of occurrence of Q_MAXM in each year
Winter half annual maximum daily flow timing (days)	Q_MAXT _{wi}	Day of occurrence of Q_MAXM in each winter half-year (Nov–Apr)
Summer half annual maximum daily flow timing (days)	Q_MAXT _{su}	Day of occurrence of Q_MAXM in each summer half-year (May–Oct)
Mean day of flood (days)	MDF	Mean day of occurrence of the Q_MAXM series in each year

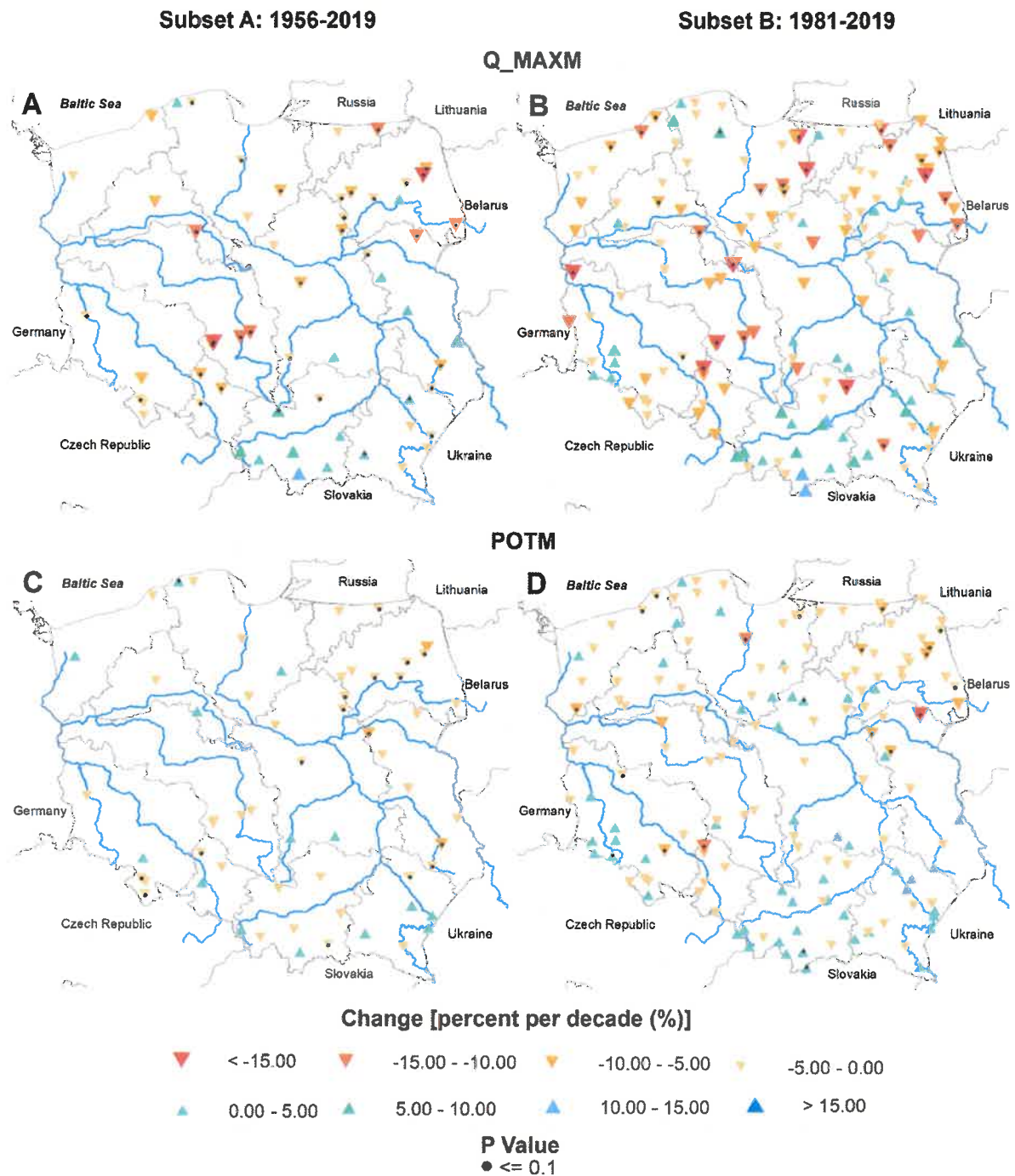


Fig. 2. Trends in Q_MAXM and POTM for the period 1956–2019 (subset A) and 1981–2019 (subset B). Triangle symbols indicate positive (blue palette) and negative (red palette) changes expressed as % change per decade. Point symbols indicate statistically significant changes with $P \leq 0.1$. (For interpretation of the references to colour in this figure legend, the reader is referred to the web version of this article.)

Table 2
Number and percentage of gauges per river basin with decreasing or increasing (overall and statistically significant at $p = 0.1$ level) trend in POTM and Q-MAXM for two analyzed subsets.

Region	Q-MAXM (1956–2019)			Q-MAXM (1981–2019)			POTM (1956–2019)			POTM (1981–2019)		
	Down	Up	All	Down	Up	All	Down	Up	All	Down	Up	All
Bug (7/9)	4 (57%)	3 (43%)	7 (100%)	6 (67%)	3 (33%)	9 (100%)	7 (100%)	0 (0%)	7 (100%)	6 (67%)	3 (33%)	9 (100%)
Significant $< = 0.1$	4 (57%)	0 (0%)	4 (57%)	0 (0%)	0 (0%)	0 (0%)	3 (43%)	0 (0%)	3 (43%)	3 (33%)	0 (0%)	3 (33%)
Lower Odra (2/8)	2 (100%)	0 (0%)	2 (100%)	8 (100%)	0 (0%)	8 (100%)	1 (50%)	1 (50%)	2 (100%)	6 (75%)	2 (25%)	8 (100%)
Significant $< = 0.1$	0 (0%)	0 (0%)	0 (0%)	3 (38%)	0 (0%)	3 (38%)	0 (0%)	0 (0%)	0 (0%)	3 (38%)	0 (0%)	3 (38%)
Lower Vistula (5/18)	4 (80%)	1 (20%)	5 (100%)	15 (83%)	3 (17%)	18 (100%)	3 (60%)	2 (40%)	5 (100%)	13 (72%)	5 (28%)	18 (100%)
Significant $< = 0.1$	3 (60%)	0 (0%)	3 (60%)	5 (28%)	1 (6%)	6 (33%)	0 (0%)	1 (20%)	1 (20%)	2 (11%)	0 (0%)	2 (11%)
Middle Odra (5/16)	5 (100%)	0 (0%)	5 (100%)	12 (75%)	4 (25%)	16 (100%)	4 (80%)	1 (20%)	5 (100%)	8 (50%)	8 (50%)	16 (100%)
Significant $< = 0.1$	2 (40%)	0 (0%)	2 (40%)	2 (13%)	0 (0%)	2 (13%)	2 (40%)	0 (0%)	2 (40%)	2 (13%)	1 (6%)	3 (19%)
Middle Vistula (6/15)	5 (83%)	1 (17%)	6 (100%)	11 (73%)	4 (27%)	15 (100%)	4 (67%)	2 (33%)	6 (100%)	8 (53%)	7 (47%)	15 (100%)
Significant $< = 0.1$	4 (67%)	0 (0%)	4 (67%)	0 (0%)	0 (0%)	0 (0%)	3 (50%)	0 (0%)	3 (50%)	0 (0%)	1 (7%)	1 (7%)
Narew (8/22)	7 (87.5%)	1 (12.5%)	8 (100%)	19 (86%)	3 (14%)	22 (100%)	8 (100%)	0 (0%)	8 (100%)	21 (95%)	1 (5%)	22 (100%)
Significant $< = 0.1$	7 (87.5%)	0 (0%)	7 (87.5%)	6 (27%)	1 (12.5%)	6 (27%)	4 (50%)	0 (0%)	4 (50%)	5 (23%)	0 (0%)	5 (23%)
Notec (2/8)	2 (100%)	0 (0%)	2 (100%)	7 (87.5%)	0 (0%)	7 (100%)	1 (50%)	1 (50%)	2 (100%)	7 (87.5%)	1 (12.5%)	8 (100%)
Significant $< = 0.1$	1 (50%)	0 (0%)	1 (50%)	3 (37.5%)	0 (0%)	3 (37.5%)	0 (0%)	0 (0%)	0 (0%)	0 (0%)	0 (0%)	0 (0%)
Pregolya (2/4)	1 (50%)	0 (0%)	1 (50%)	3 (75%)	1 (25%)	4 (100%)	2 (100%)	0 (0%)	2 (100%)	4 (100%)	0 (0%)	4 (100%)
Significant $< = 0.1$	1 (50%)	0 (0%)	1 (50%)	1 (25%)	0 (0%)	1 (25%)	1 (50%)	0 (0%)	1 (50%)	1 (25%)	0 (0%)	1 (25%)
Upper Odra (3/8)	3 (100%)	0 (0%)	3 (100%)	7 (87.5%)	1 (12.5%)	8 (100%)	2 (67%)	1 (33%)	3 (100%)	7 (87.5%)	1 (12.5%)	8 (100%)
Significant $< = 0.1$	3 (100%)	0 (0%)	3 (100%)	1 (12.5%)	0 (0%)	1 (12.5%)	0 (0%)	0 (0%)	1 (33%)	1 (12.5%)	0 (0%)	1 (12.5%)
Upper Vistula East (6/14)	4 (67%)	2 (33%)	6 (100%)	7 (50%)	7 (50%)	14 (100%)	2 (33%)	4 (67%)	6 (100%)	5 (36%)	9 (64%)	14 (100%)
Significant $< = 0.1$	1 (17%)	2 (33%)	3 (50%)	1 (7%)	0 (0%)	1 (7%)	1 (17%)	0 (0%)	1 (17%)	0 (0%)	0 (0%)	0 (0%)
Upper Vistula West (8/16)	1 (12.5%)	7 (87.5%)	8 (100%)	6 (37%)	10 (63%)	16 (100%)	6 (75%)	2 (25%)	8 (100%)	5 (31%)	11 (69%)	16 (100%)
Significant $< = 0.1$	1 (12.5%)	1 (12.5%)	2 (25%)	1 (6%)	0 (0%)	1 (6%)	1 (13%)	0 (0%)	1 (13%)	0 (0%)	2 (13%)	2 (13%)
Warta (4/8)	4 (100%)	0 (0%)	4 (100%)	8 (100%)	0 (0%)	8 (100%)	4 (100%)	0 (0%)	4 (100%)	7 (88%)	1 (12%)	8 (100%)
Significant $< = 0.1$	4 (100%)	0 (0%)	4 (100%)	2 (25%)	0 (0%)	2 (25%)	0 (0%)	0 (0%)	0 (0%)	0 (0%)	0 (0%)	0 (0%)
All gauges (58/146)	43 (74%)	15 (26%)	58 (100%)	109 (75%)	37 (25%)	146 (100%)	44 (76%)	14 (24%)	58 (100%)	95 (64%)	51 (36%)	146 (100%)
Significant $< = 0.1$	31 (53%)	3 (5%)	34 (58%)	25 (17%)	1 (1%)	26 (18%)	16 (28%)	1 (1%)	17 (29%)	16 (11%)	4 (3%)	20 (14%)

* The values in parentheses (X/Y) denote, respectively, the number of subset A gauges (X) and subset B gauges (Y) in a given river basin.

$$MDF_j = \varphi_j \frac{J_d}{2\pi} \quad (5)$$

where DF_{ij} is the date of occurrence of a maximum flow in a hydrological year, φ_j represents the direction of the angle, \bar{x} and \bar{y} are the cosine and sine components of the mean date of a maximum flow, J_d shows the average number of days per year (365.25 used) and P is the number of peaks in the time series. The reader is referred to literature, such as Blöschl et al. (2017) and Mediero et al. (2014), for more details on MDF calculation.

2.4. Trend analyses

Following studies on river flood indicators (Blöschl et al., 2017, 2019; Mangini et al., 2018; Mediero et al., 2014), we used the non-parametric Mann-Kendall test (MK) and Sen slope (Sen, 1968) in the trend detection process, for POTM, Q_MAXM and for flood timing based on Q_MAXT_{An}, Q_MAXT_{Wi} and Q_MAXT_{Su}. Sen method (Sen, 1968) was applied to estimate magnitude of trends due to its greater robustness to outliers than the parametric analysis (Piniewski et al., 2018). In this process, the median slope of every possible ordered pair of the time series is calculated. Additionally, the trends detected were evaluated for significance using the MK test with p-values at a significance level of 10% (0.1), in consistence with other recent flood trend studies such as Vormoor et al. (2016); Blöschl et al. (2017); Blöschl et al. (2019); Trambay et al. (2019) and Do et al. (2020).

Kundzewicz and Robson (2004) as well as Mediero et al. (2014) explained that the MK test is applicable for flood time series, especially because hydrological data usually have a non-normal distribution. For more details on trend calculation the reader is referred to Mediero et al. (2014) and Mangini et al. (2018).

In this study, the Mann-Kendall test is based on Eqs. (7, 8):

$$S = \sum_{i=1}^{n-1} \sum_{j=i+1}^n \text{sgn}(X_j - X_i) \quad (7)$$

$$\text{sgn}(X_j - X_i) = \begin{cases} 1 & \text{if } (X_j - X_i) > 0 \\ 0 & \text{if } (X_j - X_i) = 0 \\ -1 & \text{if } (X_j - X_i) < 0 \end{cases} \quad (8)$$

where X_j and X_i are the values sorted by data sequence and n is the length of the data set.

Frei and Schär (2001); Vormoor et al. (2016) and Mangini et al. (2018) detected that the chi-square test on parametric Poisson regression is a feasible alternative for trends in POTF, because it is able to fit the series of count, assuming that such count has a Poisson distribution that varies linearly over time (Mangini et al., 2018). This analysis was carried out in R ('Kendall' and 'zyp' packages) by the implementation of a code developed by Mangini et al. (2018).

Trend results of POTM and Q_MAXM were converted into a percent change per decade (Gudmundsson et al., 2019; Stahl et al., 2012) which eases interpretation and comparability of results. The percent change per decade, S_m , is defined by Eq. (9):

$$S_m = \frac{S_c \times 10 \text{ years}}{\bar{x}} \times 100 \quad (9)$$

where S_m is the trend in percentage change per decade, S_c is the Sen slope, and \bar{x} is the average of the annual flood time series.

Then, changes in POTF and Q_MAXT (with an annual and a seasonal approach) are presented in events per decade by Eq. (10):

$$S_f = (S_c \times 10 \text{ years}) \quad (10)$$

where S_f is the trend in events per decade and S_c is the Sen slope by chi-square test on parametric Poisson regression in the case of frequency.

3. Results

3.1. Trends in Q_MAX and POT magnitude

The analyses of the Q_MAXM showed a strong and consistent pattern. A general downward trend for both subsets and both approaches was observed, with statistically significant decreases of more than 15% per decade at some gauges. The time series of Q_MAXM manifests stronger changes (Fig. 2 A-B) than POTM (Fig. 2 C-D). For instance, in the north-east region (Lower Vistula - Pregolya - Narew), Q_MAXM has the highest downward tendency in both subsets in comparison to POTM (Fig. 2 C-D).

Changes are less pronounced for the subset A (with smaller number of gauges but longer time series of records) than for the subset B. This holds for POT and Q_MAX method, where a positive tendency is found in the south-east region particularly in the Upper Vistula Basin, where the percentage increase for Q_MAXM is around 5–15% (Fig. 2B) but with no statistical significance. For POTM, the variation of change is between 0% and 5% per decade in the south-east region (Fig. 2D).

The trend results for all river basins are summarized in Table 2, where the percentage of gauges exhibiting significant, positive or negative, trends is shown for the two subsets. A general downward trend is observed for almost all the river basins for both subsets. At the national level, for Q_MAXM there is a temporal stability in detected trends, with roughly 75% of gauges with decreasing trends

irrespective of the starting year. For POTM, the evidence for decreasing trends is stronger for subset A (76% of gauges and 28% with significance) than B (64% and 11% with significance). For Q_MAXM, nine river basins (all but the Upper Vistula East and West as well as the Bug) exhibit downward trends in at least 73% of gauges, for both subsets. It is interesting that although downward trend magnitude is lower for the subset A, statistical significance is much more frequent (53% of gauges) than for the subset B (17%). The largest difference between two approaches can be found for the Middle Vistula Basin in subset B, for which 47% of gauges show insignificant decreasing trend in POTM and 73% in Q_MAXM.

3.2. Trends in POT frequency

The frequency of flood events is determined on the basis of POT series. Fig. 3 illustrates the spatial changes of flood events per decade, with higher variability for the long time series. This result is similar to findings for Q_MAXM and POTM presented in Fig. 2. The pattern of POTF has a negative trend for the northern part of the country for each period, while in the southern regions various trend directions were found, but upward trends prevail. Some gauges in the eastern regions are characterized by a positive tendency in both periods. The Narew, the Bug and the Upper Vistula (West and East) have the higher values for the period 1981–2019.

Detected trends in flood frequency have low magnitude and in great majority they are insignificant in both periods (subsets A and B). None of the gauges from subset A has an upward trend higher than 0.2 events per decade and only two (one gauge in the northeast region with significant change) out of 146 gauges from the subset B have such trend. Indeed, the main similarity between the two subsets is the increasing trend in the southern part of Poland, mostly in vicinity of the Slovakian border and the decreasing tendency in the north-east region. One difference is detected in the eastern part (Bug region) with a downward pattern in the subset A and an upward in the subset B.

Table 3 supports the findings from Fig. 3 where a common decreasing trend is found. At the national level, POTF has a decreasing trend in 71% (7% with significance) and 66% (3% with significance) of gauges for the subsets A and B, respectively, which shows that the temporal stability is in place. In some river basins there is no clear pattern – for example in the Upper Vistula West half of gauges point at upward/downward trend in POT frequency, irrespective of the time period. Another extreme case is the Noteć Basin for which upward trends occur in all (two) gauges from subset A, whereas all (eight) gauges exhibit downward trends in subset B (just one with statistically significant change). An insignificant upward tendency for 67% (six out of nine) of gauges was found in the Bug Basin for the subset B, however the subset A displayed an insignificant increase of 14% (one gauge) for the same area. In addition, an insignificant downward trend in 100% of gauges for the subset A in the Pregolya and Upper Odra was detected, similar to the period of

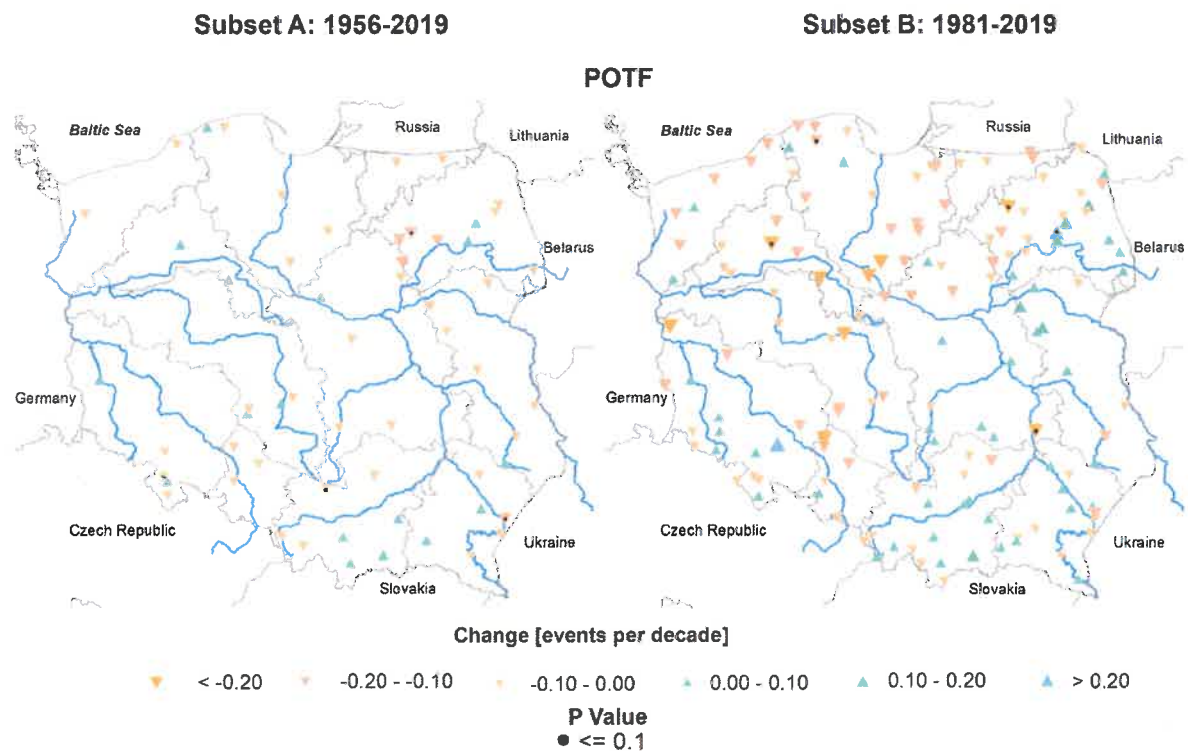


Fig. 3. Trends in POTF for the period 1956–2019 (subset A) and 1981–2019 (subset B). Triangle symbols indicate positive (blue palette) and negative (red palette) trends quantified as change in the number of events per decade. Point symbols indicate statistically significant changes as $P < 0.1$. (For interpretation of the references to colour in this figure legend, the reader is referred to the web version of this article.)

Table 3

Number and percentage of gauges per river basin with increasing or decreasing trends (overall and statistically significant at $p = 0.1$ level) in POTF for the two analyzed subsets.

Region	POTF (1956–2019)			POTF (1981–2019)		
	Down	Up	All	Down	Up	All
Bug (7/9)	6 (86%)	1 (14%)	7 (100%)	3 (33%)	6 (67%)	9 (100%)
Significant ≤ 0.1	0 (0%)	0 (0%)	0 (0%)	0 (0%)	0 (0%)	0 (0%)
Lower Odra (2/8)	2 (100%)	0 (0%)	2 (100%)	6 (75%)	2 (25%)	8 (100%)
Significant ≤ 0.1	0 (0%)	0 (0%)	0 (0%)	0 (0%)	0 (0%)	0 (0%)
Lower Vistula (5/18)	4 (80%)	1 (20%)	5 (100%)	16 (89%)	2 (11%)	18 (100%)
Significant ≤ 0.1	0 (0%)	0 (0%)	0 (0%)	1 (6%)	0 (0%)	1 (6%)
Middle Odra (5/16)	3 (60%)	2 (40%)	5 (100%)	9 (56%)	7 (44%)	16 (100%)
Significant ≤ 0.1	1 (20%)	0 (0%)	1 (20%)	0 (0%)	0 (0%)	0 (0%)
Middle Vistula (6/15)	83%	17%	6 (100%)	8 (53%)	7 (47%)	15 (100%)
Significant ≤ 0.1	0 (0%)	0 (0%)	0 (0%)	1 (7%)	0 (0%)	1 (7%)
Narew (8/22)	6 (75%)	2 (25%)	8 (100%)	13 (60%)	9 (40%)	22 (100%)
Significant ≤ 0.1	1 (13%)	0 (0%)	1 (13%)	1 (5%)	1 (5%)	2 (9%)
Notec (2/8)	0 (0%)	2 (100%)	2 (100%)	8 (100%)	0 (0%)	8 (100%)
Significant ≤ 0.1	0 (0%)	0 (0%)	0 (0%)	1 (13%)	0 (0%)	1 (13%)
Pregolya (2/4)	2 (100%)	0 (0%)	2 (100%)	4 (100%)	0 (0%)	4 (100%)
Significant ≤ 0.1	0 (0%)	0 (0%)	0 (0%)	0 (0%)	0 (0%)	0 (0%)
Upper Odra (3/8)	3 (100%)	0 (0%)	3 (100%)	6 (75%)	2 (25%)	8 (100%)
Significant ≤ 0.1	0 (0%)	0 (0%)	0 (0%)	0 (0%)	0 (0%)	0 (0%)
Upper Vistula East (6/14)	4 (67%)	2 (33%)	6 (100%)	7 (50%)	7 (50%)	14 (100%)
Significant ≤ 0.1	1 (17%)	0 (0%)	1 (17%)	0 (0%)	0 (0%)	0 (0%)
Upper Vistula West (8/16)	4 (50%)	4 (50%)	8 (100%)	8 (50%)	8 (50%)	16 (100%)
Significant ≤ 0.1	1 (13%)	0 (0%)	1 (13%)	0 (0%)	0 (0%)	0 (0%)
Warta (4/8)	2 (50%)	2 (50%)	4 (100%)	8 (100%)	0 (0%)	8 (100%)
Significant ≤ 0.1	0 (0%)	0 (0%)	0 (0%)	0 (0%)	0 (0%)	0 (0%)
All gauges (58/146)	41 (71%)	17 (29%)	58 (100%)	97 (66%)	49 (34%)	146 (100%)
Significant ≤ 0.1	4 (7%)	0 (0%)	4 (7%)	4 (3%)	1 (1%)	5 (4%)

*The values in parentheses (X/Y) denote, respectively, the number of subset A gauges (X) and subset B gauges (Y) in a given river basin.

1981–2019 with 100% and 75% for Pregolya and Upper Odra Basin, respectively. The POTF at the national scale presents an increase for the subset B of 34% of gauges with a positive trend. In summary, based on POTF results we have detected a moderate, but mostly insignificant, downward change in flood frequency, mainly in the northern part of Poland for the subset B (the Notec, the Warta, the Pregolya and the Lower Vistula basins), where the decrease is consistent and described by values not exceeding 0.2 flood events per decade.

3.3. Trends in Q_{MAX} timing

Before results on trends in Q_{MAX} timing are presented, the average timing of river floods in the observation record is shown in Fig. 4. The spatial pattern in the subsets A and B for the $Q_{MAXT_{An}}$ (Fig. 4 A-B) shows that average flood timing varies between February and April for most of the country (lowland part), whereas in mountainous south the average flood timing is from May till July. Due to different flood generation mechanisms in different parts of Poland (a mixture of snowmelt, heavy rainfall in summer and winter precipitation), the average timing of annual floods reflects both years with spring or winter floods (predominant in the Centre and North) and summer floods (prevailing in the South). A different trend pattern can arise once the flood timing is analyzed separately for winter and summer half-years, for which flood generation mechanisms are more consistent.

The $Q_{MAXT_{Su}}$ for both subsets (Fig. 4 C-D) exhibit an interesting spatial pattern, with the earliest occurrence of summer half-year flood peaks in north-eastern and central part of Poland (typically June). Gauges located close to the coast and in the upland part in the South are characterized by flood peaks occurring in July. June–July is the average flood timing period in summer half-year, for the southern-most gauges in the Carpathian and the Sudety Mountains.

A more spatially uniform pattern occurs in winter half-year flood peak timing (Fig. 4 E-F). In this case, the pattern resembles to much extent that for the annual timing, except for gauges in southern, mountainous, area. The earliest occurrence of winter floods (February) occurs in the coastal parts of the country, and the latest in the north-east.

The results of changes for the time occurrences of flood series are presented in Fig. 5. The changes are expressed as number of days per decade, which allows to detect an earlier or later incidence of flood peaks.

Spatial pattern of trends shown in Fig. 5 A-B is more complex than respective patterns in flood magnitude and frequency across Poland and there is a lower statistical significance in comparison to Q_{MAXM} . The patterns for two subsets A and B are not fully consistent and also the magnitude of trends is higher for the second subset. In general, decreasing trends prevail, especially in the southern part of the country (both mountains and upland regions). In the north-east, the pattern is highly mixed, with neighboring gauges showing changes of large magnitude and opposing directions. In the north-western part of Poland, there is a dominant increasing trend (with significant changes for one gauge in the subset B), though.

A different pattern, with more robust results for the larger subset restricted to the period 1981–2019 than for the smaller subset

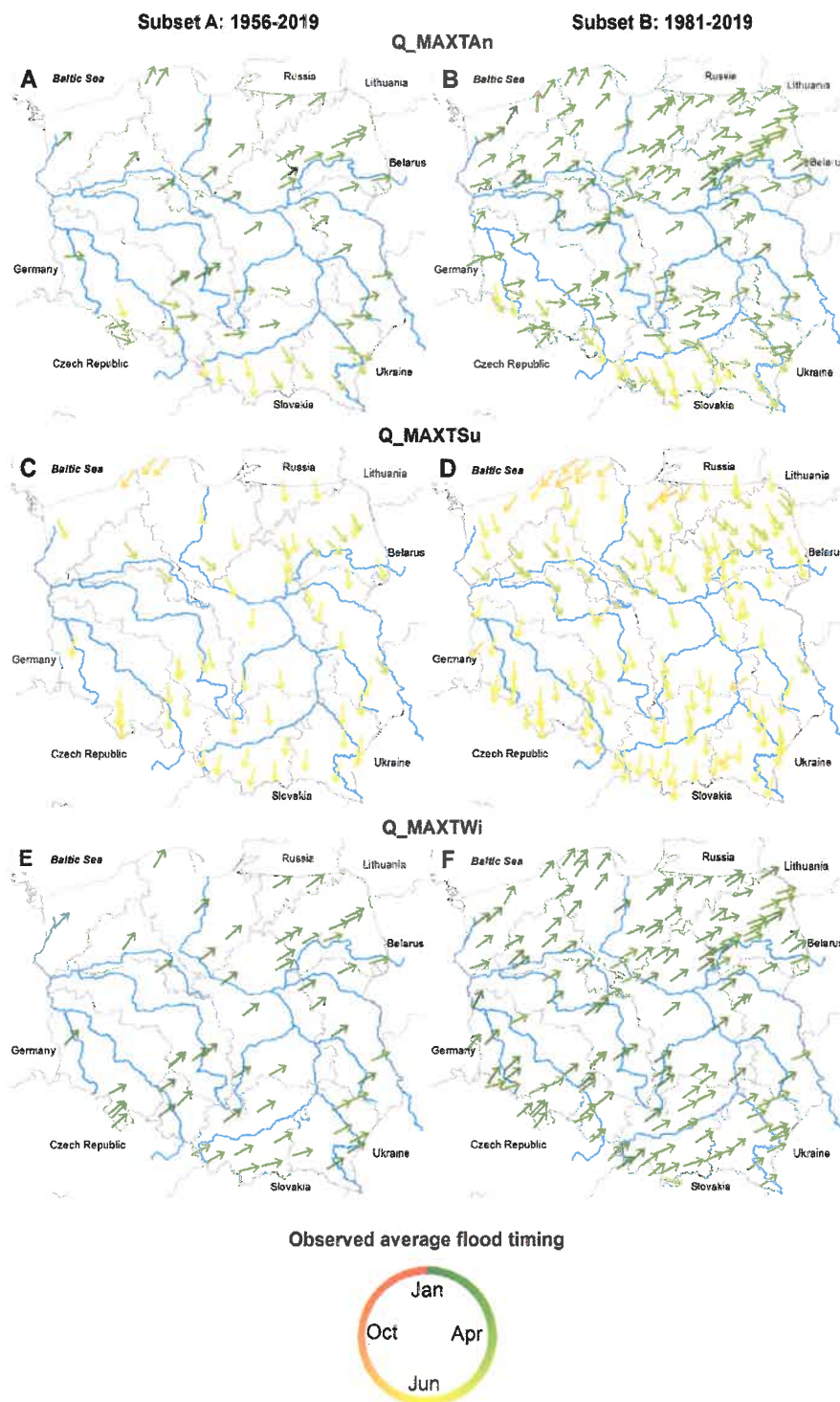


Fig. 4. Observed average timing of river floods for the period 1956–2019 (subset A) and 1981–2019 (subset B). Arrow symbols (both angle and color) show the timing of floods in analyzed periods.

restricted to 1956–2019 can be found for trends in Q_MAXT_{Su} (Fig. 5C–D). In this case, a tendency for earlier flood occurrence dominates throughout the whole country, especially for subset B. The largest magnitude of this decrease, exceeding 8 days per decade, can be observed for gauges located in the upland part in the South and in the proximity of the coast in the north. For subset A,

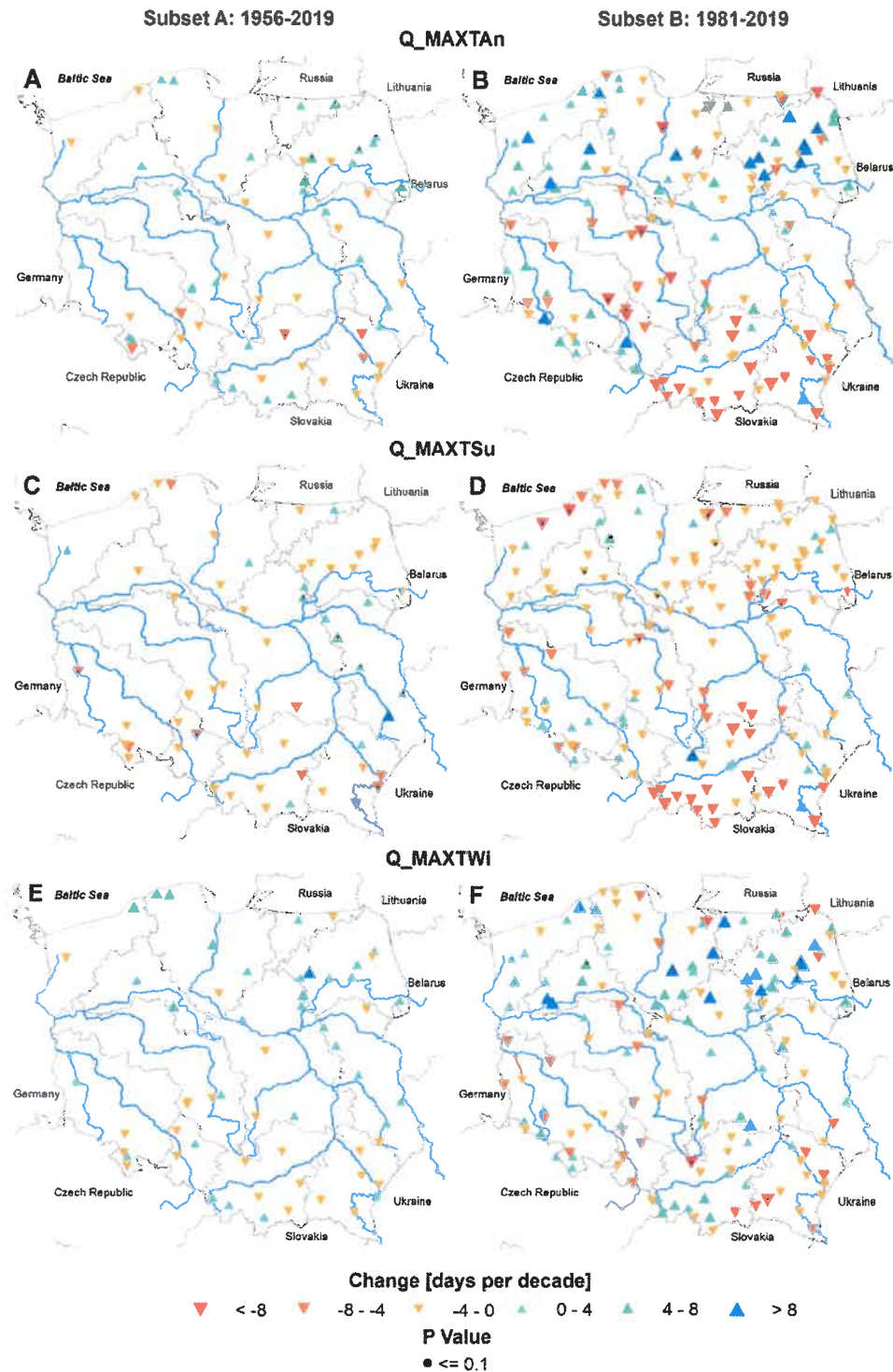


Fig. 5. Trends in Q_MAX timing for the period 1956–2019 (subset A) and 1981–2019 (subset B). Triangle symbols indicate positive (blue palette) and negative (red palette) trends expressed as change in days per decade. Panels A-B, C-D and E-F show the annual (Q_MAXTAn), summer half-year (Q_MAXTSu) and winter half-year (Q_MAXTWi) flood timing, respectively. Point symbols indicate statistically significant changes with ≤ 0.1 . (For interpretation of the references to colour in this figure legend, the reader is referred to the web version of this article.)

increasing, statistically significant, trends can be found mostly for the eastern part.

For Q_MAXT_{Wi} (Fig. 5 E-F), the country is roughly divided into two halves, with increasing trends dominating in the north (except for the northern part of the Lower Vistula basin) and decreasing in the south (except for the southern part of the Upper Vistula West basin), which generally resembles trends for the annual flood timing. The pattern is generally consistent across two subsets, with lower magnitude of trends detected for the longer period. Statistical significance occurs only in several gauges located mainly in the northeast (subset B).

In summary, the trends in Q_MAX timing for annual and sub-annual data with the percentage and number of gauges with statistical significance are presented in Tables 4 and 5, respectively. When looking at particular basins, in some cases we can observe high sensitivity to the time period selected for analysis. For example, in the Upper Odra and the Upper Vistula West basins, significantly higher fraction of gauges was pointing at insignificant decreasing trends for subset A than B. This may be related to the acceleration of warming (and, in consequence, snowmelt) in the second part of the analyzed period.

On the other hand, for summer and winter flood timing, the trends were more consistent between the two time periods (Table 5). The summer half-year illustrated a strong decreasing trend in almost all the regions of Poland for both subsets, with 10% of gauges showing statistical significance for 1956–2019 (7% for 1981–2019). An upward tendency was detected for the winter half-year timing in the northern regions, where in the Lower Odra and Narew basins, there were later occurrences in 75% and 68% of gauges for subset B, while in the Lower Vistula basin increasing trend was detected in 80% of gauges for subset A. Nevertheless, for only 5% of all streamflow gauges the change for Q_MAXT_{Win} was statistically significant.

4. Discussion

The trend detection of various flood indicators is important for understanding of the observed changes in flood pattern in Poland. The use of two complimentary methods, POT and Q_MAX series, allows for a more comprehensive examination of the magnitude, frequency and timing of high flow episodes. This topic has been rarely studied in Poland, while pan-European and global-scale studies dealing with changes in flood hazard have typically left the country out of analysis due to the lack of free access to flow data. To our knowledge, there is no study that used comparably recent data for trend detection in flood indices in this region, with an exception of Piniewski et al. (2018), who nevertheless studied only one flood indicator, Q_MAXM .

4.1. Trends in flood magnitude

The trend detection in flood magnitude via Q_MAXM showed a visible spatial variability and statistical significance in both periods, including 58% of all the gauges in subset A and 18% in subset B. The decreases were detected mainly in the northern river basins, while

Table 4

Number and percentage of gauges per river basin with later or earlier flood occurrence in Q_MAXT for annual data (overall and statistically significant at $p = 0.1$ level) for the two analysed subsets.

Region	Q_MAXT_{An} (1956–2019)			Q_MAXT_{An} (1981–2019)		
	Earlier (↓)	Later (↑)	All	Earlier (↓)	Later (↑)	All
Bug (7/9)	3 (43%)	4 (57%)	7 (100%)	7 (78%)	2 (22%)	9 (100%)
Significant ≤ 0.1	0 (0%)	0 (0%)	0 (0%)	0 (0%)	0 (0%)	0 (0%)
Lower Odra (2/8)	2 (100%)	0 (0%)	2 (100%)	1 (12%)	7 (88%)	8 (100%)
Significant ≤ 0.1	0 (0%)	0 (0%)	0 (0%)	0 (0%)	0 (0%)	0 (0%)
Lower Vistula (5/18)	2 (40%)	3 (60%)	5 (100%)	9 (50%)	9 (50%)	18 (100%)
Significant ≤ 0.1	0 (0%)	0 (0%)	0 (0%)	2 (11%)	1 (6%)	3 (17%)
Middle Odra (5/16)	2 (40%)	3 (60%)	5 (100%)	8 (50%)	8 (50%)	16 (100%)
Significant ≤ 0.1	0 (0%)	0 (0%)	0 (0%)	1 (6%)	0 (0%)	1 (6%)
Middle Vistula (6/15)	4 (67%)	2 (33%)	6 (100%)	9 (60%)	6 (40%)	15 (100%)
Significant ≤ 0.1	0 (0%)	1 (17%)	1 (17%)	0 (0%)	0 (0%)	0 (0%)
Narew (8/22)	2 (25%)	6 (75%)	8 (100%)	8 (36%)	14 (64%)	22 (100%)
Significant ≤ 0.1	0 (0%)	4 (50%)	4 (50%)	0 (0%)	4 (18%)	4 (18%)
Notec (2/8)	0 (0%)	2 (100%)	2 (100%)	3 (37.5%)	5 (62.5%)	8 (100%)
Significant ≤ 0.1	0 (0%)	0 (0%)	0 (0%)	0 (0%)	1 (13%)	1 (13%)
Pregolya (2/4)	0 (0%)	2 (100%)	2 (100%)	3 (75%)	1 (25%)	4 (100%)
Significant ≤ 0.1	0 (0%)	1 (50%)	1 (50%)	0 (0%)	0 (0%)	0 (0%)
Upper Odra (3/8)	3 (100%)	0 (0%)	3 (100%)	5 (62%)	3 (38%)	8 (100%)
Significant ≤ 0.1	0 (0%)	0 (0%)	0 (0%)	1 (13%)	0 (0%)	1 (13%)
Upper Vistula East (6/14)	6 (100%)	0 (0%)	6 (100%)	13 (93%)	1 (7%)	14 (100%)
Significant ≤ 0.1	0 (0%)	0 (0%)	0 (0%)	2 (14%)	1 (7%)	3 (21%)
Upper Vistula West (8/16)	3 (37.5%)	5 (62.5%)	8 (100%)	14 (87%)	2 (13%)	16 (100%)
Significant ≤ 0.1	1 (12.5%)	0 (0%)	1 (12.5%)	1 (6%)	0 (0%)	1 (6%)
Warta (4/8)	1 (25%)	3 (75%)	4 (100%)	7 (87%)	1 (13%)	8 (100%)
Significant ≤ 0.1	0 (0%)	0 (0%)	0 (0%)	1 (13%)	0 (0%)	1 (13%)
All gauges (58/146)	28 (48%)	30 (52%)	58 (100%)	89 (61%)	57 (39%)	146 (100%)
Significant ≤ 0.1	1 (1%)	6 (10%)	7 (11%)	8 (5%)	7 (5%)	15 (10%)

*The values in parentheses (X/Y) denote, respectively, the number of subset A gauges (X) and subset B gauges (Y) in a given river basin.

Table 5
Number and percentage of gauges per river basin with later or earlier flood occurrence in Q_{MAXT} for summer and winter half-years (overall and statistically significant at $p = 0.1$ level) for the two subsets.

Region	Q _{MAXTsu} (1956–2019)				Q _{MAXTsu} (1981–2019)				Q _{MAXTwt} (1956–2019)				Q _{MAXTwt} (1981–2019)			
	Earlier (t)	Later (t)	All		Earlier (t)	Later (t)	All		Earlier (t)	Later (t)	All		Earlier (t)	Later (t)	All	
Bug (7/9)	0 (0%)	7 (100%)	7 (100%)		7 (88%)	2 (22%)	9 (100%)		2 (25%)	5 (71%)	7 (100%)		6 (67%)	3 (33%)	9 (100%)	
Significant < = 0.1	0 (0%)	4 (57%)	4 (57%)		1 (11%)	0 (0%)	1 (11%)		0 (0%)	0 (0%)	0 (0%)		0 (0%)	0 (0%)	0 (0%)	
Lower Odra (2/8)	1 (50%)	1 (50%)	2 (100%)		6 (75%)	2 (25%)	8 (100%)		1 (50%)	1 (50%)	2 (100%)		2 (25%)	6 (75%)	8 (100%)	
Significant < = 0.1	0 (0%)	0 (0%)	0 (0%)		2 (25%)	0 (0%)	2 (25%)		0 (0%)	0 (0%)	0 (0%)		0 (0%)	0 (0%)	0 (0%)	
Lower Vistula (5/18)	4 (80%)	1 (20%)	5 (100%)		14 (88%)	4 (22%)	18 (100%)		1 (20%)	4 (80%)	5 (100%)		9 (50%)	9 (50%)	18 (100%)	
Significant < = 0.1	0 (0%)	0 (0%)	0 (0%)		3 (17%)	1 (5%)	4 (22%)		0 (0%)	0 (0%)	0 (0%)		0 (0%)	1 (6%)	1 (6%)	
Middle Odra (5/16)	5 (100%)	0 (0%)	5 (100%)		11 (69%)	5 (31%)	16 (100%)		3 (60%)	2 (40%)	5 (100%)		10 (62%)	6 (38%)	16 (100%)	
Significant < = 0.1	1 (20%)	0 (0%)	1 (20%)		0 (0%)	0 (0%)	0 (0%)		0 (0%)	0 (0%)	0 (0%)		0 (0%)	0 (0%)	0 (0%)	
Middle Vistula (6/15)	4 (67%)	2 (33%)	6 (100%)		15 (100%)	0 (0%)	15 (100%)		2 (33%)	4 (67%)	6 (100%)		6 (40%)	9 (60%)	15 (100%)	
Significant < = 0.1	1 (16.5%)	1 (16.5%)	2 (33%)		0 (0%)	0 (0%)	0 (0%)		0 (0%)	0 (0%)	0 (0%)		0 (0%)	0 (0%)	0 (0%)	
Narew (8/22)	8 (100%)	0 (0%)	8 (100%)		19 (86%)	3 (14%)	22 (100%)		1 (13%)	7 (87%)	8 (100%)		7 (32%)	15 (68%)	22 (100%)	
Significant < = 0.1	0 (0%)	0 (0%)	0 (0%)		0 (0%)	0 (0%)	0 (0%)		0 (0%)	0 (0%)	0 (0%)		0 (0%)	4 (18%)	4 (18%)	
Notec (2/8)	2 (100%)	0 (0%)	2 (100%)		8 (100%)	0 (0%)	8 (100%)		0 (0%)	2 (100%)	2 (100%)		3 (38%)	5 (62%)	8 (100%)	
Significant < = 0.1	0 (0%)	0 (0%)	0 (0%)		1 (13%)	0 (0%)	1 (13%)		0 (0%)	0 (0%)	0 (0%)		0 (0%)	1 (12.5%)	1 (12.5%)	
Pregolya (2/4)	1 (50%)	1 (50%)	2 (100%)		4 (100%)	0 (0%)	4 (100%)		1 (50%)	1 (50%)	2 (100%)		1 (25%)	3 (75%)	4 (100%)	
Significant < = 0.1	0 (0%)	0 (0%)	0 (0%)		0 (0%)	0 (0%)	0 (0%)		0 (0%)	0 (0%)	0 (0%)		0 (0%)	0 (0%)	0 (0%)	
Upper Odra (3/8)	3 (100%)	0 (0%)	3 (100%)		6 (75%)	2 (25%)	8 (100%)		2 (67%)	1 (33%)	3 (100%)		6 (75%)	2 (25%)	8 (100%)	
Significant < = 0.1	1 (33%)	0 (0%)	1 (33%)		0 (0%)	0 (0%)	0 (0%)		0 (0%)	0 (0%)	0 (0%)		0 (0%)	0 (0%)	0 (0%)	
Upper Vistula East (6/14)	5 (83%)	1 (17%)	6 (100%)		10 (71%)	4 (29%)	14 (100%)		5 (83%)	1 (17%)	6 (100%)		12 (86%)	2 (14%)	14 (100%)	
Significant < = 0.1	2 (33%)	0 (0%)	2 (33%)		0 (0%)	0 (0%)	0 (0%)		0 (0%)	0 (0%)	0 (0%)		1 (7%)	0 (0%)	1 (7%)	
Upper Vistula West (8/16)	7 (87%)	1 (13%)	8 (100%)		13 (81%)	3 (19%)	16 (100%)		5 (62%)	3 (38%)	8 (100%)		9 (56%)	7 (44%)	16 (100%)	
Significant < = 0.1	1 (13%)	0 (0%)	1 (13%)		2 (13%)	1 (6%)	3 (19%)		0 (0%)	0 (0%)	0 (0%)		1 (6%)	0 (0%)	1 (6%)	
Warta (4/8)	4 (100%)	0 (0%)	4 (100%)		7 (87%)	1 (13%)	8 (100%)		3 (75%)	1 (25%)	4 (100%)		6 (75%)	2 (25%)	8 (100%)	
Significant < = 0.1	0 (0%)	0 (0%)	0 (0%)		1 (13%)	0 (0%)	1 (13%)		0 (0%)	0 (0%)	0 (0%)		0 (0%)	0 (0%)	0 (0%)	
All gauges (58/146)	44 (76%)	14 (24%)	58 (100%)		124 (85%)	22 (17%)	146 (100%)		26 (45%)	32 (55%)	58 (100%)		78 (53%)	68 (47%)	146 (100%)	
Significant < = 0.1	6 (10%)	5 (9%)	11 (19%)		10 (7%)	2 (1%)	12 (8%)		0 (0%)	1 (2%)	1 (2%)		2 (1%)	6 (4%)	8 (5%)	

* The values in parentheses (X/Y) denote, respectively, the number of subset A gauges (X) and subset B gauges (Y) in a given river basin.

the increases were present in the south of the country. The highest downward change in percent per decade in all the cases was detected in the northeast, with values about -15% per decade. The statistical significance was also most frequent in this region, for example, in the Narew basin changes at 87.5% of all gauges for the period 1956–2019 were significant for Q_{MAXM} . This overall result is in agreement with that reported by Piniewski et al. (2018), who found the strongest decreasing trend in the northern part of Poland and a moderate increase in the southern-most, mountainous, part close to the border with Slovakia.

Direct comparison of our results with those from other authors of publications on changes in flood hazard is a challenge due to different study emphases and coverage area. Nevertheless, our results show a generally coherent pattern with previous European studies of Blöschl et al. (2019), Bertola et al. (2020) and Slater et al. (2021). Blöschl et al. (2019), who studied trends in flood magnitude in Europe based on European Flood Database by Hall et al. (2015) for 1960–2010, using the time series of annual maxima of daily mean or instantaneous discharge data, found a rather complex pattern in mean annual flood change over Poland. While the majority of the territory, including the entire eastern and interior parts, exhibited downward trend (below -5% per decade), upward trends were also noted in two regions: the northern edge close to the Baltic Sea coast (weak trend) and a smaller, south-eastern edge with a slightly stronger magnitude of trend. The spatial pattern revealed by our analyses matches the one discovered by Blöschl et al. (2019) quite well, although we have not found a weak increasing trend in the coastal region.

A different pattern of trends in the northern regions of Poland was found by Bertola et al. (2020) who analyzed trends in 100-year and 2-year floods in Europe for small and large catchments, based on the same European Flood Database of Hall et al. (2015) as Blöschl et al. (2019). They found that northern Poland features a decrease in flood magnitude for both recurrence levels and catchment size classes, as supported by our findings. In contrast, Kundzewicz et al. (2018) studied the spatial-temporal change of numbers of large floods in the whole of Europe, based on flood data from the Dartmouth Flood Observatory dataset, where large floods were defined as those with severity and magnitude greater than a selected threshold. They detected larger floods between 1985 and 2016 in the southern part of Poland as our main results for Q_{MAXM} , where heavy and prolonged precipitation (2–5 days) are the most common flood generators in the area (Kundzewicz et al., 2014b and Ruiz-Villanueva et al., 2016).

Our findings are also consistent with Slater et al. (2021), who analyzed global changes in river floods with different probabilities of occurrence using annual maximum daily streamflow. They found decreases in 20- and 50-year floods for central Europe, a region containing Poland and this is consistent with our Q_{MAXM} results. The 20- and 50-year floods exhibited a clear downward pattern in most of the country, except for a few gauges located in mountainous south – a similar pattern as in our study.

In some river basins, we identified a lack of robustness between the analysis performed for two subsets, A and B, characterized by different spatial and temporal coverage. For example, in the Upper Vistula West Basin, a decreasing trend in POTM was found for the longer period (1956–2019), while an upward trend - for the shorter time period (1981–2019) (Table 2). A similar pattern was observed by Vormoor et al. (2016) who studied trends for daily peak flow series in Norway and found a higher number of stations with decrease in the longer time period than in the shorter period. In addition, Mostofi Zadeh et al. (2020) mentioned that a predominantly increasing trend in a short period (recent years) could indicate a possible common driver of floods in a specific area. This is consistent with our findings for the subset B for 1981–2019. Overall, the spatial patterns of change are different, depending on the scale, observed data and method applied. For example, Masseroni et al. (2021) who used daily streamflow data for 1950–2013, showed a general positive trend in annual streamflow volumes in the continental region of Europe but with an opposite pattern for the majority of stations in Slovakia, close to the Polish border. This is a different pattern from the majority of reported literature and our study. However, it should be noted that their main focus was on annual discharge volumes and not on river floods as in our case.

Drivers of changes in flood magnitude are still debated due to the lack of hydrometric gauges and large-scale evidence (Blöschl et al., 2019), but one common result was determined in the northeastern Europe, where studies such as Estilow et al. (2015), Blöschl et al. (2017, 2019) and Bertola et al. (2020) mentioned an association between this downward trend and the increasing air temperature and earlier snowmelt. This drop in flood magnitude closely follows larger decreases in mean snow cover depth in eastern Poland (Szwed et al., 2017), which have an impact on snow storage with low magnitude values (negative changes per decade in both methods), such as the downward trend flood in Europe that Madsen et al. (2014) found for snowmelt-dominated areas. The downward trends in the North are related to a decrease in river discharge which is the dominant factor in this region (Kundzewicz et al., 2018). Indeed, this decreasing trend over north-western regions may also be associated with a negative phase of Azores-Scandinavia Oscillation (ASO) index, defined as the sea level pressure difference between the oscillations of Gibraltar (The Azores) and Haparandain Sweden, and Gibraltar and Vestervig in Denmark, generating a dry climate over north and central-western Europe (Willems, 2013). The increases prevailing in the southern part are associated with heavy and prolonged precipitation (2–5 days), especially in the mountain areas (Kundzewicz et al., 2014b and Ruiz-Villanueva et al., 2016). In fact, both patterns (decreases in the north and small increases in the south) are corroborated by the results of Piniewski et al. (2018), who also studied Q_{MAXM} indicator for the time period reaching 2016.

4.2. Trends in flood frequency

Analysis of changes in POT frequency did not demonstrate an evident and significant trend due to the low values of changes in events per decade detected, even though the spatial distribution showed a particular decrease in northern part of Poland and a mixed behavior in the south. Statistical significance of flood frequency was the lowest among all flood indices studied in the paper. Table 3 displayed a robust result of decreasing trend for POTF in the Pregolya Basin in both subsets while a weaker robustness for the Warta and the Bug basins. Therefore, it should be noted that the increase of flood frequency in the country is less common and it refers mainly to the southern area.

There are very few studies dealing with trends in flood frequency that we could use as a reference for comparison with our results.

For example, [Mudelsee et al. \(2003\)](#) analyzed the occurrence rate of summer and winter extreme floods in the Elbe and Odra rivers and found a downward trend in winter floods for the past 50, 80 and 100 years, where the decreasing pattern was attributed to less severe freezing events during the study period. They also showed a downward trend in frequency of extreme floods for the central Europe area, but with some increase during the past decades that could be explained by nonhomogeneous historical data records. [Mangini et al. \(2018\)](#) analyzed the POT frequency for different regions in Europe using mean daily streamflow data and found consistent negative trends in POTF in the continental part of Europe, where many stations had results with change in the range from -0.2 – 0 events per decade, similarly to our findings. Unfortunately, the study did not include analyses with gauges over Poland that could be compared directly with our results. In contrast, the global-scale study of [Berghuijs et al. \(2017\)](#) reported increases in magnitude and occurrences of extreme (corresponding to 1/30 annual exceedance probability) floods in Europe, but the results were not presented at a finer than continental spatial scale, and flow data from Poland were not used in the analysis.

Similar decreasing results in flood frequency was found by [Tramblay et al. \(2019\)](#), who used daily discharge data and associated the less frequent occurrence of floods above 95th and 99th flow percentile in the Mediterranean region to the soil moisture decrease. This decrease may compensate the increasing rainfall amount, even more in areas with observed crop yields and a lack of urban areas ([Tramblay et al., 2019](#)). The general downward trend found in our paper could be directly associated with the anomalies in the soil moisture around Poland as detected by [Piniewski et al. \(2020\)](#) and [Pińskwar et al. \(2020\)](#). Also, in their study on flood regime changes in Europe, [Hall et al. \(2014\)](#) reported a marked decrease in the number of observed flood events in the east of central Europe with a variation of floods over Poland. [Strupczewski et al. \(2001\)](#) found a decreasing number of flood events between the decades of 1920 and 1990, while [Kundzewicz et al. \(2012\)](#) mentioned an increase of the number of regional flood occurrences during 1946–2010. In addition, it is difficult to have direct comparison due to a lack of trend detection studies in flood frequency in Poland and the results are still debated due to the lack of large-scale evidence. Moreover, the frequency, as well as magnitude, of floods could vary due to different factors such as deforestation, river regulations, climate variations and land-use change for a specific area, which would have a direct effect on the occurrence of flood events ([Kundzewicz and Schellnhuber, 2004](#)). In fact, a recent finding of [Seneviratne et al. \(2021\)](#) at the Sixth Assessment Report of Climate Change 2021, showed that the changes in frequency and magnitude of fluvial floods are more complex, while pluvial floods are on the rise with increasing intense precipitation.

4.3. Trends in flood timing

The river basins in northern and central Poland showed a concentrated annual flood timing in February–April, while May–June was the period of average flood timing in the southern-most basins. This is in agreement with studies of flood timing in Europe based on observed data ([Blöschl et al., 2017](#); [Hall and Blöschl, 2018](#)). [Wasko et al. \(2020\)](#), who studied trends in flood timing based on daily streamflow data at global scale, showed an average flood timing in February–March for the eastern part of Germany and a limited part of western Poland (not fully included in the study), which coincides with our results as well. The flood timing between March–May could be linked with the North Atlantic Oscillation (NAO) and the snowmelt processes, determining the runoff generation in spring (March–May) due to the increasing winter temperature and changing precipitation pattern ([Kaczmarek, 2003](#)). Moreover, NAO, characterized by a quasi-cyclical change of atmospheric pressure in the Icelandic Low and the Azores High, influences the winter conditions over a large part of Europe ([Kaczmarek, 2003](#) and [Kundzewicz et al., 2019](#)).

Detected trends in annual flood timing exhibited considerable spatial variability. Only 10–11% of gauges showed statistical significance which is less than for flood magnitude and more than for flood frequency. The detected pattern of trends in annual Q_{MAX} timing partly agrees with the one identified by [Blöschl et al. \(2017\)](#) who studied flood timing in Europe using the European Flood Database of [Hall et al. \(2015\)](#). They detected two large clusters of increasing trends over north-western and south-eastern Poland. The north-western part of Poland, specifically the Lower Odra Basin and the northern part of the Notec Basin, coincide completely with the increasing trend (later occurrences) for the subset B and partially for the subset A. However, in our study the south-eastern region was characterized mostly by trends in the opposite direction, especially for the subset of gauges with higher data availability (1981–2019). The end year of gauge data in the study of [Blöschl et al. \(2017\)](#) was 2010, which may partly explain the different behavior, given that the decade of 2010 s was extremely warm in this region of Europe. [Blöschl et al. \(2017\)](#) also identified a strong trend of earlier flood timing in Lithuania, neighboring Poland in the northeast. In our case, the results are slightly different, because in the north-eastern Poland (e.g., the Narew and Pregolya basins) the pattern is mixed, but increasing trends slightly dominate.

Advances in timing of floods were found in the southern basins and the Lower Vistula Basin for the annual data and for winter half-years, where the increased river runoff in winter is associated with a positive NAO phase in this particular area of Poland and over the north and north-east Europe ([Wrzesiński, 2008](#); [Wrzesiński and Paluszkievicz, 2011](#) and [Kundzewicz et al., 2019](#)). Also, [Wrzesiński and Paluszkievicz \(2011\)](#) mentioned that after occurrence of a positive NAO phase in a warmer winter with less snow, meltwater floods are visibly lower. This trend is also associated with the general behavior of North-Eastern parts of Europe, with warming and spring incidence of snowmelt ([Blöschl et al., 2017](#); [Blöschl et al., 2019](#)). In addition, the floods in the lower Vistula Basin and the southern region of Poland have been associated with cyclones, which can move from the Mediterranean region to Central-Eastern Europe that generates high precipitation amounts in the area ([van Bebber, 1891](#); [Wyżga et al., 2016](#)). In fact, [Volosciuk et al. \(2016\)](#) and [Tabari and Willems \(2018\)](#) mentioned that factors from the Mediterranean Sea such as atmospheric moisture and evaporation can be associated to flood events in Central-Europe caused by intense precipitation in summer.

A global study of [Do et al. \(2020\)](#), investigating trends in the ordinal year of annual maximum streamflow, showed that prediction of flood timing in Central European region, including Poland, is associated with low confidence, which may partly explain the complex pattern of trends in this indicator in our study. Interestingly, they also showed that three out of five global hydroclimate zones intersect Poland, which confirms the complexity of flood generation mechanisms and resulting flood timing patterns across the country.

5. Concluding remarks

This study analyzed trends in magnitude, frequency and timing of river floods, over two periods (1956–2019 and 1981–2019) in Poland. The indices described annual maximum discharge and peak-over-threshold flow series. The use of both methods allowed for a better understanding of changes in river flood indicators. Comparison of two different subsets of flow gauges demonstrates stronger trends for the more abundant subset with shorter time series (1981–2019) than for the less abundant subset with longer time series (1956–2019).

Trends in magnitude of floods calculated for POT and Q_MAX series illustrate a visible spatial variability over the river basins of the country with an evident statistical significance, especially for the longer of two considered periods (1956–2019). A relatively strong downward pattern was found in the northeastern part of Poland for both subsets analyzed, while an increasing trend was obtained usually in the southern part of the country. Evidence for changes in frequency of river floods in Poland was weak. In contrast, a strong pattern of advanced river flood timing was found over southern Poland and an opposite trend in northeastern and northwestern Poland. All these changes, that were detected for recent years, may not necessarily continue in the future due to climate change and other factors. This leaves an opportunity to study the attribution of changes in river floods as well as their future projections as a next step.

In addition, the influence of climate variation on trend detection should be considered. Tabari and Willems (2018) and Tabari et al. (2020) stated that climate fluctuations occur on different times and scales over a region (e.g. in the rhythm of multi-decadal oscillations), which may impact the precipitation patterns that can turn into flood events. In this case, precipitation variability over Europe is influenced mainly by ocean-atmosphere circulation, especially, the North Atlantic Oscillation (NAO). Therefore, the complexity of interaction between oceans and atmosphere makes it difficult to detect the principal driving forces of the oscillations and their influence on the variation of floods over the region (Willems, 2013).

Finally, the observed changes in magnitude, frequency and timing of floods obtained in our research provide one of the first analyses of this under-studied topic in Poland. We show that the patterns are complex and not always consistent with previous research, which means that further studies are required. It is especially important to enrich the knowledge enhancing flood risk reduction in areas where flood events cause human and economic losses.

CRediT authorship contribution statement

Nelson Venegas-Cordero: Conceptualization, Investigation, Methodology, Data curation, Software, Validation, Formal analysis, Visualization, Writing – original draft, Writing – review & editing. **Zbigniew W. Kundzewicz:** Conceptualization, Writing – original draft, Writing – review & editing. **Shoaib Jamro:** Data curation, Software. **Mikołaj Piniewski:** Conceptualization, Investigation, Writing – original draft, Writing – review & editing, Supervision.

Declaration of Competing Interest

The authors declare that they have no known competing financial interests or personal relationships that could have appeared to influence the work reported in this paper.

Acknowledgements

The authors acknowledge the Institute of Meteorology and Water Management – National Research Institute (IMGW-PIB) for providing river flow data. Two anonymous referees provided insightful comments that helped improve the quality of the manuscript. This study was supported financially by the Warsaw University of Life Sciences (SGGW) Financial Support Mechanism for Researchers and Research Teams granted in 2021.

Appendix A. Supporting information

Supplementary data associated with this article can be found in the online version at [doi:10.1016/j.ejrh.2022.101098](https://doi.org/10.1016/j.ejrh.2022.101098).

References

- Alfieri, L., Burek, P., Feyen, L., Forzieri, G., 2015. Global warming increases the frequency of river floods in Europe. *Hydrol. Earth Syst. Sci.* 19 (5), 2247–2260.
- Berghuijs, W.R., Aalbers, E.E., Larsen, J.R., Trancoso, R., Woods, R.A., 2017. Recent changes in extreme floods across multiple continents. *Environ. Res. Lett.* 12 (11), 114035.
- Bertola, M., Viglione, A., Lun, D., Hall, J., Blöschl, G., 2020. Flood trends in Europe: are changes in small and big floods different? *Hydrol. Earth Syst. Sci.* 24 (4), 1805–1822.
- Błazejczyk, K., 2006. Climate and bioclimate of Poland. Natural and human environment of Poland. A geographical overview, Ed. M. Degórski Polish Academy of Sciences, Inst. of Geography and Spatial Organization Polish Geographical Society, p. 31–48.
- Blöschl, G., et al., 2017. Changing climate shifts timing of European floods. *Science* 357 (6351), 588–590.
- Blöschl, G., et al., 2019. Changing climate both increases and decreases European river floods. *Nature* 573 (7772), 108–111.

- Blöschl, G., Nester, T., Komma, J., Parajka, J., Perdigão, R.A., 2013. The June 2013 flood in the upper danube Basin, and comparisons with the 2002, 1954 and 1899 floods. *Hydrol. Earth Syst. Sci.* 17 (12), 5197–5212.
- Bryndal, T., Franczak, P., Krocak, R., Cabaj, W., Kolodziej, A., 2017. The impact of extreme rainfall and flash floods on the flood risk management process and geomorphological changes in small Carpathian catchments: a case study of the Kasiniczanka river (Outer Carpathians, Poland). *Nat. Haz.* 88 (1), 95–120.
- Burn, D.H., Whitfield, P.H., 2017. Changes in cold region flood regimes inferred from long-record reference gauging stations. *Water Res. Res.* 53 (4), 2643–2658.
- CRED (Centre for Research on the Epidemiology of Disasters), 2015. *The human cost of natural disasters: A global perspective*. Université Catholique de Louvain, Brussels: Centre for Research on the Epidemiology of Disasters.
- Cunnane, C., 1973. A particular comparison of annual maxima and partial duration series methods of flood frequency prediction. *J. Hydrol.* 18 (3–4), 257–271.
- Davison, A.C., Smith, R.L., 1990. Models for exceedances over high thresholds. *J. R. Statist. Soc. Series B Methodol.* 52 (3), 393–425.
- Do, H.X., Westra, S., Leonard, M., Gudmundsson, L., 2020. Global-scale prediction of flood timing using atmospheric reanalysis. *Water Res. Research* 56 (1) e2019WR024945.
- Duan, L., Cai, T., 2018. Changes in magnitude and timing of high flows in large rain-dominated watersheds in the cold region of north-eastern China. *Water* 10 (11), 1658.
- Estilow, T.W., Young, A.H., Robinson, D.A., 2015. A long-term Northern Hemisphere snow cover extent data record for climate studies and monitoring. *Earth System Science, Data* 7 (1), 137–142.
- Field, C.B., Barros, V., Stocker, T.F., Dahe, Q., 2012. Managing the risks of extreme events and disasters to advance climate change adaptation: special Report of the Intergovernmental Panel on Climate Change (IPCC). Cambridge University Press.
- Frei, C., Schär, C., 2001. Detection probability of trends in rare events: theory and application to heavy precipitation in the Alpine region. *J. Clim.* 14 (7), 1568–1584.
- Grygoruk, M., Kochanek, K., Mirosław-Świątek, D., 2021. Analysis of long-term changes in inundation characteristics of near-natural temperate riparian habitats in the Lower Basin of the Biebrza Valley, Poland. *J. Hydrol. Region. Stud.* 36, 100844.
- Gudmundsson, L., Leonard, M., Do, H.X., Westra, S., Seneviratne, S.I., 2019. Observed trends in global indicators of mean and extreme streamflow. *Geophys. Res. Lett.* 46 (2), 756–766.
- Gupta, D., Dhanya, C., 2020. The potential of GRACE in assessing the flood potential of Peninsular Indian River basins. *Int. J. Rem. Sens.* 41 (23), 9009–9038.
- Hall, J., et al., 2014. Understanding flood regime changes in Europe: a state-of-the-art assessment. *Hydrol. Earth Syst. Sci.* 18 (7), 2735–2772.
- Hall, J., Blöschl, G., 2018. Spatial patterns and characteristics of flood seasonality in Europe. *Hydrol. Earth Syst. Sci.* 22 (7), 3883–3901.
- Hall, J. et al., 2015. *A European Flood Database: facilitating comprehensive flood research beyond administrative boundaries*. Proceedings of the International Association of Hydrological Sciences, 370: 89–95.
- Hu, P., Zhang, Q., Shi, P., Chen, B., Fang, J., 2018. Flood-induced mortality across the globe: spatiotemporal pattern and influencing factors. *Sci. Total Environ.* 643, 171–182.
- Jonkman, S.N., 2005. Global perspectives on loss of human life caused by floods. *Nat. Hazards* 34 (2), 151–175.
- Kaczmarek, Z., 2003. The impact of climate variability on flood risk in Poland. *Risk Anal.* 23 (3), 559–566.
- Kemter, M., Merz, B., Marwan, N., Vorogushyn, S. and Blöschl, G., 2020. Joint Trends in Flood Magnitudes and Spatial Extents across Europe. *Geophysical Research Letters*, 47(7): e2020GL087464.
- F. Kreienkamp et al. Rapid attribution of heavy rainfall events leading to the severe flooding in Western Europe during July 2021. *World Weather Attribution*.
- Kumar, M., Sharif, M., Ahmed, S., 2020. Flood estimation at Hathnikund Barrage, river Yamuna, India using the peak-over-threshold method. *ISH J. Hydraulic Engineering* 26 (3), 291–300.
- Kundzewicz, Z., Kowalczak, P., 2014. Urban flooding and sustainable land management—polish perspective. *Problemy ekorozwoju—problems of sustainable development*, 9 (2), 131–138.
- Kundzewicz, Z.W., Ulbrich, U., Graczyk, D., Krüger, A., Leckebusch, G.C., Menzel, L., Pińskwar, I., Radziejewski, M., Szwed, M., 2005. Summer floods in central europe – climate change track? *Nat. Hazards* 36 (1), 165–189.
- Kundzewicz, Z.W., Kanae, S., Seneviratne, S.I., Handmer, J., Nicholls, N., Peduzzi, P., Mechler, R., Bouwer, L.M., Arnell, N., Mach, K., Muir-Wood, R., 2014a. Flood risk and climate change: global and regional perspectives. *Hydrol. Sci. J.* 59 (1), 1–28.
- Kundzewicz, Z.W., Stoffel, M., Kaczka, R.J., Wyżga, B., Niedźwiedz, T., Pińskwar, I., Ruiz-Villanueva, V., Łupikasza, E., Czajka, B., Ballesteros-Canovas, J.A., Malarzewski, L., 2014b. Floods at the northern foothills of the Tatra Mountains—a Polish-Swiss research project. *Acta Geophys.* 62 (3), 620–641.
- Kundzewicz, Z.W., Matczak, P., 2012. Climate change regional review: Poland. *Wiley Interdisciplinary Reviews: Climate Change* 3 (4), 297–311.
- Kundzewicz, Z.W., Robson, A.J., 2004. Change detection in hydrological records—a review of the methodology. *Hydrol. Sci. J.* 49 (1), 7–19.
- Kundzewicz, Z.W., Schellnhuber, H.J., 2004. Floods in the IPCC TAR perspective. *Nat. Hazards* 31 (1), 111–128.
- Kundzewicz, Z.W., Pińskwar, I., Brakenridge, G.R., 2018. Changes in river flood hazard in Europe: a review. *Hydrol. Res.* 49 (2), 294–302.
- Kundzewicz, Z.W., Szwed, M., Pińskwar, I., 2019. Climate variability and floods—a global review. *Water* 11 (7), 1399.
- Kundzewicz, Z. W., Dobrowolski, A., Lorenc, H., Niedźwiedz, T., Pińskwar, I., and Kowalczak, P., 2012. *Floods in Poland*. W: Kundzewicz, Z. W. (ed.) *Changes in Flood Risk in Europe*, Special Publication No. 10, IAHS Press, Wallingford, Oxfordshire, UK, Ch. 17, 319–334.
- Macdonald, N., Phillips, I.D., Mayle, G., 2010. Spatial and temporal variability of flood seasonality in Wales. *Hydrol. Process.* 24 (13), 1806–1820.
- Madsen, H., Rasmussen, P.F., Rosbjerg, D., 1997. Comparison of annual maximum series and partial duration series methods for modeling extreme hydrologic events: 1. At-site Modeling. *Water Resources Research* 33 (4), 747–757.
- Madsen, H., Lawrence, D., Lang, M., Martinkova, M., Kjeldsen, T.R., 2014. Review of trend analysis and climate change projections of extreme precipitation and floods in Europe. *J. Hydrol.* 519, 3634–3650.
- Mallakpour, I., Villarini, G., 2015. The changing nature of flooding across the central United States. *Nat. Clim. Change* 5 (3), 250–254.
- Mangini, W., et al., 2018. Detection of trends in magnitude and frequency of flood peaks across Europe. *Hydrol. Sci. J.* 63 (4), 493–512.
- Masseroni, D., et al., 2021. The 63-year changes in annual streamflow volumes across Europe with a focus on the Mediterranean basin. *Hydrol. Earth Syst. Sci.* 25 (10), 5589–5601.
- Mediero, L., Santillán, D., Garrote, L., Granados, A., 2014. Detection and attribution of trends in magnitude, frequency and timing of floods in Spain. *J. Hydrol.* 517, 1072–1088.
- Mediero, L., Kjeldsen, T.R., Macdonald, N., Kohnova, S., Merz, B., Vorogushyn, S., Wilson, D., Alburquerque, T., Blöschl, G., Bogdanowicz, E., Castellarin, A., 2015. Identification of coherent flood regions across Europe by using the longest streamflow records. *J. Hydrol.* 528, 341–360.
- Mostofi Zadeh, S., Burn, D.H., O'Brien, N., 2020. Detection of trends in flood magnitude and frequency in Canada. *J. Hydrol. Region. Stud.* 28, 100673.
- Mudelsee, M., Börngen, M., Tetzlaff, G., Grinewald, U., 2003. No upward trends in the occurrence of extreme floods in central Europe. *Nature* 425 (6954), 166–169.
- Petrow, T., Merz, B., 2009. Trends in flood magnitude, frequency and seasonality in Germany in the period 1951–2002. *J. Hydrol.* 371 (1–4), 129–141.
- Piniewski, M., et al., 2020. Model-based reconstruction and projections of soil moisture anomalies and crop losses in Poland. *Theor Appl Climatol* 140 (691–708), 2020. <https://doi.org/10.1007/s00704-020-03106-6>.
- Piniewski, M., Marcinkowski, P., Kundzewicz, Z.W., 2018. Trend detection in river flow indices in Poland. *Acta Geophysica* 66 (3), 347–360.
- Pińskwar, I., Choryński, A., Kundzewicz, Z.W., 2020. Severe drought in the spring of 2020 in Poland—more of the same? *Agronomy* 10 (11), 1646.
- Poff, N.L., et al., 1997. The natural flow regime. *BioScience* 47 (11), 769–784.
- Richter, B.D., Baumgartner, J.V., Powell, J., Braun, D.P., 1996. A method for assessing hydrologic alteration within ecosystems. *Conservation Biology* 10 (4), 1163–1174.
- Ruiz-Villanueva, V., et al., 2016. Decadal variability of floods in the northern foreland of the Tatra mountains. *Regional Environ. Change* 16 (3), 603–615.
- Schröter, K., Kunz, M., Elmer, F., Mühr, B., Merz, B., 2015. What made the June 2013 flood in Germany an exceptional event? a hydro-meteorological evaluation. *Hydrology and Earth System Sciences* 19 (1), 309–327.
- Sen, P.K., 1968. Estimates of the regression coefficient based on Kendall's tau. *J. Am. Stat. Assoc.* 63 (324), 1379–1389.

- Seneviratne, S. I., Zhang, X., Adnan, M., et al., 2021. Weather and Climate Extreme Events in a Changing Climate. In: *Climate Change 2021: The Physical Science Basis. Contribution of Working Group I to the Sixth Assessment Report of the Intergovernmental Panel on Climate Change* [Masson-Delmotte, V., P. Zhai, A. Pirani, S. L. et al. (eds.)]. Cambridge University Press.
- Slater, L., et al., 2021. Global changes in 20-Year, 50-Year, and 100-Year River floods. *Geophysical Research Letters* 48 (6) e2020GL091824.
- Stahl, K., et al., 2010. Streamflow trends in Europe: evidence from a dataset of near-natural catchments. *Hydrol. Earth System Sci.* 14 (12), 2367–2382.
- Stahl, K., Tallaksen, L.M., Hannaford, J., Van Lanen, H., 2012. Filling the white space on maps of European runoff trends: estimates from a multi-model ensemble. *Hydrol. Earth Syst. Sci.* 16 (7), 2035–2047.
- Strupczewski, W., Singh, V., Mitosek, H., 2001. Non-stationary approach to at-site flood frequency modelling. III. Flood Analysis of Polish Rivers. *J. Hydrol.* 248 (1–4), 152–167.
- Szwed, M., Pińskwar, I., Kundzewicz, Z.W., Graczyk, D., Mezghani, A., 2017. Changes of snow cover in Poland. *Acta Geophysica* 65 (1), 65–76.
- Tabari, H., Willems, P., 2018. Lagged influence of Atlantic and Pacific climate patterns on European extreme precipitation. *Sci. Rep.* 8 (1), 1–10.
- Tabari, H., Madani, K., Willems, P., 2020. The contribution of anthropogenic influence to more anomalous extreme precipitation in Europe. *Environ. Res. Lett.* 15 (10), 104077.
- Tramblay, Y., Mimeau, L., Neppel, L., Vinet, F., Sauquet, E., 2019. Detection and attribution of flood trends in Mediterranean basins. *Hydrol. Earth Syst. Sci.* 23 (11), 4419–4431.
- van Bebber, J.W., 1891. Die Zugstraßen der barometrischen Minima. (The tracks of the barometric minima.). *Meteor. Zeitschr.* 8, 361–366.
- Villarini, G., Smith, J.A., Ntelekos, A.A., Schwarz, U., 2011a. Annual maximum and peaks-over-threshold analyses of daily rainfall accumulations for Austria. *J. Geophys. Res. Atmos.* 116 (D5).
- Villarini, G., Smith, J.A., Serinaldi, F., Ntelekos, A.A., 2011b. Analyses of seasonal and annual maximum daily discharge records for central Europe. *J. Hydrol.* 399 (3), 299–312.
- Volosciuk, C., Maraun, D., Semenov, V.A., Tilinina, N., Gulev, S.K., Latif, M., 2016. Rising Mediterranean Sea surface temperatures amplify extreme summer precipitation in Central Europe. *Sci. Rep.* 6 (1), 1–7.
- Vommoor, K., Lawrence, D., Schlichting, L., Wilson, D., Wong, W.K., 2016. Evidence for changes in the magnitude and frequency of observed rainfall vs. snowmelt driven floods in Norway. *J. Hydrol.* 538, 33–48.
- Ward, P.J., et al., 2018. Dependence between high sea-level and high river discharge increases flood hazard in global deltas and estuaries. *Environ. Res. Lett.* 13 (8), 084012.
- Wasko, C., Nathan, R., Peel, M.C., 2020. Trends in global flood and streamflow timing based on local water Year. *Water Res. Res.* 56 (8) e2020WR027233.
- Willems, P., 2013. Multidecadal oscillatory behaviour of rainfall extremes in Europe. *Climatic Change* 120 (4), 931–944.
- Wrzesiński, D., Pałuszkiewicz, R., 2011. Spatial differences in the impact of the North Atlantic oscillation on the flow of rivers in Europe. *Hydrol. Res.* 42 (1), 30–39.
- Wrzesiński, D., 2008. Impact of the North Atlantic Oscillation on river runoff in Poland, IWRA 13th World Water Congress Montpellier, France, 1–4 September 2008.
- Wyżga, B., Kundzewicz, Z.W., Ruiz-Villanueva, V. and Zawiejska, J., 2016. Flood Generation Mechanisms and Changes in Principal Drivers. In: Z.W. Kundzewicz, M. Stoffel, T. Niedźwiedz and B. Wyżga (Editors), *Flood Risk in the Upper Vistula Basin*. Springer International Publishing, Cham, pp. 55–75.
- Zhang, M., Wei, X., 2014. Alteration of flow regimes caused by large-scale forest disturbance: a case study from a large watershed in the interior of British Columbia. *Can. Ecohydrol.* 7 (2), 544–556.
- Zhang, X., et al., 2021. The detection of flood characteristics alteration induced by the danjiangkou reservoir at Han River, China. *Water* 13 (4), 496.

Co-author statements - Article 1

Appendix no. 2 – co-authorship statement

Warsaw, 01-04-2024

Nelson Enrique Venegas Cordero
nelson_venegas@sggw.edu.pl

Department of Hydrology, Meteorology
and Water Management, Warsaw
University of Life Sciences

Co-authorship statement

I hereby represent that in the article: Detection of trends in observed river floods in Poland. Authors: Nelson Venegas-Cordero, Zbigniew W. Kundzewicz, Shoaib Jamro, and Mikołaj Piniewski. Journal of Hydrology: Regional Studies, Volume 41, June 2022, 101098, my individual contribution in the development thereof involved: Conceptualization, Investigation, Methodology, Data curation, Software, Validation, Formal analysis, Visualization, Writing – original draft, Writing – review & editing.



Nelson Enrique Venegas Cordero

Appendix no. 2 – co-authorship statement

Poznań, 01-04-2024

Zbigniew W. Kundzewicz
kundzewicz@yahoo.com

**Meteorology Lab, Department of
Construction and Geoengineering,
Faculty of Environmental
Engineering and Mechanical
Engineering, Poznań University of
Life Sciences, Poznań, Poland**

Co-authorship statement

I hereby represent that in the article: Detection of trends in observed river floods in Poland. Authors: Nelson Venegas-Cordero, Zbigniew W. Kundzewicz, Shoaib Jamro, and Mikołaj Piniewski. Journal of Hydrology: Regional Studies, Volume 41, June 2022, 101098], my individual contribution in the development thereof involved: Conceptualization, Writing – original draft, Writing – review & editing.



Zbigniew W. Kundzewicz

Appendix no. 2 – co-authorship statement

Bridgwater, 01-04-2024

Shoaib Jamro
shoaib@balanced-energy.co.uk

**Balance Energy Ltd, Bridgwater,
Somerset, TA6 3DT**

Co-authorship statement

I hereby represent that in the article: Detection of trends in observed river floods in Poland. Authors: Nelson Venegas-Cordero, Zbigniew W. Kundzewicz, Shoaib Jamro, and Mikołaj Piniewski. Journal of Hydrology: Regional Studies, Volume 41, June 2022, 101098, my individual contribution in the development thereof involved: Data curation and Software.



Shoaib Jamro

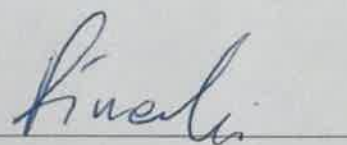
Appendix no. 2 – co-authorship statement

Warsaw, 01-04-2024

Mikołaj Piniewski
Department of Hydrology, Meteorology and Water Management,
Warsaw University of Life Sciences
mikolaj_piniewski@sggw.edu.pl

Co-authorship statement

I hereby represent that in the article: Detection of trends in observed river floods in Poland. Authors: Nelson Venegas-Cordero, Zbigniew W. Kundzewicz, Shoaib Jamro, and Mikołaj Piniewski. Journal of Hydrology: Regional Studies, Volume 41, June 2022, 101098, my individual contribution in the development thereof involved: Conceptualization, Investigation, Writing – original draft, Writing – review & editing, Supervision.

A handwritten signature in dark ink, appearing to read 'Piniewski', is written over a horizontal line.

Mikołaj Piniewski

Annex 2: Model-based assessment of flood generation mechanisms over Poland: The roles of precipitation, snowmelt, and soil moisture excess. *Science of the Total Environment*, 891, 164626 (IF = 9.8). <https://doi.org/10.1016/j.scitotenv.2023.164626>



Model-based assessment of flood generation mechanisms over Poland: The roles of precipitation, snowmelt, and soil moisture excess

Nelson Venegas-Cordero^a, Cyrine Cherrat^b, Zbigniew W. Kundzewicz^c, Jitendra Singh^d, Mikołaj Piniewski^{a,*}

^a Department of Hydrology, Meteorology and Water Management, Warsaw University of Life Sciences, Nowoursynowska 166, 02-787 Warsaw, Poland

^b Department of Bioresource Engineering, Faculty of Agricultural and Environmental Sciences, McGill University, Montreal, QC, Canada

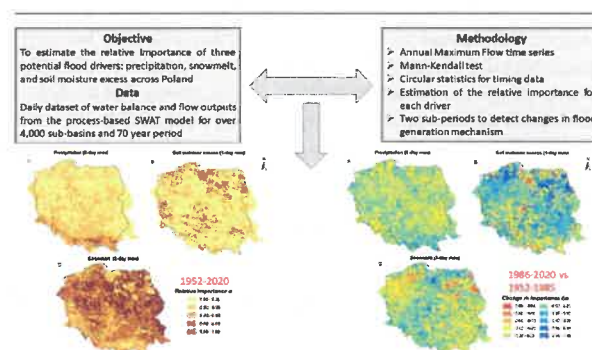
^c Meteorology Lab, Department of Construction and Geoenvironment, Faculty of Environmental Engineering and Mechanical Engineering, Poznań University of Life Sciences, Poznań, Poland

^d Institute for Atmospheric and Climate Science, ETH Zürich, Universitätsstrasse 16, 8092, Zürich, Switzerland

HIGHLIGHTS

- We used a process-based model to explain flood-generating mechanisms for over 4,000 sub-basins in Poland.
- Snowmelt is the primary cause of flooding throughout the country.
- Soil moisture excess gained importance as a flood driver in large parts of northern Poland after 1986.

GRAPHICAL ABSTRACT



ARTICLE INFO

Editor: Fernando A.L. Pacheco

Keywords:

Flood mechanisms
Trend
Timing
Relative importance
Poland

ABSTRACT

Hydrometeorological variability, such as changes in extreme precipitation, snowmelt, or soil moisture excess, in Poland can lead to fluvial flooding. In this study we employed the dataset covering components of the water balance with a daily time step at the sub-basin level over the country for 1952–2020. The data set was derived from the previously calibrated and validated Soil & Water Assessment Tool (SWAT) model for over 4000 sub-basins. We applied the Mann Kendall test and circular statistics-based approach on annual maximum floods and various potential flood drivers to estimate the trend, seasonality, and relative importance of each driver. In addition, two sub-periods (1952–1985 and 1986–2020) were considered to examine changes in flood mechanism in the recent decades. We show that floods in the northeast Poland were decreasing, while in the south the trend showed a positive behavior. Moreover, the snowmelt is a primary driver of flooding across the country, followed by soil moisture excess and precipitation. The latter seemed to be the dominant driver only in a small, mountain-dominated region in the south. Soil moisture excess gained importance mainly in the northern part, suggesting that the spatial pattern of flood generation mechanisms is also governed by other features. We also found a strong signal of climate change in large parts of northern Poland, where snowmelt is losing importance in the second sub-period in favor of soil moisture excess, which can be explained by the temperature warming and diminishing role of snow processes.

Abbreviations: Q_{max} , Annual maximum daily discharge; PCP_{max} , Annual maximum 3-day precipitation; SN_{max} , Annual maximum 3-day snowmelt; SME_{max} , Annual maximum soil moisture excess.

* Corresponding author.

E-mail addresses: nelson_venegas@sggw.edu.pl (N. Venegas-Cordero), cyrine.cherrat@mail.mcgill.ca (C. Cherrat), jitendra.singh@env.ethz.ch (J. Singh), mikolaj_piniewski@sggw.edu.pl (M. Piniewski).

<http://dx.doi.org/10.1016/j.scitotenv.2023.164626>

Received 23 March 2023; Received in revised form 26 May 2023; Accepted 31 May 2023

Available online 5 June 2023

0048-9697/© 2023 The Authors. Published by Elsevier B.V. This is an open access article under the CC BY license (<http://creativecommons.org/licenses/by/4.0/>).

1. Introduction

Floods, as hydroclimate-related disasters, result in major economic and human losses, and their severity, frequency and exposure are increasing in many countries of the world (Blöschl et al., 2017; Dottori et al., 2018; Fang et al., 2022; Kundzewicz et al., 2014a; Merz et al., 2021; Tellman et al., 2021; Trambly et al., 2022). In recent decades, destructive floods have occurred on rivers across all continents besides Antarctica (Kundzewicz et al., 2014a; Kundzewicz et al., 2019; Venegas-Cordero et al., 2022). These events have attracted the attention of researchers attempting to understand their dynamics and potential causes. In this paper, the term “flood” follows the definition of the annual maximum flow (AMF) adopted by many scientific papers on flood trend detection (Berghuijs et al., 2019; Bertola et al., 2021; Blöschl et al., 2019; Mediero et al., 2014; Kemter et al., 2023; Singh et al., 2021; Venegas-Cordero et al., 2022).

In Central and Eastern Europe, great historic floods have occurred on the trans-national rivers Oder (1997) and Elbe (2002), each causing numerous fatalities and billions of euros in material damage (Kundzewicz et al., 1999; Ulbrich et al., 2003; Kundzewicz et al., 2013). Recently, devastating floods hit western Germany, Belgium, and the Netherlands triggering extensive infrastructure damage and causing over two hundred casualties in July 2021 (Koks et al., 2021; Kreienkamp et al., 2021). All these floods were caused by intense and long-lasting precipitation in the summer time. As these and other flood events have exceeded past recorded levels, there is a robust physical argument for an intensification of the global hydrological cycle, increasing the intensity and frequency of extreme weather events including floods and droughts (Blöschl et al., 2017; Blöschl et al., 2019; Hall et al., 2014; IPCC, 2013). In Poland, climate change is expected to cause a significant increase in the frequency and intensity of extreme precipitation, leading to pluvial and fluvial floods (Kundzewicz and Pińskwar, 2022).

In recent years, different techniques, such as hydrological model simulations and machine learning approaches have been used in different flood analyses worldwide (e.g. Arheimer and Lindström, 2015; Bevacqua et al., 2020; Brunner et al., 2021; Ekwueme, 2022; El Kasri et al., 2021; Jiang et al., 2022a, 2022b; Tarasova et al., 2023). Moreover, research efforts have been carried out to gain a better understanding of existing trends in the magnitude, frequency, and seasonality of such events, as well as their potential physical drivers (Bertola et al., 2020; Bertola et al., 2021; Blöschl et al., 2019; Do et al., 2020a, 2020b; Fang et al., 2022; Jiang et al., 2022a, 2022b; Singh et al., 2021; Stein et al., 2021; Venegas-Cordero et al., 2022; Wasko and Nathan, 2019). These studies suggest that floods are influenced by various factors such as precipitation, temperature patterns, drainage basin features, snow and ice cover, or soil conditions (e.g., permeability, moisture content), which typically intervene collectively to trigger floods (Bates et al., 2008; Berghuijs et al., 2019; Kundzewicz et al., 2014a). Broadly, the flood-generating mechanisms can be explained as causal classifications of flood events based on hydrometeorological variables or catchment conditions (e.g. precipitation, soil moisture, snow depth) leading to floods (Tarasova et al., 2019; Trambly et al., 2022).

A few notable studies have recently examined the seasonality of floods and their responsible drivers in different world regions. For example, Singh et al. (2021) studied the timing of floods based on annual maximum streamflow in Canada and used circular statistics to identify the main driver of these events across the country. The results demonstrate a clear influence of snowmelt extremes on floods in the Eastern part of Canada, while an increase in extreme precipitation primarily causes floods in Western Canada. Berghuijs et al. (2019) in a pan-European study incorporated the relative importance of three flood-driving indices (i.e., soil moisture excess, precipitation, snowmelt). They demonstrate that soil moisture excess is the largest driver of floods in most European watersheds during 1960–2010. Furthermore, snowmelt was found to be a significant contributor to floods, particularly in Northern and Eastern Europe, including the majority of Poland. However, climatic change is predicted to contribute to an increase in flood incidence at the global scale, and to possible shifts in the relative importance of flood-generating mechanisms, making the awareness of such processes crucial to implement more effective flood management

strategies, mitigation measures and early warning systems (Arnell and Gosling, 2016; Berghuijs et al., 2019; Kendon et al., 2014; Winsemius et al., 2016). Research has demonstrated that many influencing factors of streamflow can reinforce or compensate for one another. As a result, temporal changes in streamflow (and therefore, flood magnitudes) are characterized by unsteady and mixed patterns at various geographical scales, which complicates the detection of magnitude trends (Piniewski et al., 2018). In addition, the behavior of hydrological mechanisms that give rise to floods is complex, spatially heterogeneous, and insufficiently investigated in flood studies. Together, these issues increase the uncertainty in both flood trends detection and flood forecasting, particularly in changing climate (Kundzewicz et al., 2014a; Berghuijs et al., 2019). Moreover, evidence of climate change is easier to detect in certain climatic variables (e.g., temperature) than in others (e.g., precipitation), further complicating a clear understanding of flood-causing processes (Piniewski et al., 2018). These issues are particularly relevant to Central Europe and Poland, as the region is located in a transition zone between Northern and Southern Europe that are projected to become wetter or drier, respectively, over the next decades (Russo et al., 2013). Trends in precipitation extremes are therefore generally uncertain and unsteady in Central Europe (Kjellström et al., 2018; Milly et al., 2008; Pińskwar, 2022).

On top of these issues, the geographical scope of quantitative flood investigations at a regional or national scale is limited, hindering a systematic mapping of dominant flood-causing mechanisms. Although such approaches have been taken for areas like the United States or Sweden, many countries have yet to be included in these assessments (Arheimer and Lindström, 2015; Berghuijs et al., 2019; Berghuijs et al., 2016). Studies also report that analyses are often methodologically inconsistent (due to e.g., lack of data uniformity, unharmonized time periods), making comparisons difficult to implement (Hall et al., 2014; Mangini et al., 2018). With regard to Poland, flood trend detection studies are generally restricted to single watersheds or small regions, and rarely encompass post-2010 data (e.g., Kundzewicz et al., 2013; Ruiz-Villanueva et al., 2016; Somorowska, 2017), although a few studies offer a more systematic assessment of trends in flow indices (e.g., Piniewski et al., 2018; Venegas-Cordero et al., 2022). In recent years, as reported by Venegas-Cordero et al. (2022) global and European flood trend studies have partially or completely left Poland out of the analyses or used data up to 2010 (e.g., Blöschl et al., 2017; Blöschl et al., 2019; Berghuijs et al., 2019; Bertola et al., 2020; Hundedcha et al., 2020; Mangini et al., 2018; Stein et al., 2020). This lack of comprehensive studies can be attributed to restricted access to hydrological data at the national scale, coupled with a scarcity of English language publications (Kundzewicz et al., 2017; Piniewski et al., 2018).

The main objective of this study is to investigate the spatio-temporal variability and relationships between floods and three flood generation mechanisms (extreme precipitation, snowmelt and soil moisture excess) over Poland. The specific objectives are to: (1) detect long-term trends in floods and flood mechanisms (drivers) over Poland; (2) determine the seasonality of floods and flood drivers over Poland; (3) assess correlation between particular flood drivers and floods as well as their joint temporal evolution for selected, geographically distinct regions; (4) investigate the relative importance of flood mechanisms and their long-term changes over Poland. This is, to our knowledge, the first study of this kind, providing a broad perspective on flood generation mechanisms for a country in central Europe. The novelty lies also in the use of a high-resolution process-based SWAT model outputs for the period 1951–2020, which allowed for a reliable consideration of snowmelt and soil moisture excess.

2. Data and methodology

2.1. Study area

This research was carried out for a large set of sub-basins (4381) distributed across Poland (~312,000 km²) and neighboring countries such as Ukraine, Belarus, the Czech Republic, Germany, Slovakia and Russia (~37,000 km²), which together enclose eight river basins (Fig. 1) draining

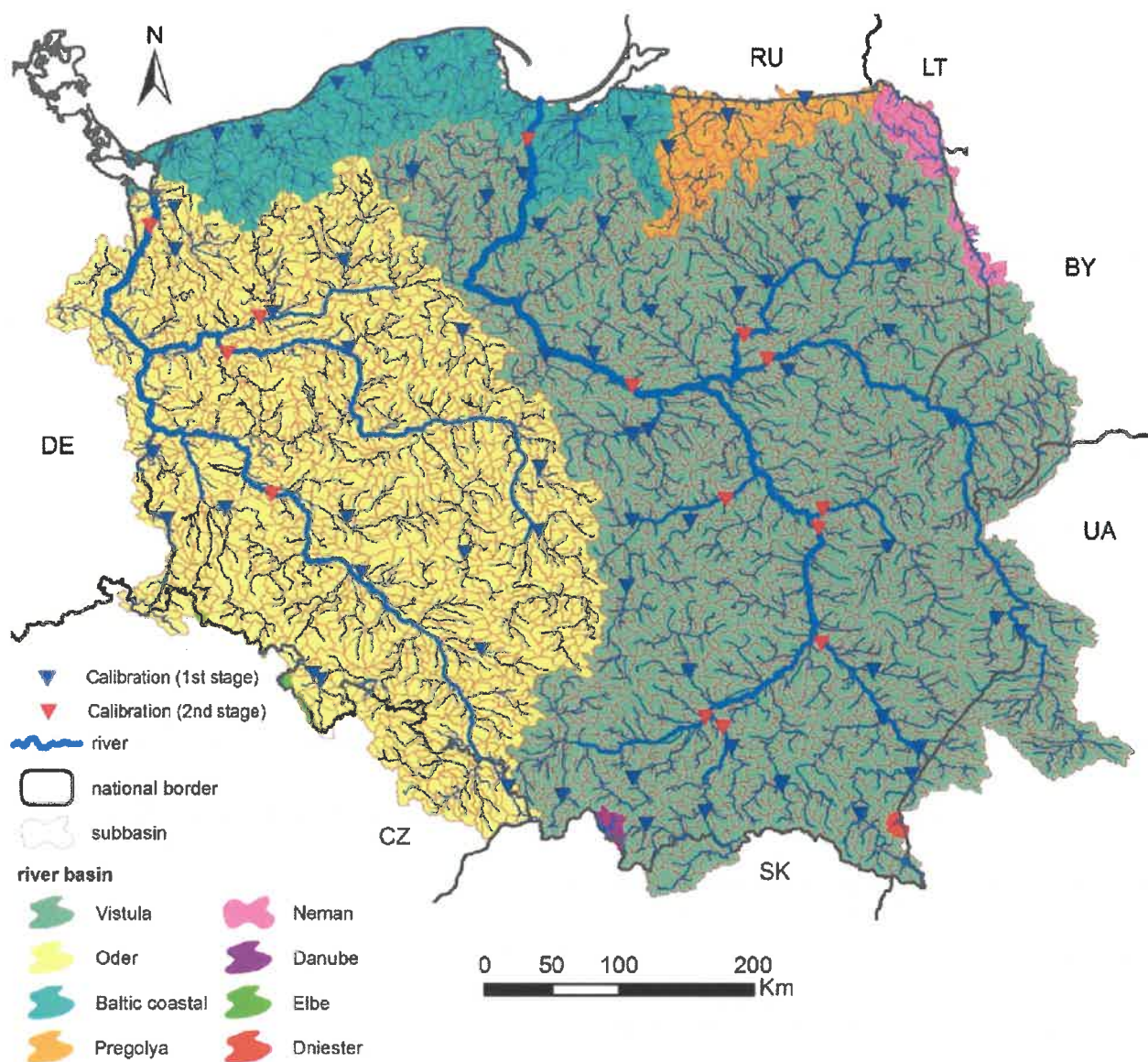


Fig. 1. Study area adopted from Marcinkowski et al. (2022).

their waters into the Baltic, Black and North Seas (Marcinkowski et al., 2022).

Poland is located in a transitional warm temperate climatic zone, characterized by air masses originating from the Atlantic Ocean and Eurasian land (Blażejczyk, 2006; Venegas-Cordero et al., 2022). The maximum annual total precipitation occurs in the southern and mountainous with values of 700–1100 mm/year and more in the mountains, while the northern and central region receive approximately 500–700 mm/year (Kundzewicz and Matczak, 2012). In addition, the mean annual temperature varies according to a spatial gradient, from around 10 °C in the southwest, to 6 °C in the northeast, while values below 0 °C are recorded in the highest mountains located in the south of the country (Blażejczyk, 2006; Venegas-Cordero et al., 2022).

2.2. Data

In this study we used daily discharge and water balance time series derived from a process-based model, a set of simulated water balance data (PL-SWAT-51_20, (Marcinkowski et al., 2022)). Simulations were made using the semi-distributed, process-based hydrological model SWAT, i.e.

Soil and Water Assessment Tool (Arnold et al., 1998) forced with the G2DC-PL + gridded climate dataset (Piniewski et al., 2021). The data considered in this study covers 70 years, between 1951 and 2020. The average size of the basic calculation units (4381 sub-basins) is 80 km² (Marcinkowski et al., 2022). Of particular interest in this study are four variables: precipitation [mm/day], snowmelt [mm/day], soil moisture content [mm] and water yield [mm/day]. While precipitation is the SWAT input, three other variables are SWAT outputs.

Snow processes in SWAT include snowfall, snow cover formation and snowmelt. A user-defined temperature threshold allows to partition precipitation into rain or snow. The snow cover component allows non-uniform cover due to shading, drifting, topography and land cover. Snowmelt is controlled by user-defined melt temperature, melt rate and areal snow cover distribution.

SWAT takes these processes related to soil water into account: infiltration, redistribution, lateral flow, soil evaporation, plant uptake and transpiration and percolation. Infiltration is modelled indirectly as a difference between precipitation and surface runoff. The initial rate of infiltration depends on the prior soil moisture conditions. The redistribution component in SWAT uses a storage routing technique to simulate flow in each layer

of the root zone. Percolation occurs when the underlying layer is not saturated, and the field capacity of a soil layer is exceeded. The saturated conductivity of the soil layer governs the downward flow rate.

Water yield is the total of surface runoff, lateral flow and baseflow. It represents the amount of water generated within sub-basin boundaries and reaching the channel on a given day. It is thus almost equivalent to discharge, but it is not affected by flow routing in channel network. Since water yield for each sub-basin can be directly transformed into discharge (a more common term), we will use the latter term throughout the study. The readers can find more details about the PL+ SWAT model hydrology data set in Marcinkowski et al. (2022) and Piniewski et al. (2021), and more details about the theoretical background of SWAT in Arnold et al. (1998) and Neitsch et al. (2011).

2.3. Flood mechanisms

This study considers three main factors that can lead to annual maximum flows (Berghuijs et al., 2019; Berghuijs et al., 2016; Bertola et al., 2021; Singh et al., 2021): extreme precipitation, snowmelt and soil moisture excess. The corresponding indices are compiled in Table 1. The annual maximum values of each variable are extracted for hydrological years (in Poland it is assumed as 1 November – 30 October). Using hydrological instead of calendar years better reflects the timing of snow cover development in the climate conditions of Poland and allows for accounting snowfall and snowmelt to the same year.

The variable SME_{max} was selected based on the fact that the soil moisture by itself does not drive flood events. Instead, the concurrence of heavy precipitation with high antecedent soil moisture can engender floods (Berghuijs et al., 2019). The daily soil moisture excess was calculated by the following equation:

$$SME = P - (SM_{max} - SM) \quad (1)$$

where SME is the soil moisture excess, P represents the daily precipitation in each sub-basin, SM_{max} is the soil moisture storage capacity, which we fixed at 125 mm as Berghuijs et al. (2019), and SM is the daily soil moisture amount in a hydrological year per sub-basin (a direct SWAT output).

2.4. Trend analysis

Trend detection for studied variables was performed using a rank-based non-parametric approach, namely the Mann-Kendall (MK) test with Sen's slope (Kendall, 1975; Mann, 1945; Sen, 1968). The MK test is designed to identify the presence of monotonic upward or downward trend, and is commonly employed in hydrometeorological data analysis (e.g., trend detection in precipitation, streamflow, flood timing) (Mediero et al., 2014; Blöschl et al., 2017; Mangini et al., 2018; Serinaldi et al., 2018; Blöschl et al., 2019; Wang et al., 2020). Sen's slope refers to the median slope between all ordered pairs of observations for a given time series. These two methods were chosen for trend estimation due to their robustness against outliers and non-normally distributed measurements (Hamed and Rao, 1998; Piniewski et al., 2018; Wang et al., 2020). The non-parametric approaches help circumvent the assumptions associated with parametric methods (e.g., Spearman correlation, linear regression). Choosing a non-parametric method can thus be especially useful in the context of a changing climate, given that hydroclimatic variables may lack stationarity and be

incompatible with certain statistical assumptions (Piniewski et al., 2018; Singh et al., 2021).

This approach was used to detect trends based on our set of indices, namely Q_{max} , PCP_{max} , SN_{max} , and SME_{max} . Moreover, the significance level of the MK test was set at 10 % ($\alpha = 0.1$), in accordance with similar flood-related studies (Blöschl et al., 2017; Blöschl et al., 2019; Do et al., 2020a, 2020b; Venegas-Cordero et al., 2022). Prior to applying the MK test to the variables of choice, a standardization procedure was applied whereby the values of interest (i.e., annual maximum or 3-day maximum values) were divided by the mean value for the given time series in each sub-basin. This enabled to analyze spatial variability of trend slopes more objectively.

In this study, the MK test is based on the following equations as shown in Venegas-Cordero et al. (2022):

$$S = \sum_{i=1}^{n-1} \sum_{j=1+i}^n \text{sgn}(X_j - X_i) \quad (2)$$

$$\text{sgn}(X_j - X_i) = \begin{cases} 1 & \text{if } (X_j - X_i) > 0 \\ 0 & \text{if } (X_j - X_i) = 0 \\ -1 & \text{if } (X_j - X_i) < 0 \end{cases} \quad (3)$$

where X_j and X_i are the values sorted by data sequence and n is the length of the data set.

2.5. Timing of floods and flood drivers

Here, we use circular statistics to examine the mean seasonality of Q_{max} , PCP_{max} , SN_{max} and SME_{max} events across the study area. The mean seasonality approach involves converting the dates of events (Q_{max} , PCP_{max} , etc.) into an angular value (Berghuijs et al., 2019; Blöschl et al., 2017; Do et al., 2020a, 2020b; Fang et al., 2022; Singh et al., 2021; Venegas-Cordero et al., 2022; Wasko et al., 2020a, 2020b). The mean seasonality is implemented from Singh et al. (2021) and Venegas-Cordero et al. (2022):

$$\varnothing_{ij} = DF_{ij} \frac{2\pi}{J_d} \quad (4)$$

$$\varnothing_j = \tan^{-1} \frac{\bar{y}}{\bar{x}}; \text{when } \bar{x} > 0, \bar{y} > 0 \quad (5a)$$

$$\varnothing_j = \tan^{-1} \frac{\bar{y}}{\bar{x}} + \pi; \text{when } \bar{x} < 0 \quad (5b)$$

$$\varnothing_j = \tan^{-1} \frac{\bar{y}}{\bar{x}} + 2\pi; \text{when } \bar{x} > 0, \bar{y} < 0 \quad (5c)$$

$$\bar{x} = \frac{1}{P} \sum_{i=1}^P \cos \varnothing_{ij} \quad (6)$$

$$\bar{y} = \frac{1}{P} \sum_{i=1}^P \sin \varnothing_{ij} \quad (7)$$

$$MDF_j = \varnothing_j \frac{J_d}{2\pi} \quad (8)$$

where \varnothing_{ij} is the date of occurrence converted into an angular value; DF_{ij} is the date of occurrence of a maximum flow in a hydrological year; \varnothing_j represents the direction of the angle; \bar{x} and \bar{y} are the cosine and sine components of the mean date of a maximum flow; P is the number of years in the time series; and J_d shows the average number of days per year.

2.6. Relative importance of flood drivers

Following Berghuijs et al. (2019), we calculated the relative importance of each flood driver from the comparison of annual flood circular statistics. Berghuijs et al. (2019) explained that the summed cosine and sine

Table 1
List of variables analyzed in this study.

Index	Abbreviation
Annual maximum daily discharge	Q_{max}
Annual maximum 3-day precipitation	PCP_{max}
Annual maximum 3-day snowmelt	SN_{max}
Annual maximum soil moisture excess	SME_{max}

components of the seasonality of the three processes (precipitation, snowmelt and soil moisture excess) allow to estimate the relative importance of each flood factor. The calculation was based on the following linear equations proposed by Berghuijs et al. (2019):

$$\bar{x}_f = \alpha_{pcp}\bar{x}_{pcp} + \alpha_{sn}\bar{x}_{sn} + \alpha_{mo}\bar{x}_{mo} \quad (9)$$

$$\bar{y}_f = \alpha_{pcp}\bar{y}_{pcp} + \alpha_{sn}\bar{y}_{sn} + \alpha_{mo}\bar{y}_{mo} \quad (10)$$

$$1 = \alpha_{pcp} + \alpha_{sn} + \alpha_{mo} \quad (11)$$

where α is the relative importance of each flood driver (pcp = precipitation, sn = snowmelt, and mo = soil moisture excess), \bar{x}_f and \bar{y}_f are the average cosine and sine components of the dates of occurrence of the drivers. Hence, the relative importance ranges from 0 to 1, where 0 indicates no influence of the driver on flooding, while 1 indicates that the driver fully explains flooding. Finally, the change in the relative importance of the three flood drivers in the period 1952–2020 was calculated separately for the periods 1952–1985 and 1986–2020 following the Eqs. (9)–(11). Then, the difference was obtained from the following equation:

$$\Delta\alpha = \alpha_{post1986} - \alpha_{pre1986} \quad (12)$$

where $\Delta\alpha$ is the relative change in time, and $\alpha_{post1986}$ and $\alpha_{pre1986}$ are the indices of relative importance of the given flood driver for each sub-period, respectively. The reader is referred to the literature, such as Berghuijs et al. (2019) for more details on indices of flood relative importance.

Finally, Spearman correlations were calculated between the magnitude (timing) of flood drivers (PCP_{max} , SN_{max} and SME_{max}), and the magnitude (timing) of floods (Q_{max}), similar to studies implemented by Berghuijs et al. (2016), Blöschl et al. (2019), Trambly et al. (2021) and Shen and Chui (2021). Additionally, we used a Multivariate Linear Regression (MLR) to explain the spatial variability of the relative importance of SME_{max} based on maps of two key soil physical properties derived from SWAT, namely available water capacity (AWC) and hydraulic conductivity (K). The soil parameters were extracted from the model described in Marcinkowski et al. (2022). The MLR method describes a response variable by implementing a linear equation which depends on two or more independent variables (Ahmadianfar et al., 2020).

2.7. Methodological flow chart

Particular steps performed to process and analyzed the data were described in the methodological flow chart in Fig. 2.

3. Results

3.1. Trends in floods and flood drivers

The analyses of the magnitude of floods and flood drivers are shown in Fig. 3. Q_{max} showed a strong and consistent pattern across the study area (Fig. 3A). Broadly, a decreasing trend is observed across the country (with slope no lower than -0.003). Moreover, a significant downward trend no lower than -0.072 in central, south-east (Ukrainian border) and north-east (Lithuanian border) Poland was detected. An increasing trend was identified in the north-west and southern regions, where the changes are higher than 0.036, with some specific sub-basin with significant changes higher than 0.007 in the north-west. The statistically significance trend is more predominant in three regions: namely the north-west (positive trend), north-east and south-east (negative trends).

The magnitude of precipitation showed a clear dominance of positive trend around the study area, with a clear significant pattern in the north-west and south-east regions (slope higher than 0.002). An insignificant decreasing trend was found in the south-west, particularly at the Czech border and in some areas in the central and north-east regions.

A different pattern with a widespread decreasing trend can be found for SN_{max} (Fig. 3C). For this variable, changes around -0.002 dominate throughout the study area, with statistical significance predominantly found in the eastern region, along with certain smaller areas in western and northern Poland. A non-significant increasing trend can be observed for a small number of sub-basins spread in the southern and western regions.

The trends in SME_{max} (Fig. 3D) are low in magnitude, whether positive or negative, and significance is concentrated in southern and eastern regions. A positive trend is detected in the east, the south, and northwest, with trend slopes between 0 and 0.02. The central and south region show a downward trend with slopes no lower than -0.02 .

Finally, Sen's slope was calculated at the reach level in Fig. 4. A non-significant trend was detected for the main reaches (Vistula and Odra)

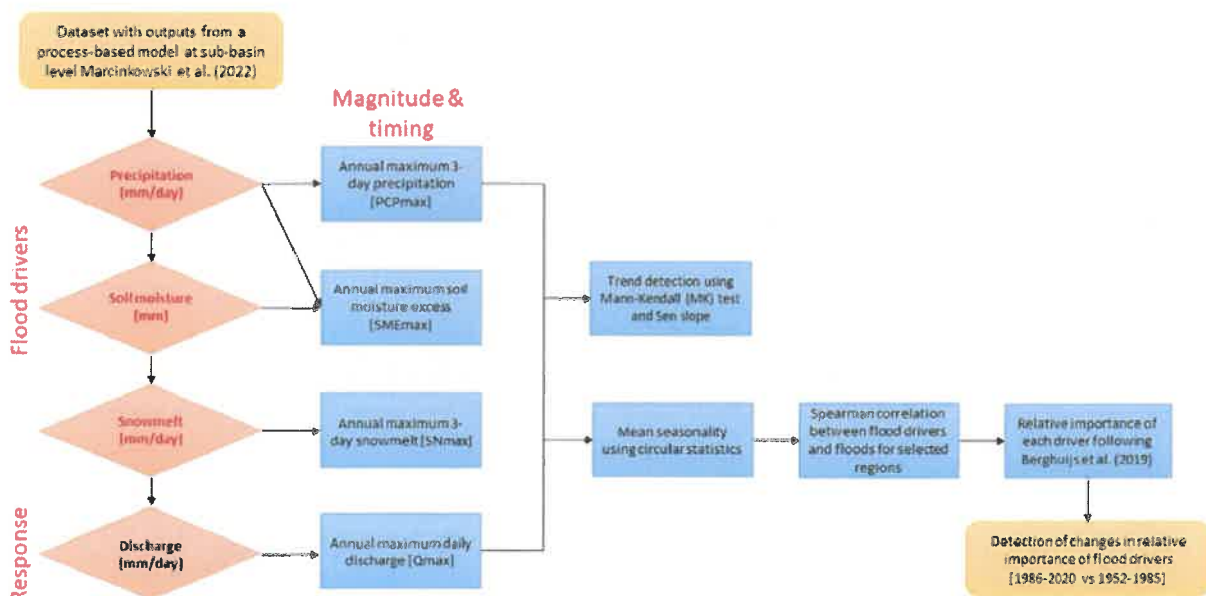


Fig. 2. Research methodology flow chart.

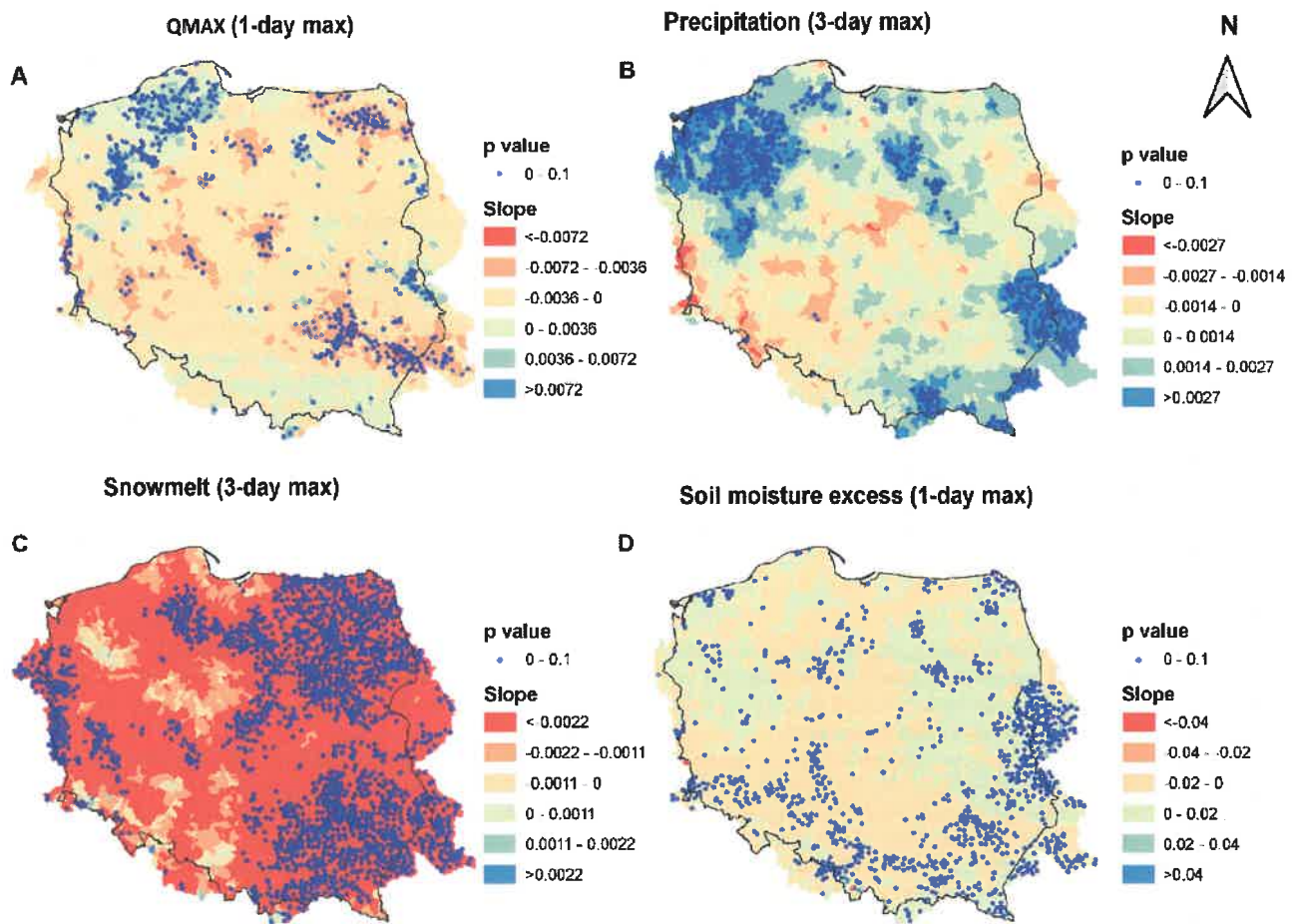


Fig. 3. Mann-Kendall test and Sen's slope for annual maximum daily discharge (A), annual maximum 3-day precipitation (B), annual maximum 3-day snowmelt (B), and annual maximum daily soil moisture excess (D) across the study area for the period 1952–2020.

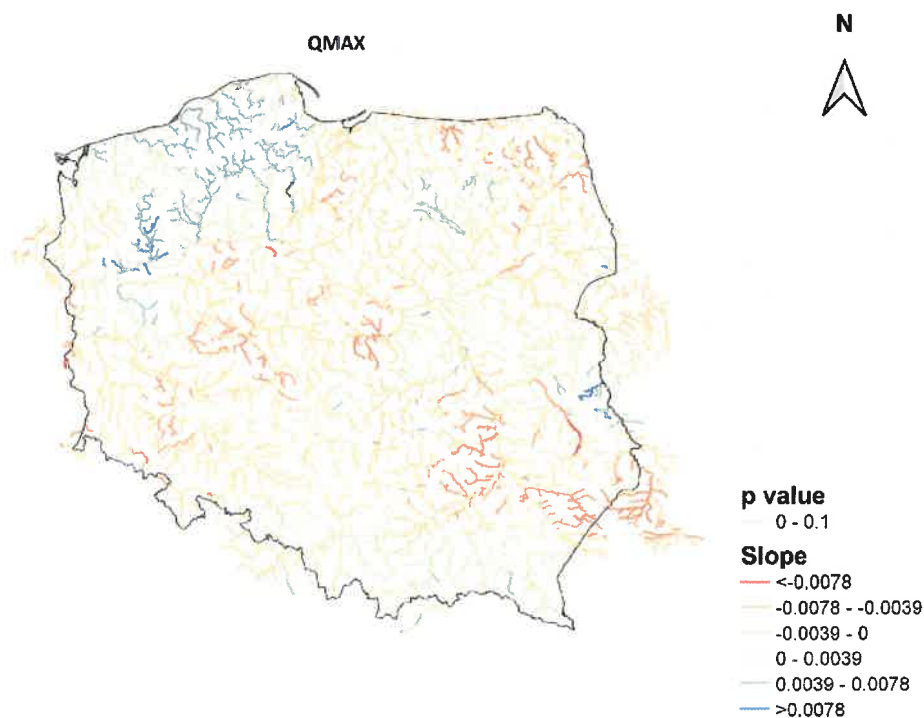


Fig. 4. Mann-Kendall test and Sen's slope for annual maximum daily discharge for the period 1952–2020 at the stream level.

with a variance between 0 and ± 0.039 . Significant trends were mainly in the north-west, and local reaches in southern Poland with slope values between 0.004 and 0.008. Generally, trends showed a non-

significant upward behavior at the southern range. Additionally, a significant decreasing trend was located mostly in the northeast and east (Ukrainian border) region.

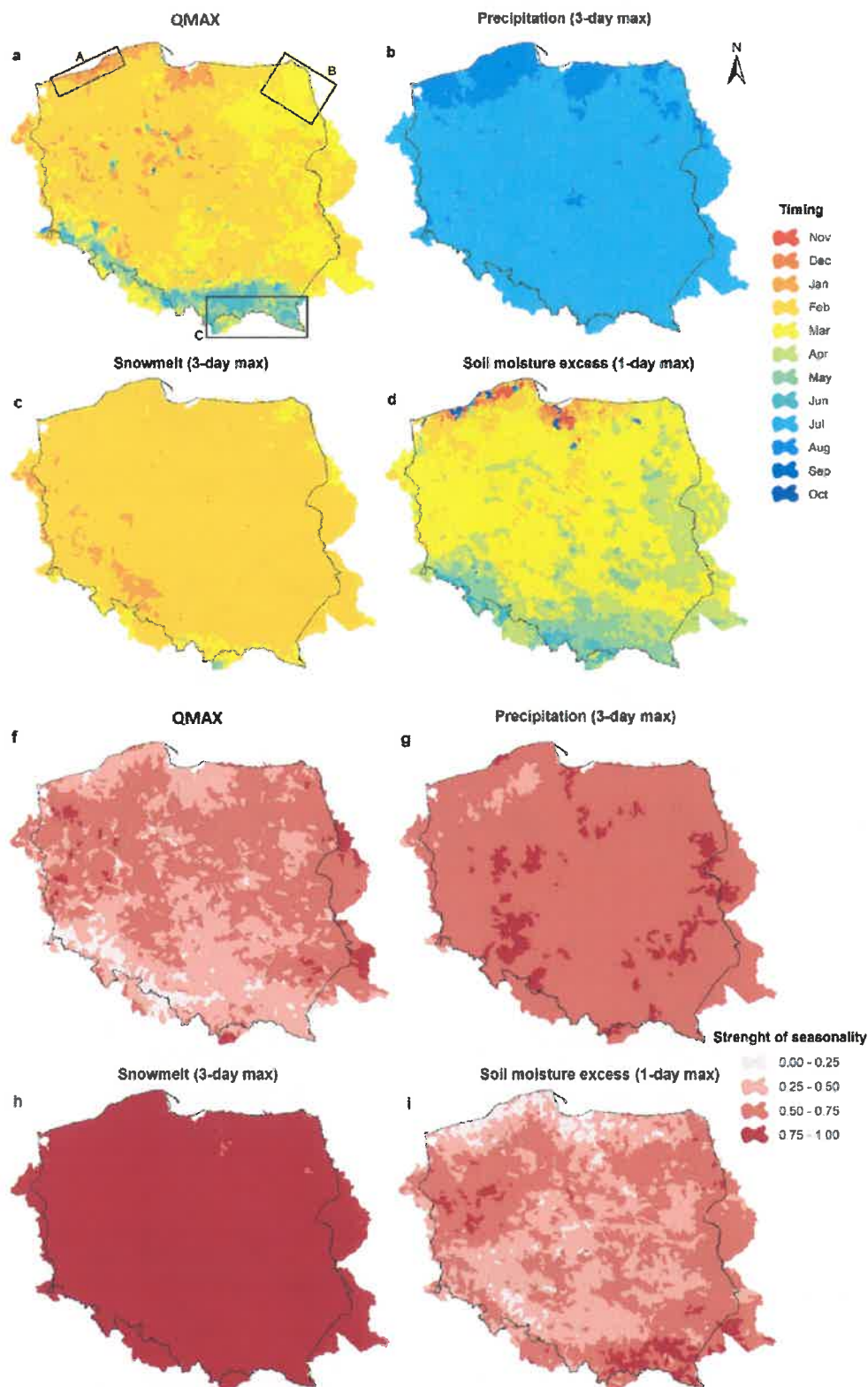


Fig. 5. Mean date of occurrence of annual maximum daily discharge (a), annual maximum 3-day precipitation (b), annual maximum 3-day snowmelt (c), and annual maximum daily soil moisture excess (d) across the study area. Panels f to i show the strength of mean seasonality of extreme events (0 being evenly distributed events and 1 meaning all events arise on the same date).

3.2. Seasonality of floods and their drivers

The analyses of the average seasonality and the seasonal strength (concentration) for Q_{\max} , PCP_{\max} , SN_{\max} , and SME_{\max} are presented in Fig. 5. The mean date of occurrence of floods showed a consistent pattern in the

study area. The Q_{\max} occurs between February and April with a strength seasonality between 0.50 and 0.75, while in the mountainous region (south) the average flood occurrence is between May and July, with the lowest strength in the southwest region (Fig. 5a, and f). The PCP_{\max} and SN_{\max} (Fig. 5b–c, and g–h, respectively) exhibited a clear and strong

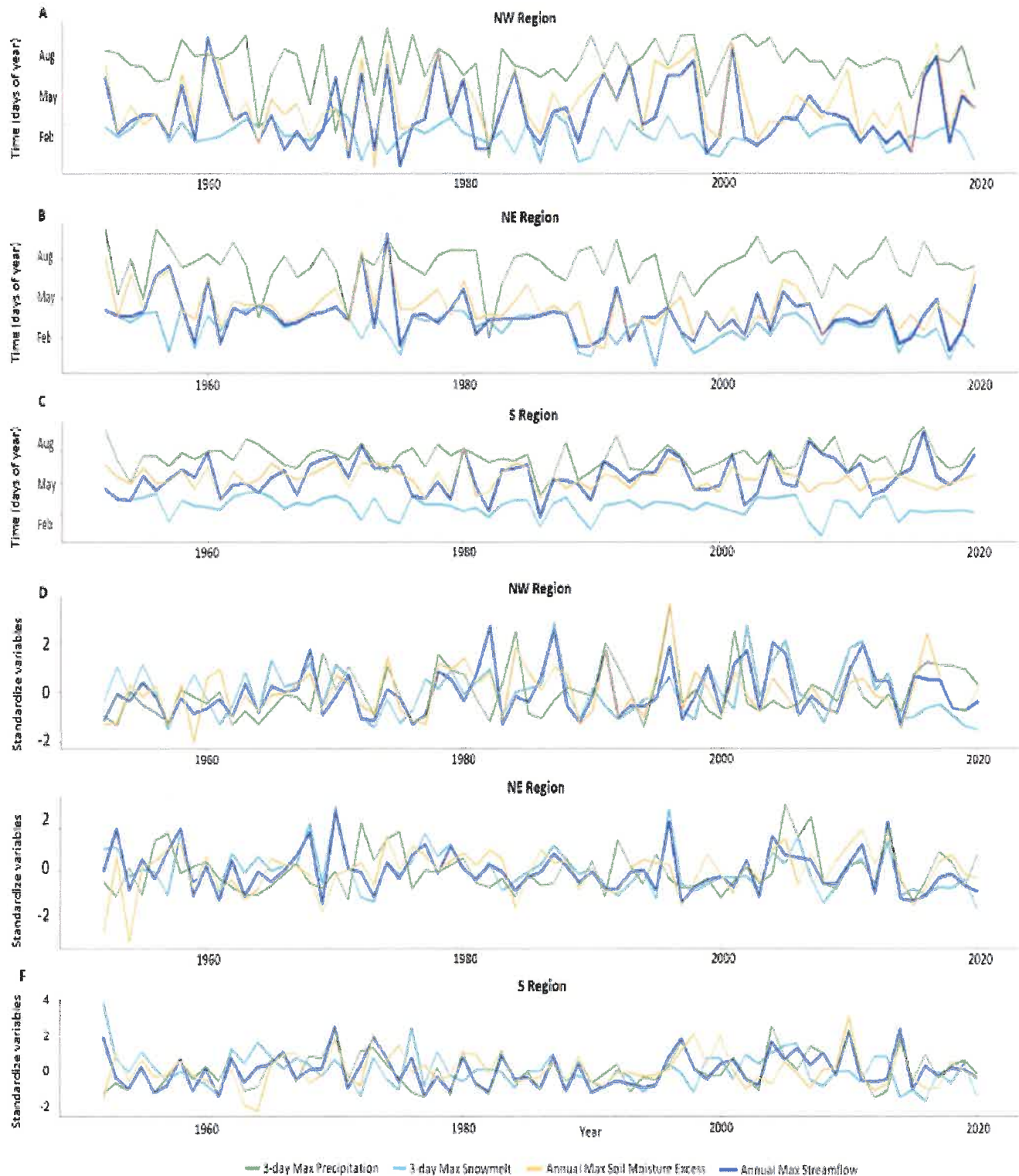


Fig. 6. Long-term temporal evolution of timing (A–C) and magnitude (D–F) of floods and their dominant drivers for three regions across Poland for the period 1952–2020. Green: annual maximum 3-day precipitation, Cyan: annual maximum 3-day snowmelt, Orange: annual maximum daily soil moisture excess, and Blue: Annual maximum daily flood. Flood and flood driver magnitude data (panels D–F) have undergone standardization.

incidence. Extreme precipitation occurred in July in the inland part, while more frequently in August closer to the Baltic Sea coast. The occurrence of SN_{max} was predominantly in February in most of the study area and in January in certain isolated zones in the western part of the territory. This variable was also characterized by having the highest concentration value (close to 1), which can be interpreted as high stability of maximum snowmelt timing. Finally, the results for SME_{max} (Fig. 5d, and i) showed a mixed mean occurrence over the study area, with soil moisture excess peaking around March or April in the lowland areas, and between October and December close to the Baltic Sea (with rather low concentration value). Moreover, a different pattern can be observed in the southern region, where these events mainly occurred between May and June, similar to Q_{max} .

Further, we analyzed the relationship between Q_{max} and PCP_{max} , SN_{max} , and SME_{max} in three focus regions (marked with black rectangles in Fig. 5a), as shown in Fig. 6. The three regions help to better understand the evolution of the flood drivers across Poland. Fig. 6 clearly confirms that the long-term temporal dynamics of the flood timing and magnitude is rather weakly related to extreme precipitation. Indeed, these variables have stronger connections to soil moisture excess in the north-western region (with a Spearman correlation of 0.83 for timing and 0.72 for magnitude) and snowmelt in the north-eastern region (with a Spearman correlation of 0.51 for timing and 0.80 for magnitude).

In region A (north-western Poland (Fig. 6A, and D), Q_{max} timing and magnitude are mostly connected to soil moisture excess (orange line), since Q_{max} time series follows the same seasonality as this variable. Additionally, extreme precipitation shows a marked seasonality in the summer months, indicating a weaker link with flood events. Soil moisture excess presented the highest Spearman correlation with Q_{max} timing ($R = 0.83$). Interestingly, while the maximum snowmelt and flood timing have a very weak relationship in this region ($R = 0.2$), the corresponding magnitude characteristics have a much higher correlation ($R = 0.64$). This may stem from the timing of maximum snowmelt being more concentrated than flood timing, whereas extreme snowmelt magnitude has higher inter-annual variability, which matches the Q_{max} magnitude variability quite well.

In region B (north-eastern Poland (Fig. 6B, and E), the evolution of Q_{max} timing and its magnitude follow patterns similar to those of maximum snowmelt and soil moisture excess. Indeed, the former has the highest correlation value with magnitude, while the latter has the highest correlation with timing. Snowmelt gains in importance compared to region A, especially for timing data. To illustrate, the Spearman correlation between SN_{max} and Q_{max} timing is 0.51, but it is 0.80 for magnitude, which is in fact the maximum correlation among the drivers (Table 2). In contrast, the PCP_{max} has the weakest relationship with Q_{max} for both timing and magnitude, with a correlation of 0.27 and 0.25, respectively. This might be due to this region being a snow-dominated area where extreme summer precipitation does not lead to significant flood events, as in other parts of the country.

Region C Southern Poland (Fig. 6C, and F) differs substantially from other regions, as it is the only region where extreme precipitation is an important flood driver. Indeed, the temporal evolution of Q_{max} magnitude follows a similar pattern to that of PCP_{max} ($R = 0.75$). The corresponding relationship for timing is weaker than the one for magnitude, but also weaker from the relationship between flood and soil moisture excess

timing. Moreover, the influence of snowmelt is close to negligible. Overall, in the southern region, high discharges are the result of extreme precipitation and its interaction with soil moisture excess.

3.3. Relative importance of flood drivers and their changes over time

Spatial pattern of relative importance of flood drivers is shown in Fig. 7. The patterns for PCP_{max} (panel A) show the least influence compared to the other studied drivers. In general, a high relative importance (α above 0.6) was detected in isolated mountainous areas in the southern-most part of the country.

A different pattern with more areas and high relative importance can be found for SME_{max} (panel B). In this case, the SME_{max} dominates as the flood driver throughout the northern and some other areas in the west. The highest relative importance can be observed for sub-basins located in the proximity of the coast of the Baltic Sea, while the lowest values (0–0.2) were detected around the whole country, especially in the southern and eastern Poland. The high relative importance of SME_{max} could be linked to certain soil properties (i.e., available water capacity, AWC and hydraulic conductivity, K, Fig. 8) as presented in Table 3.

A visual inspection of spatial variability of the SME_{max} relative importance (Fig. 7B) and the maps of selected soil properties (Fig. 8) shows a high level of agreement, particularly for hydraulic conductivity (Fig. 8A). Areas with high values of K frequently have relatively high relative importance of SME_{max} .

Table 3 confirms a statistically significant effect of K and AWC on the relative importance of SME_{max} (probability of 0.00 and 0.01, respectively). For K, a positive correlation of 13.99 was obtained, while for AWC a negative trend of -2.57 was detected. This further proves the interactions of soil properties in the high relative importance of flooding drivers over Poland.

Finally, SN_{max} (panel C in Figs. 7 and 9) is the most important flood driver, with a relative importance above 0.60 for this variable in most sub-basins. Although snowmelt is the dominant flood driver across the north-eastern region (particularly in Belarus and Ukraine) and in many west-central sub-basins, it is progressively less important in the southern region, where relative importance falls below 0.4 over a large area. Similarly, there are several sub-regions in the north and north-east, where snowmelt has lower importance than soil moisture excess.

The results of changes of the relative importance are presented in Fig. 9. These changes are based on the comparison of two time periods (1952–1985 and 1986–2020), which allows to detect the presence of a climate change signal in the studied variables.

Fig. 9A (PCP_{max}) shows a clear pattern with a positive change mainly in the mountain range in the south (higher than 0.20). A slightly negative change is detected over the majority of the country, with values between 0 and -0.20 , but a small positive change is also relatively noticeable in certain areas. The PCP_{max} is losing importance over several small areas such as in the south-west (Kłodzko basin) and in the east near the Belarusian and Ukrainian borders. The patterns are consistent with the relative importance of PCP_{max} showed in Fig. 7. In general, increasing trends prevail, especially in the southern part of the country (both mountainous and upland regions).

A different pattern with more complex results can be found for the changes in SME_{max} (Fig. 9B), where a mix of positive and negative changes are detected over the study area. However, an increasing tendency dominates throughout the north-western and eastern part of the country, especially in the Narew River basin. A decreasing change is spread over different regions, for example in the central and southern areas. For SN_{max} (Fig. 9C), the spatial pattern is to some extent the opposite of the pattern detected for SME_{max} . A decreasing trend was detected over a large part of eastern and north-western Poland. However, in the very central part of Poland, certain sub-basins show an increasing importance for snowmelt. In general, the strongest detected signal shows that snowmelt is losing importance in favor of soil moisture excess over large parts of the country.

Table 2
Spearman correlation of Q_{max} timing and magnitude with flood drivers.

	Variable	Northwest	Northeast	South
Timing	Precipitation	0.34	0.27	0.43
	Soil moisture excess	0.83	0.68	0.55
	Snowmelt	0.20	0.51	-0.20
	Precipitation	0.25	0.25	0.75
Magnitude	Soil moisture excess	0.72	0.65	0.45
	Snowmelt	0.64	0.80	0.31

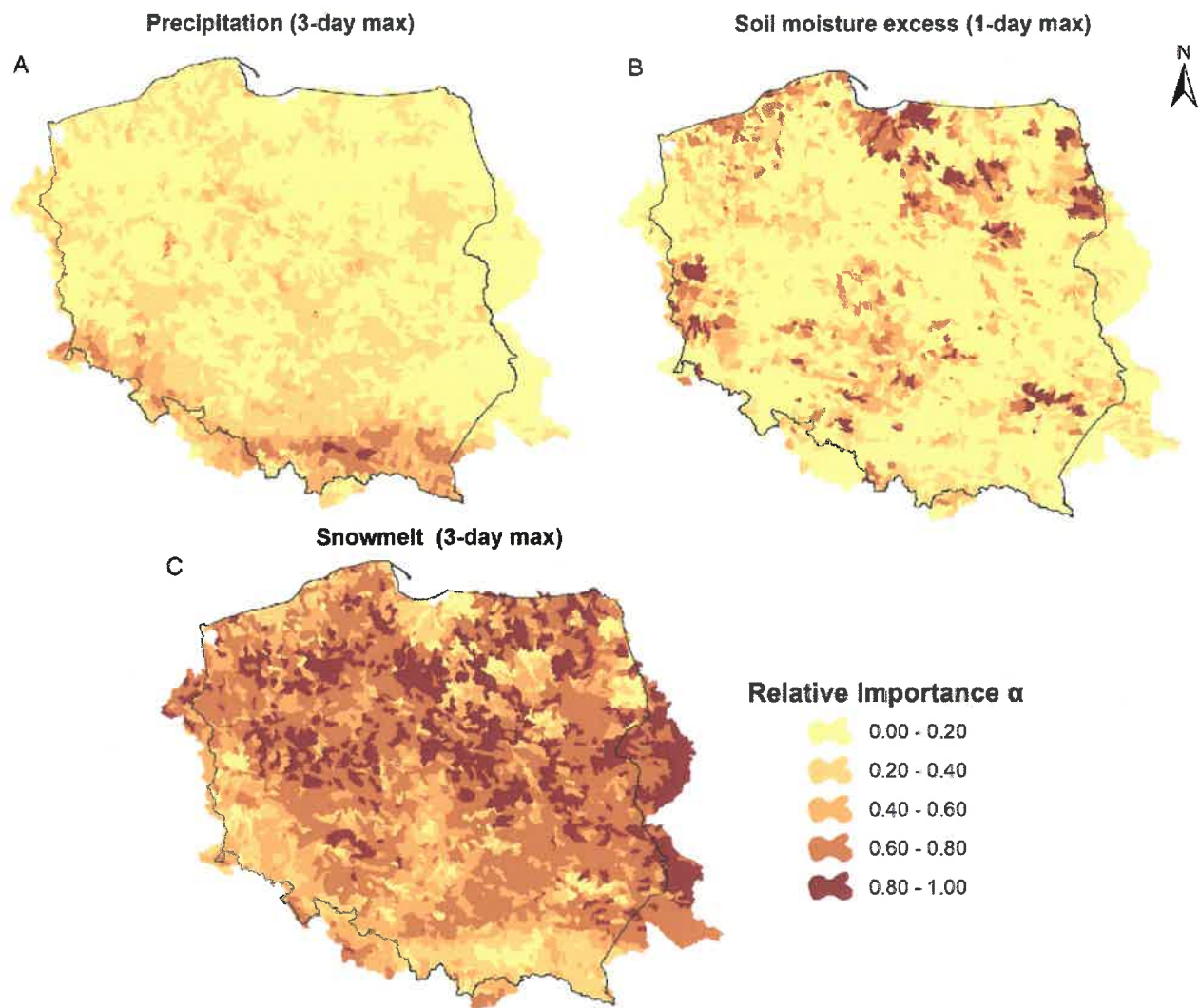


Fig. 7. Relative importance of annual maximum 3-day precipitation (A), annual maximum daily soil moisture excess (B), and annual maximum 3-day snowmelt (C) for the period 1952–2020.

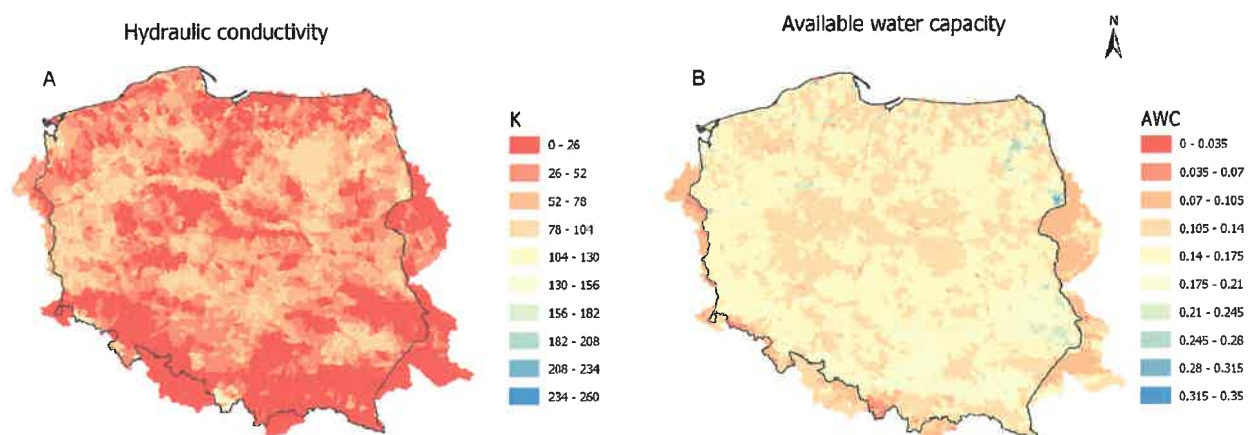


Fig. 8. Spatial variability in soil hydraulic conductivity (panel A) and available water capacity (panel B) based on the input maps from the SWAT model (Marcinkowski et al., 2022).

Table 3

Multivariate linear regression, where available water capacity (AWC) and hydraulic conductivity (K) are predictors and the relative importance of SME_{max} is response variable.

Variable	t-Statistic	Probability
K	13.99	0.00
AWC	-2.57	0.01
Multiple R-squared		0.048

4. Discussion

4.1. Trends in floods and flood drivers

The trend detection in flood magnitude (Q_{max}), both at the sub-basin and reach level showed a clear pattern over time. The decreasing trend is the dominant result detected over the study area, with a statistical significance in the northeast region. The increases were presented mainly in the south (non-significant) and northwest of the country (significant), with other focal sub-basin groups. Notably, this result is largely in line with the analysis of Piniewski et al. (2018), Blöschl et al. (2019), Bertola et al. (2020) Slater et al. (2021) and Venegas-Cordero et al. (2022) who found the strongest decreasing trend in the northeast and central parts of

Poland. Moreover, significant increasing trends were detected in the north-western Poland and non-significant increasing patterns in the south, consistent with Blöschl et al. (2019). The general decreasing trend found for the annual maximum flow in our study is consistent with Di Sante et al. (2021), who studied trend in river floods in Europe using observed data and the ensemble mean of EURO-CORDEX simulations for 1985–2014. Slater et al. (2021), studied the global changes in river floods with different probabilities of occurrence, where a clear downward pattern was found in most of the country, and a few gauges located in mountainous south were showing a positive behavior in the 20- and 50-year floods. However, our results might be sensitive to the factors such as time period considered in the trend analysis, for example, Kemter et al. (2020) in their study of flood magnitudes across Europe, detected an increasing trend of flood magnitude over most of Poland for 1960–2010. While, Venegas-Cordero et al. (2022) analyzed trends in observed river floods in Poland, founding a decreasing tendency in the northwest region for two different periods (1956–2019 and 1981–2019). Here we confirmed that the results might change due to different factors such as the uncertainty in the observations and simulations used for the analysis (Di Sante et al., 2021).

The pattern for PCP_{max} showed an increasing trend over the greater part of the study area. Likewise, Szwed (2019), who studied the variability of precipitation in Poland for 1951–2013, found a similar pattern for the mean annual precipitation over the country with the greatest changes in the northwest and in the southern region, near the Slovakian and Ukrainian

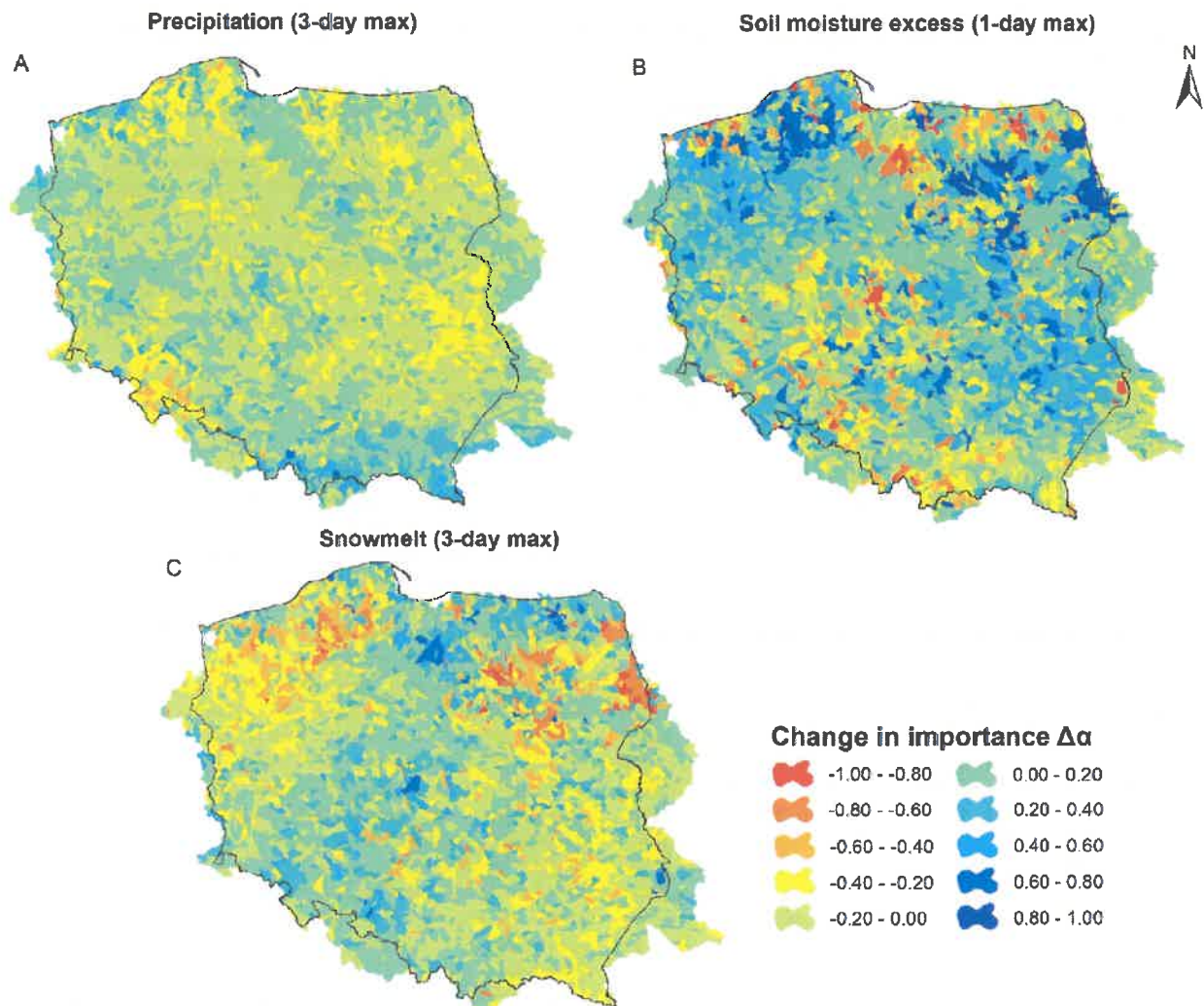


Fig. 9. Changes in the relative importance of precipitation (A), soil moisture excess (B), and snowmelt (C) for the comparison of 1952–1985 and 1986–2020.

borders. The downward trend was detected in southwest Poland (Czech and German border) which also matched the results found by [Szwed \(2019\)](#). Additionally, [Pińskwar et al. \(2019\)](#) studied the changes in extreme precipitation over Poland for 1991–2015 versus 1961–1990 (using maximum 5-day precipitation totals) and found an increasing trend over the country and a decreasing trend in some gauges in the west (near to German and Czech border) and in the north-east (near to Belarusian border), similar to our findings. The downward change in central and south-western Poland was also detected in a long-term precipitation trend analysis in Europe by [Caloiero et al. \(2018\)](#), which validates our results. Meanwhile, [Hänsel et al. \(2022\)](#) who studied heavy precipitation during record summers in Europe found a positive trend in the gauges located in Poland. Also in global scale studies, such as [Sun et al. \(2021\)](#), they analyzed annual maximum 1- and 5-day precipitation, showed similar results over Poland, with a general increasing trend over most of the country, with decreasing changes in the west and some stations in the central and eastern regions of the country, consistent with previous studies at the European scale ([Zolina, 2012](#); [van den Besselaar et al., 2013](#)). However, we detect a large change if we compare our results with studies with limited data up to the early 2000s, e.g., [Lupikasza \(2010\)](#), where the variability of extreme precipitation in Poland was studied in the period 1951–2006. They found small upward trends and mainly confined to northwest Poland, while the rest of the country was characterized by a declining trend.

The SN_{max} trend showed a negative behavior for the entire study area, with a few sub-basin groups exhibiting a non-robust increasing tendency. This decreasing pattern is associated with higher temperatures lessening flood events in the eastern part of Europe ([Bertola et al., 2020](#); [Blöschl et al., 2019](#); [Venegas-Cordero et al., 2022](#)). In addition, this decrease in SN_{max} might be associated with snow cover duration. For instance, [Szwed et al. \(2017\)](#) studied the changes of snow cover in Poland and detected a negative change in the number of days with snow cover for 1952–2013 in all the observed gauges analyzed. Another process associated with this is the North Atlantic Oscillation (NAO), where a positive phase results in less snowfall during winters ([Szwed et al., 2017](#)). In general, the snowmelt processes associated with rises in temperatures may be crucial in flood events and in catchment hydrology. For instance, it was shown that floods tend to occur later (around February–March) with less snow cover and higher rainfall events ([Blöschl et al., 2017](#); [Meresa et al., 2017](#); [Pińskwar, 2022](#); [Venegas-Cordero et al., 2022](#)). [Wu et al. \(2018\)](#) did not focus their analysis on Poland, their results confirm ours (decreasing trend) as snowmelt processes are slower over the northern hemisphere due to the warmer climate. Overall, the decreasing trend detected could be also related with the snow depth over the region. For example, [Fontrodona Bach et al. \(2018\)](#) who used daily snow depth data for 1951–2017, showed a general downward trend over the Central Europe (southwest Poland included) but with an opposite pattern for some local gauges on the Polish-Slovak border.

There is a lack of studies dealing with magnitude trends in soil moisture excess, which could have been used for comparison. Several studies exist for soil moisture related indicators, without considering precipitation aspect. Notably, [Zawadzki and Kędzior \(2014\)](#) analyzed soil moisture content changes in Central Europe (Poland, Czech Republic) from 1979 to 2011 by using the Global Land Data Assimilation System (GLDAS) dataset. They detected a general and statistically significant decreasing trend over the study area, with a slight increase during 1999–2000. [Almendra-Martín et al. \(2022\)](#) studied soil moisture anomaly trends in Europe using a rank-based, empirical decomposition method in monthly and annual series from ERA5-Land and Lisflood model. The main findings of this analysis agree with our results, with an increasing trend over the north-west of Poland and spread groups in the eastern part. In contrast, the results exhibited a negative or non-significant change using any of the dataset along with a MK test. Similar to the previous results, [Deng et al. \(2020\)](#) used a combined product for an average annual soil moisture trend analysis in 1979–2017, which demonstrated a general decreasing trend in the eastern European Plain, Poland included. Global studies have showed no clear pattern over Poland due to the product and method used. For example, no

changes found for monthly surface soil moisture using ERA/Land data, while a general downward trend in summer soil moisture using ERA5 and CMIP6 products, but an increase in the trend for the northeastern region of Poland when they used GLDAS dataset ([Albergel et al., 2013](#); [Qiao et al., 2021](#); [Qin et al., 2023](#)). Overall, it is difficult to make a direct comparison with our results due to the lack of trend analysis of soil moisture excess in Poland, which makes our results a valuable contribution, being one of the first studies of this nature at the national scale.

4.2. Seasonality of flood drivers

The Q_{max} results showed a clear pattern for the studied area. Typically, annual maximum flows occur in winter and spring across large parts of the study area, especially during February and March over the north-eastern Polish border. In contrast, Q_{max} often occurs between May and July in southern Poland. These patterns have been described in detail in previous global and pan-European studies ([Berghuijs et al., 2019](#); [Fang et al., 2022](#); [Hall and Blöschl, 2018](#); [Jiang et al., 2022a](#); [Wasko et al., 2020a, 2020b](#)). In general, the annual maximum flows occur in different months in the southern Poland, as [Blöschl et al. \(2017\)](#) reported. They found the mean time between May–July, while the rest of the country showed a more established behavior between January–March. Similar behavior was found by [Fang et al. \(2022\)](#) for central Europe. The behavior in the southern part are associated with heavy and prolonged precipitation (2–5 days) in the summer period ([Kundzewicz et al., 2014b](#); [Ruiz-Villanueva et al., 2016](#); [Venegas-Cordero et al., 2022](#)). Additionally, the seasonal characteristics of the annual maximum floods for 1953–2004 in the Danube basin (located in central Europe) showed a mean occurrence during the spring months, which is related to snowmelt processes ([Mao et al., 2019](#)). Trends in flood timing are explained in detail in the study based on observed river floods ([Venegas-Cordero et al., 2022](#)). The reader is referred to this literature for more details on the annual maximum flows seasonality.

The PCP_{max} occurs in July in most of the study area, and in August at the northern border with the Baltic Sea. These observations are in agreement with the results of [Berghuijs et al. \(2019\)](#). In general, this extreme precipitation behavior over the region could be associated with atmospheric rivers, which [Lavers and Villarini \(2015\)](#) described as narrow corridors in which most of the water vapor is transported towards the poles. Indeed, [Lavers and Villarini \(2013\)](#), who studied the link between atmospheric rivers and extreme precipitation in Europe, demonstrated that these phenomena occur during the summer in eastern Europe (especially across Poland), which may lead to the heavy and prolonged precipitation described by certain studies over the study area. For example, [Kundzewicz et al. \(2018\)](#) and [Pińskwar et al. \(2019\)](#) indicated heavy precipitation in the north-western part of Poland. In addition, the timing of PCP_{max} in northern Poland (August) is considered a typical characteristic of the coastal zone, where the sea's influence can delay the rise in temperature and shift the maximum precipitation to August ([Kirschenstein, 2009](#)). Intense summer rainfall is also associated with atmospheric humidity and evaporation from the Mediterranean Sea ([Tabari and Willems, 2018](#); [Venegas-Cordero et al., 2022](#)). This study confirms that extreme precipitation over Poland is strongly associated with the summer season. For example, previous studies reconfirmed this statement. [Gvoždíková et al. \(2019\)](#) studied the time distribution of central European extreme precipitation between 1961 and 2013 and revealed that the events over Oder occurred mostly in July–August. While, [Chan et al. \(2020\)](#) analyzed simulations and observed data on maximum precipitation events, showing that extreme precipitation events over Central Europe tend to occur in summer. The mean date of occurrence of SN_{max} is highly concentrated in February, with some scattered points in January (western) and March (northeast and south), which agree with the results of [Berghuijs et al. \(2019\)](#). The western region's behavior is associated with typical German winter with minor precipitation falling as snowfall ([Berghuijs et al., 2019](#)). The average date of last snow occurrence is late winter and early spring (February–March) in the region ([Bednorz, 2009](#); [Steirou et al., 2017](#)). In the northeast, inland, and the Gorce Mountains (southern region), flood occurrence might be related with warmer

temperatures which can generate a single snowmelt flood between January and March (Ionita et al., 2020; Kijowska-Strugała and Bucala-Hrabia, 2019). Previous studies confirmed that the snowmelt process in Poland occurred mainly between the months of January and March, which is due to an earlier snowmelt in the country that may cause a shift in the floods and in the extreme snowmelt events from March–April to January–February (Stocker, 2014; Romanowicz et al., 2016). In general, global warming with the increases in temperature during the winter, has led to a major winter snowmelt event over most of the northern countries (Aygün et al., 2020; Ford et al., 2020; Lin and Chen, 2022; Somorowska, 2023).

Finally, SME_{max} demonstrates a mixed mean occurrence that resembles Q_{max} timing. However, there is a lack of studies dealing with the seasonality of soil moisture excess for comparison with our results. Berghuijs et al. (2019) analyzed the occurrence of maximum soil moisture excess, but our results are significantly different, as the authors found a mean date of SME_{max} occurrence in the summer months. The soil moisture is one the primary factors that trigger flood in continental Europe, as these events occur under wet conditions (Bryndal, 2015; Marchi et al., 2010). For example, the mean date of occurrence in the southern region is highly similar to that of Q_{max} , due to a high soil moisture and extreme precipitation during the summer months in the mountain range (Bryndal, 2015; Siwek et al., 2013). Finally, our results showed that the timing of soil moisture excess is similar that the annual maximum flow (same time or just after), which is also confirmed by Wasko et al. (2020b) who analyzed the changes in the antecedent soil moisture on flood seasonality.

4.3. Relative importance of flood drivers and its changes over time

Extreme precipitation-dominated sub-basins are mostly located in the mountains in southern Poland, which is consistent with the nation-wide study by Venegas-Cordero et al. (2022) and regional studies in the Tatra Mountains by Kundzewicz et al. (2014b) and Ruiz-Villanueva et al. (2016). These authors explained that floods in the southern region can mostly be attributed to heavy, prolonged rainfall. In addition, previous studies such as Bryndal (2015) and Alfieri and Thielen (2015), who studied local flash floods in Central Europe and extreme rain-storm and the relation with flash flood over Europe, respectively, detected that flood events in the south are more frequent between May and July and linked with heavy rainstorms. Indeed, Berghuijs et al. (2019) who also studied the relative importance of the extreme precipitation across Europe, found results similar to this study, with the extreme precipitation being the principal mechanism of floods in the southern Poland.

In a similar pan-European flood analysis, Kemter et al. (2020) and Bertola et al. (2021) showed the spatial pattern of a high relevance for stratiform rainfall and relative contributions for extreme precipitation over the south of Poland. A global study on river flood-generating processes and their classification detected excess rainfall as the dominant flood driver in most European regions, including southern and western Poland (Stein et al., 2020). In a recent study of the changes in the flood mechanism in Europe, Tarasova et al. (2023) found the south of Poland with a positive change in the frequency of flood events generated by rainfall on dry soils. While, Jiang et al. (2022a) detected the southern Poland with a mix dominant flooding mechanisms (antecedent precipitation, recent precipitation and snowmelt). Thus, our study reconfirmed the extreme precipitation as the main flood mechanism over the south region of the county. Moreover, the changes in the relative importance for 1960–1984 and 1985–2010 on extreme precipitation from Berghuijs et al. (2019) are in agreement with our results for the southern region (Polish Carpathians) with a positive change in recent decades (1986–2020), where air flow conditions from the north and northeast cause the heaviest rains in the area (Wypych et al., 2018). Meanwhile, a contrast was found in the north-west, where an increase in the changes in relative importance for extreme precipitation was noted. This can be associated with the findings of Bevacqua et al. (2019) who identified changes in precipitation as the main driver of future changes in the probability of compound floods in Europe. In addition, the Scandinavian Blocking condition is the dominant pattern in western

Poland for the extreme precipitation during the summer (Barton et al., 2022).

The high relative importance of maximum soil moisture excess (SME_{max}) was principally seen in the northern region, with some local areas in the west and southeast. In general, our results show a high concordance with the findings of Kemter et al. (2020), who detected similar patterns in the northwest, northeast and southeast. Tarasova et al. (2023) found localities in the northeastern and western region of Poland with an increasing change in the frequency of precipitation-generated floods on wet soils, which is in agreement with our results. In contrast, Bertola et al. (2021) who studied the antecedent soil moisture (based on precipitation) found no substantial relative contributions for Poland. Overall, the changes in the relative importance for the driver varied due to the established condition of the soil moisture, which may have a direct influence on the generation of floods. For example, if the soil moisture is high, even small precipitation amount could produce a flood event (Blöschl et al., 2019). Indeed, it is a common mis-conception to think that increasing precipitation extremes on their own should lead to increased floods (Sharma et al., 2018). It is antecedent soil moisture condition that modulates precipitation signal and corresponding flood response. Moreover, our results showed a significant positive correlation with soil hydraulic conductivity, which has important consequences for hydrological properties and flood prevention (Bens et al., 2007). For example, Kerr et al. (2016) point out that high hydraulic conductivity in soil could be a favorable factor in flood events, due to a faster saturation of the soil layer (Nivedya et al., 2020) showing how our study contributes to new knowledge in the domain. Furthermore, the changes in the relative importance are not in agreement with the results of Berghuijs et al. (2019). Soil moisture excess increased over northern Poland, with strong signs that snowmelt is losing importance in favor of soil moisture excess over large parts of this region. This observation is in agreement with Kemter et al. (2020), who highlighted that the importance of soil moisture excess increased in the Central and Northern parts of Europe. They also showed that the relevance of snowmelt decreased in Eastern Europe, similarly to our results. Finally, previous studies mentioned the importance of soil moisture and precipitation as mechanisms generating floods during cold periods, because the decreasing temperatures will lead to higher soil moisture and less evapotranspiration, which might result in floods with the same amount of precipitation in a region (Blöschl et al., 2020; Grillakis et al., 2016).

Maximum snowmelt (SN_{max}) is the most important flood driver for the studied area, which agrees with pan-European studies focusing on flood drivers (Berghuijs et al., 2019; Bertola et al., 2021; Kemter et al., 2020). For instance, Berghuijs et al. (2019) and Kemter et al. (2020) demonstrated that snowmelt is the principal flood mechanism across Poland. This high relative importance closely follows the snowmelt flood regime detected in selected catchment around Poland (Romanowicz et al., 2016). Likewise, Brunner and Fischer (2022) found snowmelt flood to be the most frequent type of floods across Central Europe. More specifically, the highest relative importance of snowmelt flood type was detected in catchments located in the central-west part of our study region. This behavior should also be associated with the mean date of occurrence of Q_{max} , since most of the studied area is dominated by winter floods with the exception of the southern region. For example, Bertola et al. (2021), detected that in the northeastern Europe (Poland included), the snowmelt is the dominant mechanism of flooding in both the median and 100-year floods. Hence, the influence of snowmelt emerges as the dominant mechanism in regions where floods occur in winter (Brunner and Fischer, 2022; Tarasova et al., 2020).

Although our results identify snowmelt as the principal flood driver, data from recent decades shows signs of decreasing relative importance in certain areas such as north-eastern Poland. Kemter et al. (2020) has confirmed this downward snowmelt relevance in Eastern Europe and an increase in the soil moisture excess for the same area. These facts demonstrate the complexity of flood mechanisms across the country, with mixed patterns that can be attributed to a combination of factors. In a recent study, no changes in the mean frequency per decade in Poland during 1960–2010 of snowmelt flood generation have been observed (Tarasova

et al., 2023). Nevertheless, it can be concluded overall that the number of snowmelt-induced floods is likely to decrease in the future due to higher temperatures (Kis et al., 2020). Although using a process-based model for studying flood generation mechanisms over large domain and at high resolution is novel, it has some limitations. Modeling carries its own uncertainties that have not been thoroughly investigated. While the model was extensively calibrated for discharge (Marcinkowski et al., 2022), its behavior in soil moisture dynamics and snow processes has not been analyzed. Future studies should consider using remote sensing products for multi-objective calibration of simulated processes other than discharge, such as soil moisture (Eini et al., 2023) or snow (Grusson et al., 2015).

5. Conclusions

This study analyzed the trend magnitude, timing and flood drivers of PCP_{max} , SN_{max} and SME_{max} for the period of 1952–2020 in Poland and neighboring countries, using a process-based model. A significant decreasing trend in the annual maximum discharge, Q_{max} , was detected in the north-east, with a mean date occurring during winter, especially in January and February and a clear pattern in the south with occurrence between May and July. The maximum precipitation, PCP_{max} , is characterized by a general positive trend over the country (especially in the north-western and southern regions) with a high strength of seasonality in July and August; while the maximum snowmelt, SN_{max} shows a general decreasing trend over the study area, occurring mostly between January and February. In contrast, the maximum soil moisture excess, SME_{max} exhibited a behavior similar to Q_{max} . High flows could be attributed to a combination of factors in certain areas. Furthermore, the relative importance of flood drivers identified SN_{max} as the principal driving mechanism across Poland, followed by SME_{max} and PCP_{max} respectively. Additionally, the climate change influence is detected in the recent years, especially in north-eastern Poland, where snowmelt is losing importance in favor of excess soil moisture. Likewise, the increasing role of extreme precipitation in the south of Poland has been prominent in recent years.

Our study presents, for the first time, the flood mechanism and trend analysis using a high-resolution data set of simulated flows. The quality of simulated data was confirmed, as our results are highly similar to pan-European and local studies done in recent years. While the great majority of published flood trend studies relies on gauge data, our study highlights a potential of using hydrological model outputs to investigate floods at regional scale, in line with some previous continental-scale studies (Prudhomme et al., 2011; Stahl et al., 2012). A clear advantage of using models is the ability to fill the white spaces on maps (Stahl et al., 2012) and extending the analysis period (69 years in this study is well above the average). It was found that some soil properties have a strong correlation with the flood relative importance of SME_{max} , such as hydraulic conductivity, which showed a high level of agreement. This demonstrates that examination of the relative importance of flood drivers requires more attention in future studies to clarify the causes of river floods under climate change.

We show that the spatial and temporal patterns of generation mechanisms of annual maximum discharges are complex. Furthermore, their relative importance does change with time, which indicates that examination of updated records is required on a regular basis. It is worthy of trying to introduce well-auguring new methodological approaches. For instance, machine learning techniques have been successfully applied across different regions (Jiang et al., 2022a, 2022b) to interpret the main flood drivers. They may possibly lend themselves well also to application in studies of flood generation mechanisms in Poland. In general, this study provides a better understanding of the flood mechanism and could be used to support flood protection across Poland. Finally, as the methodology does not depend on the case studied, the study flood generation mechanisms and their relative importance is applicable to any scale level (e.g., local, regional or global), hence its great importance in advancing the knowledge of flood characterization and modeling.

CRedit authorship contribution statement

Nelson Venegas-Cordero: Conceptualization, Investigation, Methodology, Software, Validation, Formal analysis, Visualization, Writing – original draft, Writing – review & editing. **Cyrine Cherrat:** Conceptualization, Investigation, Methodology, Visualization, Writing – original draft, Writing – review & editing. **Zbigniew W. Kundzewicz:** Writing – original draft, Writing – review & editing. **Jitendra Singh:** Methodology, Writing – original draft, Writing – review & editing. **Mikołaj Piniewski:** Conceptualization, Investigation, Writing – original draft, Writing – review & editing, Supervision.

Data availability

Data will be made available on request.

Declaration of competing interest

The authors declare that they have no known competing financial interests or personal relationships that could have appeared to influence the work reported in this paper.

Acknowledgements

This study is supported financially by the National Science Centre (NCN) in Poland under the research project "ATtribution of changes in River FLOODs in Poland (ATRIFLOP)", grant 2022/45/N/ST10/03551. The publication was (co)financed by Science development fund of the Warsaw University of Life Sciences - SGGW.

References

- Ahmadianfar, I., Jamei, M., Chu, X., 2020. A novel hybrid wavelet-locally weighted linear regression (W-LWLR) model for electrical conductivity (EC) prediction in surface water. *J. Contam. Hydrol.* 232, 103641.
- Albergel, C., Dorigo, W., Balsamo, G., Muñoz-Sabater, J., de Rosnay, P., Isaksen, I., Brocca, L., De Jeu, R., Wagner, W., 2013. Monitoring multi-decadal satellite earth observation of soil moisture products through land surface reanalyses. *Remote Sens. Environ.* 138, 77–89.
- Alfieri, L., Thielen, J., 2015. A European precipitation index for extreme rain-storm and flash flood early warning. *Meteorol. Appl.* 22, 3–13.
- Almendra-Martín, L., Martínez-Fernández, J., Piles, M., González-Zamora, Á., Benito-Verdugo, P., Gaona, J., 2022. Analysis of soil moisture trends in Europe using rank-based and empirical decomposition approaches. *Glob. Planet. Chang.* 215, 103868.
- Arheimer, B., Lindström, G., 2015. Climate impact on floods: changes in high flows in Sweden in the past and the future (1911–2100). *Hydrol. Earth Syst. Sci.* 19, 771–784.
- Arnell, N.W., Gosling, S.N., 2016. The impacts of climate change on river flood risk at the global scale. *Clim. Chang.* 134, 387–401.
- Arnold, J.G., Srinivasan, R., Muttiah, R.S., Williams, J.R., 1998. Large area hydrologic modeling and assessment part I: model development 1. *J. Am. Water Resour. Assoc.* 34, 73–89.
- Aygün, O., Kinnard, C., Campeau, S., 2020. Impacts of climate change on the hydrology of northern midlatitude cold regions. *Prog. Phys. Geogr. Earth Environ.* 44, 338–375.
- Barton, Y., Rivoire, P., Koh, J., Ali, S.M., Kopp, J., Martius, O., 2022. On the temporal clustering of European extreme precipitation events and its relationship to persistent and transient large-scale atmospheric drivers. *Weather Clim. Extrem.* 38, 100518.
- Bates, B., Kundzewicz, Z., Wu, S., 2008. *Climate Change and Water*. Technical Paper Intergovernmental Panel on Climate Change Secretariat.
- Bednorz, E., 2009. Synoptic conditions for rapid snowmelt in the Polish-German lowlands. *Theor. Appl. Climatol.* 97, 279–286.
- Bens, O., Wahl, N.A., Fischer, H., Hüttl, R.F., 2007. Water infiltration and hydraulic conductivity in sandy cambisols: impacts of forest transformation on soil hydrological properties. *Eur. J. For. Res.* 126, 101–109.
- Berghuis, W.R., Woods, R.A., Hutton, C.J., Sivapalan, M., 2016. Dominant flood generating mechanisms across the United States. *Geophys. Res. Lett.* 43, 4382–4390.
- Berghuis, W.R., Harrigan, S., Molnar, P., Slater, L.J., Kirchner, J.W., 2019. The relative importance of different flood-generating mechanisms across Europe. *Water Resour. Res.* 55, 4582–4593.
- Bertola, M., Viglione, A., Lun, D., Hall, J., Blöschl, G., 2020. Flood trends in Europe: are changes in small and big floods different? *Hydrol. Earth Syst. Sci.* 24, 1805–1822.
- Bertola, M., Viglione, A., Vorogushyn, S., Lun, D., Merz, B., Blöschl, G., 2021. Do small and large floods have the same drivers of change? A regional attribution analysis in Europe. *Hydrol. Earth Syst. Sci.* 25, 1347–1364.
- Bevacqua, E., Maraun, D., Voudoukas, M.I., Voukouvalas, E., Vrac, M., Mentaschi, L., Widmann, M., 2019. Higher probability of compound flooding from precipitation and storm surge in Europe under anthropogenic climate change. *Sci. Adv.* 5, eaaw5531.
- Bevacqua, E., Voudoukas, M.I., Shepherd, T.G., Vrac, M., 2020. Brief communication: the role of using precipitation or river discharge data when assessing global coastal compound flooding. *Nat. Hazards Earth Syst. Sci.* 20, 1765–1782.

- Blazewicz, K., 2006. Climate and bioclimate of Poland. Natural and human environment of Poland. A geographical overview. pp. 31–48.
- Blöschl, G., Hall, J., Parajka, J., Perdigão, R.A., Merz, B., Arheimer, B., Aronica, G.T., Bilbashi, A., Bonacci, O., Borge, M., 2017. Changing climate shifts timing of European floods. *Science* 357, 588–590.
- Blöschl, G., Hall, J., Viglione, A., Perdigão, R.A.P., Parajka, J., Merz, B., Lun, D., Arheimer, B., Aronica, G.T., Bilbashi, A., Boháč, M., Bonacci, O., Borge, M., Čančevac, I., Castellari, A., Chirico, G.B., Claps, P., Frolova, N., Ganora, D., Gorbachova, L., Güll, A., Hannaford, J., Harrigan, S., Kireeva, M., Kiss, A., Kjeldsen, T.R., Kohnová, S., Koskela, J.J., Ledvinka, O., Macdonald, N., Mavrova-Guigouina, M., Mediero, L., Merz, R., Molnar, P., Montanari, A., Murphy, C., Osuch, M., Ovcharuk, V., Radevski, I., Salinas, J.L., Sauquet, E., Šraj, M., Szolgay, J., Volpi, E., Wilson, D., Zaimi, K., Živković, N., 2019. Changing climate both increases and decreases European river floods. *Nature* 573, 108–111.
- Blöschl, G., Kiss, A., Viglione, A., Barriendos, M., Böhm, O., Brázdil, R., Coeur, D., Damaré, G., Lasat, M.C., Macdonald, N., Retsö, D., 2020. Current European flood-rich period exceptional compared with past 500 years. *Nature* 583, 560–566.
- Brunner, M.I., Fischer, S., 2022. Snow-influenced floods are more strongly connected in space than purely rainfall-driven floods. *Environ. Res. Lett.* 17, 104038.
- Brunner, M.I., Melsen, L.A., Wood, A.W., Rakovec, O., Mizukami, N., Knoben, W.J., Clark, M.P., 2021. Flood spatial coherence, triggers, and performance in hydrological simulations: large-sample evaluation of four streamflow-calibrated models. *Hydrol. Earth Syst. Sci.* 25, 105–119.
- Bryndal, T., 2015. Local flash floods in Central Europe: a case study of Poland. *Nor. Geol. Tidsskr.* 69, 288–298.
- Caloiero, T., Caloiero, P., Frustaci, F., 2018. Long-term precipitation trend analysis in Europe and in the Mediterranean basin. *Water Environ. J.* 32, 433–445.
- Chan, S.C., Kendon, E.J., Berthou, S., Fossier, G., Lewis, E., Fowler, H.J., 2020. Europe-wide precipitation projections at convection permitting scale with the Unified Model. *Clim. Dyn.* 55, 409–428.
- Deng, Y., Wang, S., Bai, X., Luo, G., Wu, L., Cao, Y., Li, H., Li, C., Yang, Y., Hu, Z., 2020. Variation trend of global soil moisture and its cause analysis. *Ecol. Indic.* 110, 105939.
- Di Sante, F., Coppola, E., Giorgi, F., 2021. Projections of river floods in Europe using EURO-CORDEX, CMIP5 and CMIP6 simulations. *Int. J. Climatol.* 41, 3203–3221.
- Do, H.X., Westra, S., Leonard, M., Gudmundsson, L., 2020a. Global-scale prediction of flood timing using atmospheric reanalysis. *Water Resour. Res.* 56, e2019WR024945.
- Do, H.X., Mei, Y., Gronewold, A.D., 2020b. To what extent are changes in flood magnitude related to changes in precipitation extremes? *Geophys. Res. Lett.* 47 (18), e2020GL088684.
- Dottori, F., Szewczyk, W., Ciscar, J.-C., Zhao, F., Alfieri, L., Hirabayashi, Y., Bianchi, A., Mongelli, I., Frieler, K., Betts, R.A., Feyen, L., 2018. Increased human and economic losses from river flooding with anthropogenic warming. *Nat. Clim. Chang.* 8, 781–786.
- Eini, M.R., Massari, C., Piniewski, M., 2023. Satellite-based soil moisture enhances the reliability of agro-hydrological modeling in large transboundary river basins. *Sci. Total Environ.* 873, 162396.
- Ekwueme, B.N., 2022. Machine learning based prediction of urban flood susceptibility from selected rivers in a tropical catchment area. *Civ. Eng. J.* 8 (09).
- El Kasri, J., Lahmili, A., Soussi, H., Jaouda, I., Bentaher, M., 2021. Trend analysis of meteorological variables: rainfall and temperature. *Civ. Eng. J.* 7, 1868–1879.
- Fang, G., Yang, J., Li, Z., Chen, Y., Duan, W., Amory, C., De Maeyer, P., 2022. Shifting in the global flood timing. *Sci. Rep.* 12, 18853.
- Fontronoda Bach, A., Van der Schrier, G., Melsen, L.A., Klein Tank, A.M.G., Teuling, A.J., 2018. Widespread and accelerated decrease of observed mean and extreme snow depth over Europe. *Geophys. Res. Lett.* 45, 12–312.
- Ford, C.M., Kendall, A.D., Hyndman, D.W., 2020. Effects of shifting snowmelt regimes on the hydrology of non-alpine temperate landscapes. *J. Hydrol.* 590, 125517.
- Grillakis, M.G., Koutroulis, A.G., Komma, J., Tsanis, I.K., Wagner, W., Blöschl, G., 2016. Initial soil moisture effects on flash flood generation—a comparison between basins of contrasting hydro-climatic conditions. *J. Hydrol.* 541, 206–217.
- Grusson, Y., Sun, X., Gascoin, S., Sauvage, S., Raghavan, S., Antil, F., Sánchez-Pérez, J.M., 2015. Assessing the capability of the SWAT model to simulate snow, snow melt and streamflow dynamics over an alpine watershed. *J. Hydrol.* 531, 574–588.
- Gvoždíková, B., Müller, M., Kašpar, M., 2019. Spatial patterns and time distribution of central European extreme precipitation events between 1961 and 2013. *Int. J. Climatol.* 39, 3282–3297.
- Hall, J., Blöschl, G., 2018. Spatial patterns and characteristics of flood seasonality in Europe. *Hydrol. Earth Syst. Sci.* 22, 3883–3901.
- Hall, J., Arheimer, B., Borge, M., Brázdil, R., Claps, P., Kiss, A., Kjeldsen, T., Kriaučiūnienė, J., Kundzewicz, Z.W., Lang, M., 2014. Understanding flood regime changes in Europe: a state-of-the-art assessment. *Hydrol. Earth Syst. Sci.* 18, 2735–2772.
- Hamed, K.H., Rao, A.R., 1998. A modified Mann-Kendall trend test for autocorrelated data. *J. Hydrol.* 204, 182–196.
- Hänsel, S., Hoy, A., Brendel, C., Maugeri, M., 2022. Record summers in Europe: Variations in drought and heavy precipitation during 1901–2018. *Int. J. Climatol.* 42 (12), 6235–6257.
- Hundecha, Y., Parajka, J., Viglione, A., 2020. Assessment of past flood changes across Europe based on flood-generating processes. *Hydrol. Sci. J.* 65, 1830–1847.
- Ionita, M., Nagavciuc, V., Guan, B., 2020. Rivers in the sky, flooding on the ground: the role of atmospheric rivers in inland flooding in central Europe. *Hydrol. Earth Syst. Sci.* 24, 5125–5147.
- IPCC, 2013. Climate change 2013: the physical science basis. Contribution of Working Group I to the Fifth Assessment Report of the Intergovernmental Panel on Climate Change. 1535.
- Jiang, S., Bevacqua, E., Zscheischler, J., 2022a. River flooding mechanisms and their changes in Europe revealed by explainable machine learning. *Hydrol. Earth Syst. Sci.* 26, 6339–6359.
- Jiang, S., Zheng, Y., Wang, C., Babovic, V., 2022b. Uncovering flooding mechanisms across the contiguous United States through interpretive deep learning on representative catchments. *Water Resour. Res.* 58 (1), e2021WR030185.
- Kemter, M., Merz, B., Marwan, N., Vorogushyn, S., Blöschl, G., 2020. Joint trends in flood magnitudes and spatial extents across Europe. *Geophys. Res. Lett.* 47, e2020GL087464.
- Kemter, M., Marwan, N., Villarini, G., Merz, B., 2023. Controls on flood trends across the United States. *Water Resour. Res.* 59, e2021WR031673.
- Kendall, M., 1975. Rank Correlation Methods. Oxford University Press, USA, London.
- Kendon, E.J., Roberts, N.M., Fowler, H.J., Roberts, M.J., Chan, S.C., Senior, C.A., 2014. Heavier summer downpours with climate change revealed by weather forecast resolution model. *Nat. Clim. Chang.* 4, 570–576.
- Kerr, H., Johnson, K., Toll, D.G., Mansfield, F., 2016. Flood holding capacity: a novel concept to evaluate the resilience of amended soils. *Geo-Chicago 2016 (Abstr.)*.
- Kijowska-Strugała, M., Bucała-Hrabia, A., 2019. Floods types in a mountain catchment: the Ochotnica River, Poland. *Acta Geogr. Slov.* 59, 23–36.
- Kirschenstein, M., 2009. Extreme twenty-four-hour precipitation sums in north-western Poland. *Baltic Coastal Zone. J. Ecol. Prot. Coastline* 13.
- Kis, A., Pongrácz, R., Bartholy, J., Szabó, J.A., 2020. Projection of runoff characteristics as a response to regional climate change in a Central/Eastern European catchment. *Hydrol. Sci. J.* 65, 2256–2273.
- Kjellström, E., Nikulin, G., Strandberg, G., Christensen, O.B., Jacob, D., Keuler, K., Lenderink, G., van Meijgaard, E., Schär, C., Somot, S., 2018. European climate change at global mean temperature increases of 1.5 and 2 C above pre-industrial conditions as simulated by the EURO-CORDEX regional climate models. *Earth Syst. Dyn.* 9, 459–478.
- Koks, E., Van Ginkel, K., Van Marle, M., Lemnitzer, A., 2021. Brief communication: critical infrastructure impacts of the 2021 mid-July western European flood event. *Nat. Hazards Earth Syst. Sci. Discuss.* 1–11.
- Kreienkamp, F., Philip, S.Y., Tradowsky, J.S., Kew, S.F., Lorenz, P., Arrighi, J., Belleflamme, A., Bettmann, T., Caluwaerts, S., Chan, S.C., 2021. Rapid attribution of heavy rainfall events leading to the severe flooding in Western Europe during July 2021. *World Weather Attribution*.
- Kundzewicz, Z.W., Matczak, P., 2012. Climate change regional review: Poland. *Wiley Interdiscip. Rev. Clim. Chang.* 3, 297–311.
- Kundzewicz, Z.W., Pińskwar, I., 2022. Are pluvial and fluvial floods on the rise? *Water* 14, 2612.
- Kundzewicz, Z.W., Szamalek, K., Kowalczak, P., 1999. The Great Flood of 1997 in Poland. *Hydrol. Sci. J.* 44, 855–870.
- Kundzewicz, Z.W., Pińskwar, I., Brakenridge, G.R., 2013. Large floods in Europe, 1985–2009. *Hydrol. Sci. J.* 58, 1–7.
- Kundzewicz, Z.W., Kanae, S., Seneviratne, S.I., Handmer, J., Nicholls, N., Peduzzi, P., Mechler, R., Bouwer, L.M., Arnell, N., Mach, K., Muir-Wood, R., Brakenridge, G.R., Kron, W., Benito, G., Honda, Y., Takahashi, K., Sherstyukov, B., 2014a. Flood risk and climate change: global and regional perspectives. *Hydrol. Sci. J.* 59, 1–28.
- Kundzewicz, Z.W., Stoffel, M., Kaczka, R.J., Wyżga, B., Niedźwiedź, T., Pińskwar, I., Ruiz-Villanueva, V., Lupikasza, E., Czajka, B., Ballesteros-Canovas, J.A., 2014b. Floods at the northern foothills of the Tatra Mountains—a Polish-Swiss research project. *Acta Geophys.* 62, 620–641.
- Kundzewicz, Z.W., Førland, E.J., Piniewski, M., 2017. Challenges for developing national climate services—Poland and Norway. *Clim. Serv.* 8, 17–25.
- Kundzewicz, Z.W., Piniewski, M., Mezghani, A., Okruszko, T., Pińskwar, I., Kardel, I., Hov, Ø., Szczepniak, M., Szwed, M., Benestad, R.E., 2018. Assessment of climate change and associated impact on selected sectors in Poland. *Acta Geophys.* 66, 1509–1523.
- Kundzewicz, Z.W., Szwed, M., Pińskwar, I., 2019. Climate variability and floods—a global review. *Water* 11, 1399.
- Lavers, D.A., Villarini, G., 2013. The nexus between atmospheric rivers and extreme precipitation across Europe. *Geophys. Res. Lett.* 40, 3259–3264.
- Lavers, D.A., Villarini, G., 2015. The contribution of atmospheric rivers to precipitation in Europe and the United States. *J. Hydrol.* 522, 382–390.
- Lin, W., Chen, H., 2022. Changes in the spatial-temporal characteristics of daily snowfall events over the Eurasian continent from 1980 to 2019. *Int. J. Climatol.* 42, 1841–1853.
- Lupikasza, E., 2010. Spatial and temporal variability of extreme precipitation in Poland in the period 1951–2006. *Int. J. Climatol.* 30, 991–1007.
- Mangini, W., Viglione, A., Hall, J., Hundecha, Y., Ceola, S., Montanari, A., Rogger, M., Salinas, J.L., Borzi, I., Parajka, J., 2018. Detection of trends in magnitude and frequency of flood peaks across Europe. *Hydrol. Sci. J.* 63, 493–512.
- Mann, H.B., 1945. Nonparametric tests against trend. *Econometrica* 245–259.
- Mao, Y., Zhou, T., Leung, L.R., Tesfa, T.K., Li, H.Y., Wang, K., Tan, Z., Getirana, A., 2019. Flood inundation generation mechanisms and their changes in 1953–2004 in global major river basins. *J. Geophys. Res.-Atmos.* 124, 11672–11692.
- Marchi, L., Borge, M., Preciso, E., Gaume, E., 2010. Characterisation of selected extreme flash floods in Europe and implications for flood risk management. *J. Hydrol.* 394, 118–133.
- Marcinkowski, P., Kardel, I., Płaczowska, E., Giełczewski, M., Osuch, P., Okruszko, T., Venegas-Cordero, N., Ignar, S., Piniewski, M., 2022. High-resolution simulated water balance and streamflow data set for 1951–2020 for the territory of Poland. *Geosci. Data J.* 00, 1–13.
- Mediero, L., Santillán, D., Garrote, L., Granados, A., 2014. Detection and attribution of trends in magnitude, frequency and timing of floods in Spain. *J. Hydrol.* 517, 1072–1088.
- Meresa, H.K., Romanowicz, R.J., Napiorkowski, J.J., 2017. Understanding changes and trends in projected hydroclimatic indices in selected Norwegian and Polish catchments. *Acta Geophys.* 65, 829–848.
- Merz, B., Blöschl, G., Vorogushyn, S., Dottori, F., Aerts, J.C.J.H., Bates, P., Bertola, M., Kemter, M., Kreibich, H., Lall, U., Macdonald, E., 2021. Causes, impacts and patterns of disastrous river floods. *Nat. Rev. Earth Environ.* 2, 592–609.
- Milly, P.C.D., Betancourt, J., Falkenmark, M., Hirsch, R.M., Kundzewicz, Z.W., Lettenmaier, D.P., Stouffer, R.J., 2008. Stationarity is dead: whither water management? *Science* 319, 573–574.
- Neitsch, S.L., Arnold, J.G., Kiniry, J.R., Williams, J.R., 2011. Soil And Water Assessment Tool Theoretical Documentation Version 2009. Texas Water Resources Institute.

- Nivedya, M.K., Tao, M., Mallick, R.B., Daniel, J.S., Jacobs, J.M., 2020. A framework for the assessment of contribution of base layer performance towards resilience of flexible pavement to flooding. *Int. J. Pavement Eng.* 21, 1223–1234.
- Piniewski, M., Marcinkowski, P., Kundzewicz, Z.W., 2018. Trend detection in river flow indices in Poland. *Acta Geophys.* 66, 347–360.
- Piniewski, M., Szcześniak, M., Kardel, I., Chattopadhyay, S., Berezowski, T., 2021. G2DC-PL+: a gridded 2 km daily climate dataset for the union of the Polish territory and the Vistula and Odra basins. *Earth Syst. Sci. Data* 13, 1273–1288.
- Pińskwar, I., 2022. Complex changes of extreme precipitation in the warming climate of Poland. *Int. J. Climatol.* 42, 817–833.
- Pińskwar, I., Choryński, A., Graczyk, D., Kundzewicz, Z.W., 2019. Observed changes in extreme precipitation in Poland: 1991–2015 versus 1961–1990. *Theor. Appl. Climatol.* 135, 773–787.
- Prudhomme, C., Parry, S., Hannaford, J., Clark, D.B., Hagemann, S., Voss, F., 2011. How well do large-scale models reproduce regional hydrological extremes in Europe? *J. Hydrometeorol.* 12 (6), 1181–1204.
- Qiao, L., Zuo, Z., Xiao, D., Bu, L., 2021. Detection, attribution, and future response of global soil moisture in summer. *Front. Earth Sci.* 9, 745185.
- Qin, T., Feng, J., Zhang, X., Li, C., Fan, J., Zhang, C., Dong, B., Wang, H., Yan, D., 2023. Continued decline of global soil moisture content, with obvious soil stratification and regional difference. *Sci. Total Environ.* 864, 160982.
- Romanowicz, R.J., Bogdanowicz, E., Debele, S.E., Doroszkiewicz, J., Hisdal, H., Lawrence, D., Meresa, H.K., Napiórkowski, J.J., Osuch, M., Strupczewski, W.G., Wilson, D., Wong, W.K., 2016. Climate change impact on hydrological extremes: preliminary results from the Polish-Norwegian project. *Acta Geophys.* 64, 477–509.
- Ruiz-Villanueva, V., Stoffel, M., Wyżga, B., Kundzewicz, Z.W., Czajka, B., Niedźwiedź, T., 2016. Decadal variability of floods in the northern foreland of the Tatra Mountains. *Reg. Environ. Chang.* 16, 603–615.
- Russo, S., Dosio, A., Sterl, A., Barbosa, P., Vogt, J., 2013. Projection of occurrence of extreme dry-wet years and seasons in Europe with stationary and nonstationary Standardized Precipitation Indices. *J. Geophys. Res.-Atmos.* 118 (14), 7628–7639.
- Sen, P.K., 1968. Estimates of the regression coefficient based on Kendall's tau. *J. Am. Stat. Assoc.* 63, 1379–1389.
- Serinaldi, F., Kilsby, C.G., Lombardo, F., 2018. Untenable nonstationarity: an assessment of the fitness for purpose of trend tests in hydrology. *Adv. Water Resour.* 111, 132–155.
- Sharma, A., Wasko, C., Lettenmaier, D.P., 2018. If precipitation extremes are increasing, why aren't floods? *Water Resour. Res.* 54, 8545–8551. <https://doi.org/10.1029/2018WR023749>.
- Shen, M., Chui, T.F.M., 2021. Contrasting scaling relationships of extreme precipitation and streamflow to temperature across the United States. *Environ. Res. Commun.* 3, 125008.
- Singh, J., Ghosh, S., Simonovic, S.P., Karmakar, S., 2021. Identification of flood seasonality and drivers across Canada. *Hydrol. Process.* 35, e14398.
- Siwek, J., Siwek, J.P., Żelazny, M., 2013. Environmental and land use factors affecting phosphate hysteresis patterns of stream water during flood events (Carpathian Foothills, Poland). *Hydrol. Process.* 27, 3674–3684.
- Slater, L., Villarini, G., Archfield, S., Faulkner, D., Lamb, R., Khouakhi, A., Yin, J., 2021. Global changes in 20-year, 50-year, and 100-year river floods. *Geophys. Res. Lett.* 48, e2020GL091824.
- Somorowska, U., 2017. Climate-driven changes to streamflow patterns in a groundwater-dominated catchment. *Acta Geophys.* 65, 789–798.
- Somorowska, U., 2023. Warming air temperature impacts snowfall patterns and increases cold-season baseflow in the Liwiec River basin (Poland) of the central European lowland. *Resources* 12, 18.
- Stahl, K., Tallaksen, L.M., Hannaford, J., Van Lanen, H.A.J., 2012. Filling the white space on maps of European runoff trends: estimates from a multi-model ensemble. *Hydrol. Earth Syst. Sci.* 16 (7), 2035–2047.
- Stein, L., Pianosi, F., Woods, R., 2020. Event-based classification for global study of river flood generating processes. *Hydrol. Process.* 34, 1514–1529.
- Stein, L., Clark, M.P., Knoben, W.J.M., Pianosi, F., Woods, R.A., 2021. How do climate and catchment attributes influence flood generating processes? A large-sample study for 671 catchments across the contiguous USA. *Water Resour. Res.* 57, e2020WR028300.
- Steirou, E., Gerlitz, L., Apel, H., Merz, B., 2017. Links between large-scale circulation patterns and streamflow in Central Europe: a review. *J. Hydrol.* 549, 484–500.
- Stocker, T. (Ed.), 2014. *Climate Change 2013: The Physical Science Basis: Working Group I Contribution to the Fifth Assessment Report of the Intergovernmental Panel on Climate Change*. Cambridge University Press.
- Sun, Q., Zhang, X., Zwiers, F., Westra, S., Alexander, L.V., 2021. A global, continental, and regional analysis of changes in extreme precipitation. *J. Clim.* 34, 243–258.
- Szwed, M., 2019. Variability of precipitation in Poland under climate change. *Theor. Appl. Climatol.* 135, 1003–1015.
- Szwed, M., Pińskwar, I., Kundzewicz, Z.W., Graczyk, D., Mezghani, A., 2017. Changes of snow cover in Poland. *Acta Geophys.* 65, 65–76.
- Tabari, H., Willems, P., 2018. Lagged influence of Atlantic and Pacific climate patterns on European extreme precipitation. *Sci. Rep.* 8, 5748.
- Tarasova, L., Merz, R., Kiss, A., Basso, S., Blöschl, G., Merz, B., Viglione, A., Plötner, S., Guse, B., Schumann, A., Fischer, S., 2019. Causative classification of river flood events. *Wiley Interdiscip. Rev. Water* 6, e1353.
- Tarasova, L., Basso, S., Merz, R., 2020. Transformation of generation processes from small runoff events to large floods. *Geophys. Res. Lett.* 47, e2020GL090547.
- Tarasova, L., Lun, D., Merz, R., Blöschl, G., Basso, S., Bertola, M., Miniussi, A., Rakovec, O., Samaniego, L., Thober, S., Kumar, R., 2023. Shifts in flood generation processes exacerbate regional flood anomalies in Europe. *Commun. Earth Environ.* 4, 49.
- Tellman, B., Sullivan, J.A., Kuhn, C., Kettner, A.J., Doyle, C.S., Brakenridge, G.R., Erickson, T.A., Slayback, D.A., 2021. Satellite imaging reveals increased proportion of population exposed to floods. *Nature* 596 (7870), 80–86.
- Tramblay, Y., Villarini, G., El Khalki, E.M., Gründemann, G., Hughes, D., 2021. Evaluation of the drivers responsible for flooding in Africa. *Water Resour. Res.* 57, e2021WR029595.
- Tramblay, Y., Villarini, G., Saidi, M.E., Massari, C., Stein, L., 2022. Classification of flood-generating processes in Africa. *Sci. Rep.* 12, 18920.
- Ulbrich, U., Brücher, T., Fink, A.H., Leckebusch, G.C., Krüger, A., Pinto, J.G., 2003. The central European floods of August 2002: part 1 – rainfall periods and flood development. *Weather* 58, 371–377.
- Van den Besselaar, E.J.M., Klein Tank, A.M.G., Buishand, T.A., 2013. Trends in European precipitation extremes over 1951–2010. *Int. J. Climatol.* 33, 2682–2689.
- Venegas-Cordero, N., Kundzewicz, Z.W., Jamro, S., Piniewski, M., 2022. Detection of trends in observed river floods in Poland. *J. Hydrol. Reg. Stud.* 41, 101098.
- Wang, F., Shao, W., Yu, H., Kan, G., He, X., Zhang, D., Ren, M., Wang, G., 2020. Re-evaluation of the power of the Mann-Kendall test for detecting monotonic trends in hydrometeorological time series. *Front. Earth Sci.* 8, 14.
- Wasko, C., Nathan, R., 2019. Influence of changes in rainfall and soil moisture on trends in flooding. *J. Hydrol.* 575, 432–441.
- Wasko, C., Nathan, R., Peel, M.C., 2020a. Trends in global flood and streamflow timing based on local water year. *Water Resour. Res.* 56, e2020WR027233.
- Wasko, C., Nathan, R., Peel, M.C., 2020b. Changes in antecedent soil moisture modulate flood seasonality in a changing climate. *Water Resour. Res.* 56, e2019WR026300.
- Winsemius, H.C., Aerts, J.C., Van Beek, L.P., Bierkens, M.F., Bouwman, A., Jongman, B., Kwadijk, J.C., Ligtoet, W., Lucas, P.L., Van Vuuren, D.P., 2016. Global drivers of future river flood risk. *Nat. Clim. Chang.* 6, 381–385.
- Wu, X., Che, T., Li, X., Wang, N., Yang, X., 2018. Slower snowmelt in spring along with climate warming across the Northern Hemisphere. *Geophys. Res. Lett.* 45, 12–331.
- Wypych, A., Ustrnul, Z., Czekierda, D., Palarz, A., Sulikowska, A., 2018. Extreme precipitation events in the Polish Carpathians and their synoptic determinants. *Időjárás* 122, 145–158.
- Zawadzki, J., Kędzior, M., 2014. Statistical analysis of soil moisture content changes in Central Europe using GLDAS database over three past decades. *Open Geosci.* 6, 344–353.
- Zolina, O., 2012. Changes in intense precipitation in Europe. *Changes in Flood Risk in Europe*. 10, pp. 97–119.

Co-author statements - Article 2

Appendix no. 2 – co-authorship statement

Warsaw, 01-04-2024

Nelson Enrique Venegas Cordero
nelson_venegas@sggw.edu.pl

**Department of Hydrology, Meteorology
and Water Management, Warsaw
University of Life Sciences**

Co-authorship statement

I hereby represent that in the article: Model-based assessment of flood generation mechanisms over Poland: The roles of precipitation, snowmelt, and soil moisture excess. Authors: Authors: Nelson Venegas-Cordero, Cyrine Cherrat, Zbigniew W Kundzewicz, Jitendra Singh, and Mikołaj Piniewski. Journal Science of The Total Environment, Volume 891, 15 September 2023, 164626, my individual contribution in the development thereof involved: Conceptualization, Investigation, Methodology, Software, Validation, Formal analysis, Visualization, Writing – original draft, Writing – review & editing.



Nelson Enrique Venegas Cordero

Montreal, 01-04-2024

Cyrine Cherrat
cyrine.cherrat@mail.mcgill.ca

**Department of Bioresource
Engineering, Faculty of Agricultural
and Environmental Sciences, McGill
University, Montreal, QC, Canada**

Co-authorship statement

I hereby represent that in the article: Model-based assessment of flood generation mechanisms over Poland: The roles of precipitation, snowmelt, and soil moisture excess. Authors: Authors: Nelson Venegas-Cordero, Cyrine Cherrat, Zbigniew W Kundzewicz, Jitendra Singh, and Mikołaj Piñiewski. Journal Science of The Total Environment, Volume 891, 15 September 2023, 164626, my individual contribution in the development thereof involved: Conceptualization, Methodology, Visualization, Writing – original draft, Writing – review & editing.



Cyrine Cherrat

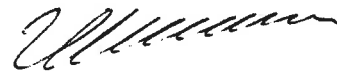
Poznań, 01-04-2024

Zbigniew W. Kundzewicz
kundzewicz@yahoo.com

**Meteorology Lab, Department of
Construction and Geoengineering,
Faculty of Environmental
Engineering and Mechanical
Engineering, Poznań University of
Life Sciences, Poznań, Poland**

Co-authorship statement

I hereby represent that in the article: Model-based assessment of flood generation mechanisms over Poland: The roles of precipitation, snowmelt, and soil moisture excess. Authors: Authors: Nelson Venegas-Cordero, Cyrine Cherrat, Zbigniew W Kundzewicz, Jitendra Singh, and Mikołaj Piniewski. Journal Science of The Total Environment, Volume 891, 15 September 2023, 164626, my individual contribution in the development thereof involved: Writing – original draft, Writing – review & editing].



Zbigniew W. Kundzewicz

Appendix no. 2 – co-authorship statement

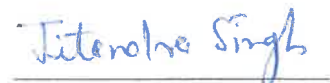
Zürich, 01-04-2024

Jitendra Singh
jitendra.singh@env.ethz.ch

**Institute for Atmospheric and
Climate Science, ETH Zürich,
Universitätstrasse 16, 8092, Zürich,
Switzerland**

Co-authorship statement

I hereby represent that in the article: Model-based assessment of flood generation mechanisms over Poland: The roles of precipitation, snowmelt, and soil moisture excess. Authors: Authors: Nelson Venegas-Cordero, Cyrine Cherrat, Zbigniew W Kundzewicz, Jitendra Singh, and Mikołaj Piniewski. Journal Science of The Total Environment, Volume 891, 15 September 2023, 164626, my individual contribution in the development thereof involved: Methodology, Writing – original draft, Writing – review & editing.



Jitendra Singh

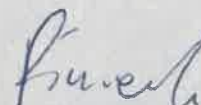
Appendix no. 2 – co-authorship statement

Warsaw, 01-04-2024

Mikołaj Piniewski
Department of Hydrology, Meteorology and Water Management,
Warsaw University of Life Sciences
mikolaj_piniewski@sggw.edu.pl

Co-authorship statement

I hereby represent that in the article: Model-based assessment of flood generation mechanisms over Poland: The roles of precipitation, snowmelt, and soil moisture excess. Authors: Nelson Venegas-Cordero, Cyrine Cherrat, Zbigniew W Kundzewicz, Jitendra Singh, and Mikołaj Piniewski. Journal Science of The Total Environment, Volume 891, 15 September 2023, 164626, my individual contribution in the development thereof involved: Conceptualization, Investigation, Writing – original draft, Writing – review & editing, Supervision.



Mikołaj Piniewski

Annex 3: Urbanization vs climate drivers: investigating changes in fluvial floods in Poland.
Stochastic Environmental Research and Risk Assessment (IF = 4.2).
<https://doi.org/10.1007/s00477-024-02717-z>



Urbanization vs. climate drivers: investigating changes in fluvial floods in Poland

Nelson Venegas-Cordero¹ · Luis Mediero² · Mikołaj Piniewski¹

Accepted: 30 March 2024

© The Author(s), under exclusive licence to Springer-Verlag GmbH Germany, part of Springer Nature 2024

Abstract

Fluvial floods are a severe hazard resulting from the interplay of climatic and anthropogenic factors. The most critical anthropogenic factor is urbanization, which increases land imperviousness. This study uses the paired catchment approach to investigate the effect of urbanization vs. climate drivers on river floods in Poland. Long-term daily river flow data until 2020 was used for four selected urban catchments and their non-urban counterparts, along with extreme precipitation, soil moisture excess, and snowmelt data generated from the process-based Soil & Water Assessment Tool (SWAT) model. Changes in impervious areas were assessed using two state-of-the-art Copernicus products, revealing a consistent upward trend in imperviousness across all selected urban catchments. A range of statistical methods were employed to assess changes in the magnitude and frequency of floods and flood drivers, including the Pettitt test, the Mann Kendall (MK) multitemporal test, the Poisson regression test, multi-temporal correlation analysis and multiple linear regression. The MK test results showed a contrasting behaviour between urban (increases) and non-urban (no change) catchments for three of the four analysed catchment pairs. Flood frequency increased significantly in only one urban catchment. Multiple regression analysis revealed that non-urban catchments consistently exhibited stronger relationships between floods and climate drivers than the urban ones, although the results of residual analysis were not statistically significant. In summary, the evidence for the impact of urbanization on floods was found to be moderate. The study highlights the significance of evaluating both climatic and anthropogenic factors when analysing river flood dynamics in Poland.

Keywords Flood · Extreme precipitation · Soil moisture excess · Snowmelt · Peak-over-threshold · Imperviousness

1 Introduction

River floods can be caused by various mechanisms, including extreme precipitation, soil moisture excess, snowmelt and rain-on-snow events (Berghuijs et al. 2019; Venegas-Cordero et al. 2023). Floods have caused substantial property damage and casualties globally. Climate change projections suggest that the frequency and intensity of extreme precipitation events will increase over large parts of the world

(Kundzewicz et al. 2014; Madsen et al. 2014; Prein et al. 2017; Tabari 2020), which could lead to further damage and casualties. In addition, studies have mentioned that around 75% of the population of the European Union is settled in urban areas, with an expected increase of urban extension for the future. This expansion has led to economic and social consequences, including changes in lifestyle, infrastructure demands and exposure to hazards such as river floods (Bulti and Abebe 2020; Depietri et al. 2012; Guerreiro et al. 2018; Hebbert 2012; Mediero et al. 2022; Skougaard Kaspersen et al. 2017).

Human activities, such as urbanization and changes in land use, can significantly alter catchment characteristics by increasing impermeable surfaces (soil sealing). This can reduce the absorption of precipitation during storms, leading to an increase in fast runoff processes (Bian et al. 2020; Du et al. 2015; Smith et al. 2023). Fluctuations in flows, and therefore the magnitude of floods, can increase due to alterations such as precipitation, excess soil moisture, snowmelt,

✉ Mikołaj Piniewski
mikolaj_piniewski@sggw.edu.pl

¹ Department of Hydrology, Meteorology and Water Management, Warsaw University of Life Sciences, Nowoursynowska 166, Warsaw 02-787, Poland

² Department of Civil Engineering: Hydraulics, Energy and Environment, Universidad Politécnica de Madrid, Madrid 28040, Spain

and other factors (Davenport et al. 2020; Hodgkins et al. 2017; Trambly et al. 2019; Venegas-Cordero et al. 2022, 2023). Urban areas worldwide have faced flooding events triggered by heavy precipitation in recent years (Francipane et al. 2021; Hoeppe 2016; Mou et al. 2022; Wang et al. 2019; Wasko and Nathan 2019). This issue is further compounded by global warming, which is predicted to intensify the hydrological cycle, resulting in more frequent and intense precipitation events on a global scale (Allan et al. 2020; Brunner et al. 2021; Giorgi et al. 2019; Tabari 2020).

Several recent studies have investigated the impact of land use change and urbanization on floods (Bayazit et al. 2021; Beckers et al. 2013; Brody et al. 2014; Skougaard Kaspersen et al. 2017). These studies have employed various methods, including paired-catchment studies (Requena et al. 2017; Prosdocimi et al. 2015; Salavati et al. 2016; Shao et al. 2020) or hydrological modelling (Jodar-Abellan et al. 2019; Gao et al. 2020; Zhang et al. 2020). In a study that attributed the urbanization effect on flood events using the paired-catchment approach in the UK, Prosdocimi et al. (2015) found a significant influence of increased urbanization levels on high flow occurrences, particularly during the summer season. The expansion of urban areas can cause faster water flow during heavy or prolonged precipitation events (Fletcher et al. 2013; Kishitawal et al. 2010; McGrane 2016; Skougaard et al., 2017). Furthermore, a study conducted in Mediterranean basins (SE Spain) used the SWAT model to demonstrate that flash flood risks increased due to changes in land use, specifically impacted by urban expansion (Jodar-Abellan et al. 2019).

A variety of studies have dealt with the topic of urbanization effect on floods in Poland (Pińskwar et al. 2023; Szeląg et al. 2021; Szwagrzyk et al. 2018). Pińskwar et al. (2023) specifically investigated the effectiveness of the State Fire Service interventions in the Wielkopolska region, west of Warsaw, and found that this area is particularly vulnerable to flash floods during extreme precipitation events. Then, a probabilistic methodology was also applied to study the interactions between changes in rainfall dynamics and impervious areas in different urban watersheds in Poland. The study demonstrated that the dynamics of land use changes (urbanization) have a strong impact on the number of floods (Szeląg et al. 2021). Conclusively, Szwagrzyk et al. (2018) showed the impact of projected land use changes on flood risk in the southern Polish mountain range and concluded that urban areas are expected to increase in existing flood-prone zones. Therefore, a substantial increase in estimated economic losses due to potential flooding can be expected. Our study will assess how urbanization has changed fluvial floods by integrating high-resolution, spatio-temporal data on soil imperviousness with observed river flow data and modelled data on climatic flood drivers over a significant

historical period. It will add depth to the existing literature by providing insights into the complex relationships between urban development, land use changes, and flood risk across diverse catchment areas in Poland.

Finally, in this study, the main objective is to evaluate the impact of urbanization on fluvial floods in Poland. To achieve this, we integrate high-resolution, spatio-temporal data on soil imperviousness with observed river flow data as well as modelled data on climatic flood drivers over the period 1951–2020. The study employs a combination of methods, including the paired-catchment approach, the annual maximum flow (AMF) and peak-over-threshold (POT) approaches, the multi-temporal trend analysis, and multiple linear regression. The analysis is conducted on eight small and medium-sized catchments around Poland with variable degrees of urbanization.

2 Data and methods

2.1 Imperviousness data

This research collected imperviousness data for the entire territory of Poland from two Copernicus products: (1) the Global Human Settlement (GHS) layer, which captures the GHS built-up data for the period 1975–2020 and (2) the ‘High Resolution Layer (HRL): Imperviousness Degree’ dataset covering the period 2006–2018. The first dataset is a freely available open surface grid with global coverage, derived from a fusion of Sentinel-2 composites and Landsat imagery in five-year intervals (Pesaresi and Politis, 2022). The GHS-BUILT-S product used in this study shows the distribution of the built-up surfaces (ranging from 0 to 10 000 m²), estimated for each grid cell at a resolution of 100 m.

The second one, developed by the European Environment Agency (EEA), is designed to detect the spatial distribution and temporal evolution of artificially sealed areas at a continental scale. The product is derived from high-resolution satellite imagery (ESA’s Sentinel-1 and Sentinel-2 satellites). The HRL Imperviousness Density product used in this study provides data on sealing density ranging from 0 to 100% at 20 m resolution for the period 2006–2018 with a three-year interval.

To enable comparison between the two products, the GHS-BUILT-S raster was divided by 100 which resulted in the same unit as the HRL layer (% of imperviousness). We used the zonal statistics functions in ArcGIS to calculate catchment-averaged imperviousness indicators by taking the average value across all pixels inside the catchment.

2.2 Hydrometeorological data

Daily discharge data was extracted from the Polish Institute of Meteorology and Water Management-National Research Institute (IMGW-PIB). As a first step, catchment selection analysis, as described in Sect. 2.3, was performed only on catchments with available discharge data. Following the study by Venegas-Cordero et al. (2023), we examined three hydroclimate variables, (precipitation, snowmelt and soil moisture excess) as potential flood generation mechanisms over Poland. The relevant data were obtained from the simulated water balance dataset (PL-SWAT-51_20) developed by Marcinkowski et al. (2021) for the area of Poland. These simulations were produced using the semi-distributed, process-based hydrological model SWAT, which was driven by the G2DC-PL + gridded climate dataset (Piniewski et al. 2021). For additional information on the PL-SWAT-51_20 dataset, readers can refer to Marcinkowski et al. (2021).

2.3 Paired catchment selection

The study initially examines the evolution of impervious surfaces in Poland using GHS and HRL products for their respective periods (Fig. 1; Table 1). The results reveal a significant shift in imperviousness patterns in Poland according to both data sources. The transition from non-impervious to impervious areas is clearly illustrated, demonstrating a consistent increase in impervious surfaces over time. However, both the actual value of average imperviousness and the rate of its increase are significantly higher for the HRL product, with values of 16.71% and 21.24% for 2006 and 2018, respectively.

After conducting a country-wide analysis of imperviousness, our workflow concentrated on selecting pairs of neighbouring catchments with contrasting imperviousness characteristics. To achieve this, we employed the commonly used paired-catchment approach, a classical technique employed in hydrology. This method involves comparing the response of two catchments with similar physical characteristics (Bosch and Hewlett 1982; Kreibich et al. 2017; Prosdociimi et al. 2015; Van Loon et al. 2019). This approach involves designating one of the catchments as a treatment (referred to as ‘urban’ in our case due to its high imperviousness) and the other as a control (referred to as ‘non-urban’ in our case due to its low imperviousness). Comparison of flood response between neighbouring catchments allows us to attribute the differences to urbanization, although confounding factors such as precipitation certainly exist.

The following data were used in catchment selection procedure: (i) GIS layers of the flow gauging stations and their draining catchment areas in Poland; (ii) meta-data on daily

river flow data availability for each gauging station; (iii) GHS and HRL imperviousness products.

Catchment selection was conducted in consecutive steps, as presented in Table 2. In the first four steps, we filtered 318 potential flow gauging stations (and draining catchments) based on catchment size, record length and presence of gaps in the time series. We assumed that capturing the effect of imperviousness on floods will be more likely in small and medium-sized catchments ($A < 1,000 \text{ km}^2$), as flood changes in large catchments could be driven by multiple variables, such as the spatial variability of precipitation. In the fifth step, we applied the Zonal statistics function in ArcGIS in order to calculate average imperviousness and imperviousness change values for each catchment. We thus derived 23 catchments characterized by high imperviousness and high imperviousness change. In the sixth step, we removed nested catchments (for example, if three catchments were nested, we kept the one with the highest imperviousness characteristics), which resulted in a subset of 16 potential urban catchments. The last step of analysis dealt with matching non-urban catchments to each potential urban catchment. For the majority of potential urban catchments, it was not possible to identify a counterpart, as we prioritized non-urban catchments lying in close proximity to the urban ones (up to 50 km distance) and having similar size (area difference up to 33%). The above procedure resulted in the final selection of four pairs of urban and non-urban catchments (Table 3).

Catchments in Table 3 are ordered by their increasing imperviousness index, from U1 (1.4% in 2020) to U4 (7.3% in 2020). The first pair was located in northern Poland, while the other three were clustered in the southern part of the country (Fig. 2; see Fig. S1 in Electronic Supplementary Material for a similar figure based on HRL data). For each pair, the difference in imperviousness indicators (both the actual state and the rate of change) between the urban and non-urban catchments is evident. Figure 2 shows that the respective indices for urban catchments are considerably higher than those for non-urban catchments. The selected catchments vary in size (ranging from 74 to 497 km^2) and mean elevation (ranging from 62 to 284 m asl). Flow record length ranges from 70 years (pair 4) to 41 years (pair 1), and for each case it extends to the year 2020. Thus, there is a significant alignment between the time windows of the flow data and the temporal coverage period of the GHS product.

2.4 Flood and climate indices

This study uses two different approaches to extract flood time series: annual maximum river discharge (Q_{MAX}) and peaks-over-threshold (POT). The main goal is to determine whether increasing imperviousness in urban catchments

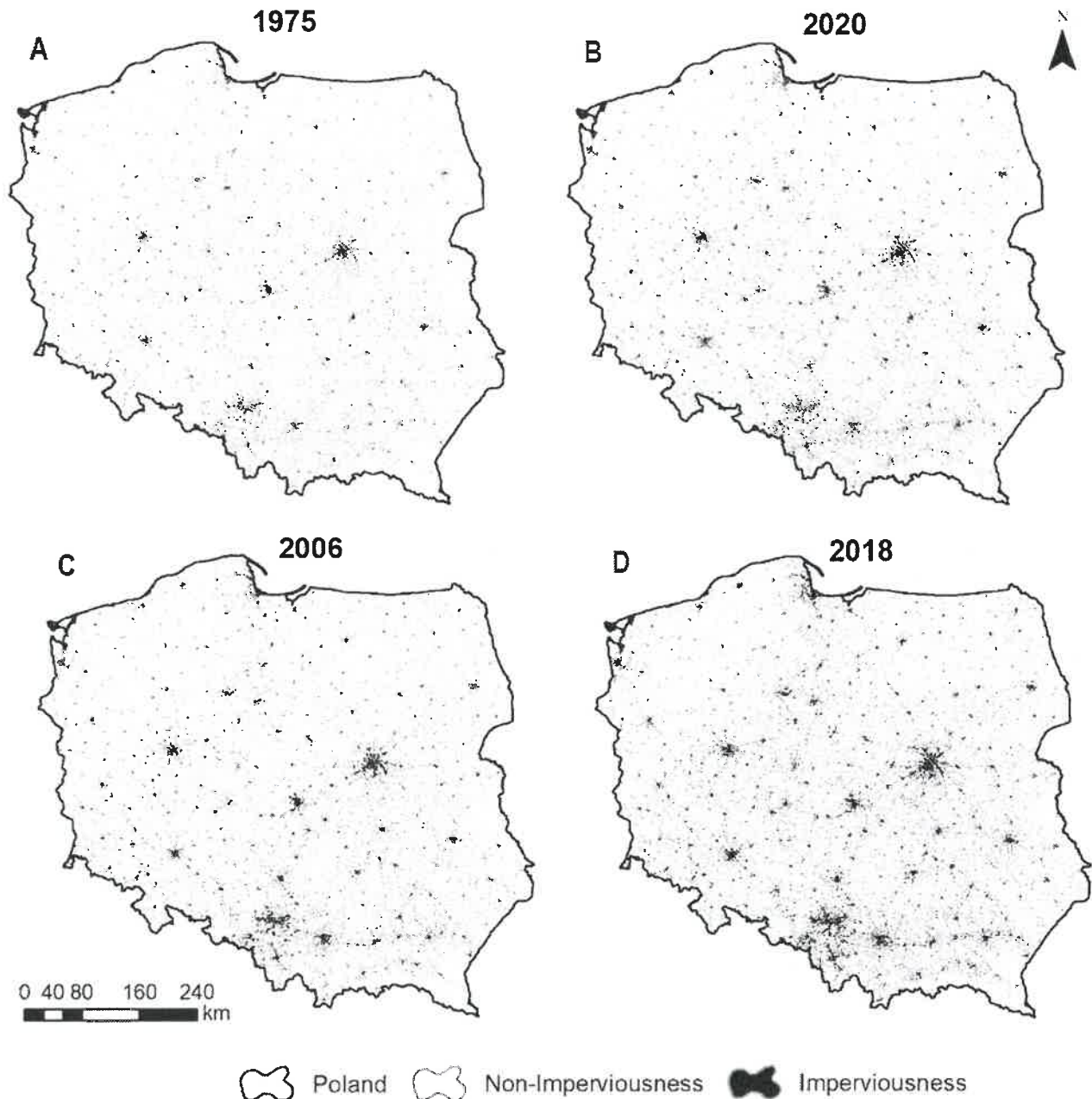


Fig. 1 Evolution of the Imperviousness in Poland according to the GHS (1975 panel **A**, 2020 panel **B**) and HRL (2006 panel **C**, 2018 panel **D**) products

Table 1 Imperviousness and non-imperviousness area percentages in Poland (1975–2020 and 2006–2018)

Year	Non-impervious (%)	Impervious (%)
GHS		
1975	87.79	12.21
2020	83.48	16.52
HRL		
2006	83.29	16.71
2018	78.76	21.24

leads to an increase in flood magnitude or frequency. However, we also include other potential drivers of flood changes, such as extreme precipitation, snowmelt and soil moisture excess (Berghuijs et al. 2019; Venegas-Cordero et al. 2023). The flood and climate indices considered in the study are listed in Table 4.

PCP_{MAX} represents the 3 day-maximum amount recorded in a year. While SME_{MAX} is based on the maximum value

Table 2 Procedure of paired catchment selection applied in this study

Step	Description	Number
1	All gauged catchments	1073
2	Filtered by area ($A < 1000 \text{ km}^2$)	706
3	Filtered by record length (≥ 30 years)	394
4	Filtered by presence of gaps (less than 1 year)	318
5	Filtered by high Imperviousness characteristics (subset of potential urban catchments)	23
6	Removal of nested catchments	16
7	Final matching of catchment pairs	4*

* 4 pairs of urban and non-urban catchments

recorded in a year, where it was calculated based in Venegas-Cordero et al. (2023) with the following equation:

$$SME = PCP - SM_{MAX} - SM \quad (1)$$

where SME is the soil moisture excess, PCP is the daily precipitation, SM_{MAX} is the soil moisture storage capacity (fixed to 125 mm) as Berghuijs et al. (2019) and Venegas-Cordero et al. (2023), and SM is the daily soil moisture amount. Furthermore, SMN_{MAX} represents the highest accumulation observed in a given year.

Q_{MAX} correspond to the maximum discharge recorded in a given year. In contrast, POT is based on the extraction of hydrograph peaks exceeding a predefined threshold regardless when the peaks occurred. Therefore, the POT approach can extract a broader range of events, which are the largest events in the time series, and allows for controlling the number of flood occurrences included in the analysis by appropriately selecting the threshold (Lang et al. 1999; Madsen et al. 1997; Mangini et al. 2018; Venegas-Cordero et al. 2022). We assess flood magnitude changes using both Q_{MAX} and POT, with a specific emphasis on the POT approach for flood frequency analysis.

The POT method is employed to effectively detect variations in flood frequency, owing to its ability to identify multiple flood events within a given year. To achieve this, we used a predefined threshold, which allowed us to detect an average of three events per year. Several flood analysis worldwide have employed thresholds based on percentiles (Jiang et al. 2022; Mallakpour and Villarini 2015;

Venegas-Cordero et al. 2022; Villarini et al. 2011). Furthermore, to prevent the double counting of peaks belonging to the same flood event, we selected the largest peak within a 15-day period (Jiang et al. 2022; Mallakpour and Villarini 2015).

2.5 Statistical analysis

The Pettitt test is a non-parametric method designed to detect change points in the mean or median of a time series. This approach was applied to the Q_{MAX} and POT3 time series extracted previously. The p-values were calculated for the test statistic using Pettitt's approximated limiting distribution, which is specifically designed for continuous variables (Pettitt 1979; Villarini et al. 2009). A significance level of 5% was considered.

The Mann-Kendall (MK) test (Kendall 1975; Mann 1945) was used to detect trends in flood magnitude indicator time series of Q_{MAX} and POT3. The Sen's slope test was used to assess trend magnitudes (Sen 1968). The MK test is designed to identify the presence of monotonic either upward or downward trends. The Sen's slope is based on the median slope between all ordered pairs of observations for a given time series (Piniewski et al. 2018; Venegas-Cordero et al. 2023). Moreover, the MK test is an appropriate method for analysing hydrological datasets with non-normal distribution characteristics (Kundzewicz and Robson 2004; Mediero et al. 2014; Venegas-Cordero et al. 2022).

The Poisson regression test was applied to POT3F time series as reported in previous publications (Aryal et al. 2018; Mangini et al. 2018; Venegas-Cordero et al. 2022; Vormoor et al. 2016). The sensitivity of the period considered in the time series was analysed for both the MK test detected trends for flood magnitude and the Poisson regression for flood frequency by using the multi-temporal trend analysis. This method detects trends for all possible combinations of starting and ending years in the time series (Hannaford et al. 2013, 2021; Mediero et al. 2014; Ruiz-Villanueva et al. 2016). The minimum time window was set to 20 years.

In this study, the MK test is based on the following equations as shown in Venegas-Cordero et al. (2023):

Table 3 Basic catchment characteristics and flow data availability

Pair ID	Gauge name	River name	Type	Code	Area (km^2)	Elevation (m)	Starting year	Ending year	Missing data
1	Krępa	Głazna	Urban	U1	73.7	61.7	1980	2020	-
	Pogorzelice	Pogorzelica	Non-Urban	N1	91.2	107.8	1980	2020	-
2	Kuźnica Skakawska	Niesób	Urban	U2	244.7	168.6	1971	2020	-
	Gorzów Śląski	Proсна	Non-Urban	N2	164.5	207.8	1971	2020	-
3	Lesiów	Mleczna	Urban	U3	338.9	164.2	1973	2020	2002
	Bzin	Kamienna	Non-Urban	N3	276.2	269.9	1973	2020	-
4	Szabelnia	Brynica	Urban	U4	496.6	283.7	1951	2020	-
	Krupski Młyn	Mała Panew	Non-Urban	N4	665.8	268.8	1951	2020	-

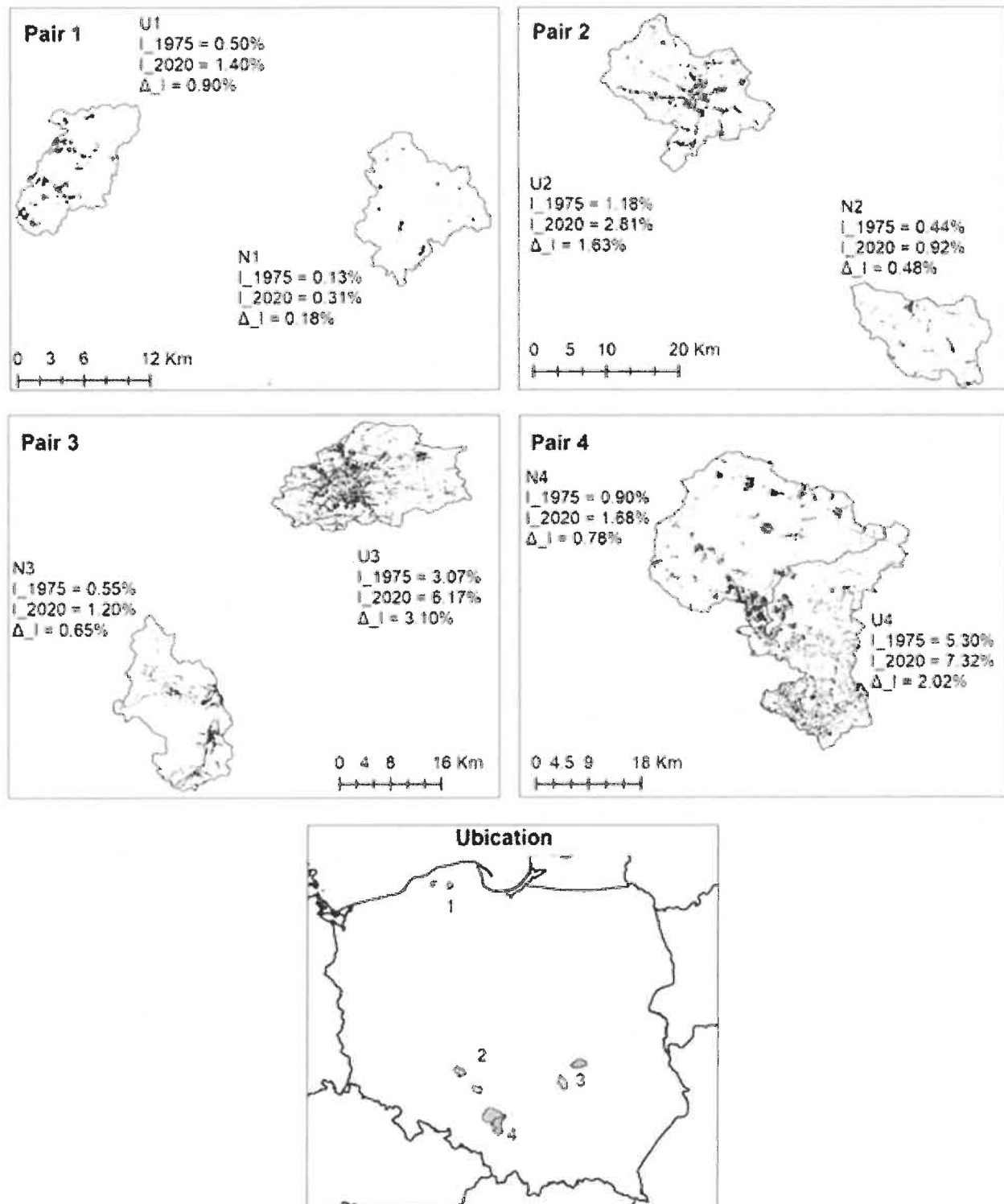


Fig. 2 Location of four pairs of catchments used in this study; Urban and non-urban catchments are shown in orange and green, respectively. Evolution of the imperviousness rate between 1975 (I_{1975}) and 2020 (I_{2020}) and relative change (Δ_I) is shown for each pair

Table 4 Flood and climate indices

Index	Abbreviation	Description
Annual maximum river discharge (m ³ /s)	Q _{MAX}	Maximum daily discharge in each year
Peak-over-threshold magnitude (m ³ /s)	POT3	Hydrograph peaks that exceed a given threshold with an average of three exceedances per year
Peak-over-threshold frequency (m ³ /s)	POT3F	Annual number of peaks that exceed the given threshold per year
Annual maximum 3-day precipitation (mm)	PCP _{MAX}	Maximum 3-day precipitation in each year
Annual maximum soil moisture excess (mm)	SME _{MAX}	Maximum daily soil moisture excess in each year
Annual maximum snowmelt (mm)	SMN _{MAX}	Maximum daily snowmelt in each year

$$S = \sum_{i=1}^{n-1} \sum_{j=1+1}^n \text{sgn}(X_j - X_i) \quad (2)$$

$$\text{sgn}(X_j - X_i) = \begin{cases} 1 & \text{if } (X_j - X_i) > 0 \\ 0 & \text{if } (X_j - X_i) = 0 \\ -1 & \text{if } (X_j - X_i) < 0 \end{cases} \quad (3)$$

where X_j and X_i are the values sorted by data sequence and n is the length of the time series.

The Z statistic is the standardized value of the trend, which is calculated with the following equations as illustrated in Hannaford et al. (2013):

$$Z = \begin{cases} \frac{S-1}{\sqrt{\text{Var}(S)}} \text{if } S > 0 \\ 0 & \text{if } S = 0 \\ \frac{S+1}{\sqrt{\text{Var}(S)}} \text{if } S < 0 \end{cases} \quad (4)$$

The multi-temporal trend analysis approach was used to analyse the sensitivity of the selected period for calculating the Pearson product moment correlations between Q_{MAX} time series and PCP_{MAX}, SME_{MAX} and SMN_{MAX} time series, respectively. The Pearson r correlation coefficient measures the strength of a linear relationship between the respective variables. Both multi-temporal trend and correlation analyses were carried out for the entire record length of each pair, as shown in Table 3.

2.6 Multi-temporal correlation analysis

We applied the Pearson correlations between the time series of flood magnitude (Q_{MAX}) and flood drivers (PCP_{MAX}, SMN_{MAX} and SME_{MAX}), following the methodology of previous studies (Lin et al. 2023; Venegas-Cordero et al. 2023; Wu and Huang 2015). Additionally, we evaluated the

sensitivity of the period, by detecting the correlation value for all possible combinations of starting and ending years with a minimum time window of 20 years.

2.7 Multiple linear regression

We determined the influence of climatic variables on Q_{MAX} time series, using a multiple linear regression in which maximum precipitation, soil moisture excess and snowmelt were used as the predictor variables of annual maximum flow, similar to the study implemented by Vicente-Serrano et al. (2019). A temporal multiple regression analysis was conducted for each paired-catchment with the following equation:

$$Q \sim PCP + SME + SMN \quad (5)$$

where Q , PCP , SME and SMN are the annual maximum flow, precipitation, soil moisture excess and snowmelt, respectively.

We then calculated a time series of regression residuals using the observed and predicted Q_{MAX}, which was obtained from the regression model in Eq. 5. We applied the MK test with the Z -statistic and a p -value (at a 10% significance level) on the residual time series to evaluate possible changes in the role of climatic variables or urbanization on the annual maximum flow, following Vicente-Serrano et al. (2019). It is assumed that the residual time series is independent of climate variables. Therefore, statistically significant trends in residuals may be attributed to increasing imperviousness in urban catchments. Therefore, in the paired-catchment context, the difference in Z values of the MK test applied to Q_{MAX} residuals between urban and non-urban catchments may also be attributed to the main differing factor between each paired catchment, which is imperviousness.

3 Results

3.1 Imperviousness change

The analysis of the change in imperviousness indicator based on the GHS product for the period 1975–2020 reveals a consistent upward pattern across all catchment pairs considered in the study (Fig. 3). For all eight studied catchments the imperviousness rate was increasing in all 5-year time intervals. However, for each pair the rate of change in imperviousness for the urban catchment was significantly higher than for the non-urban catchment.

The additional analysis based on the higher resolution of the HRL product for the shorter period 2006–2018 corroborates previous findings. However, the rate of change within

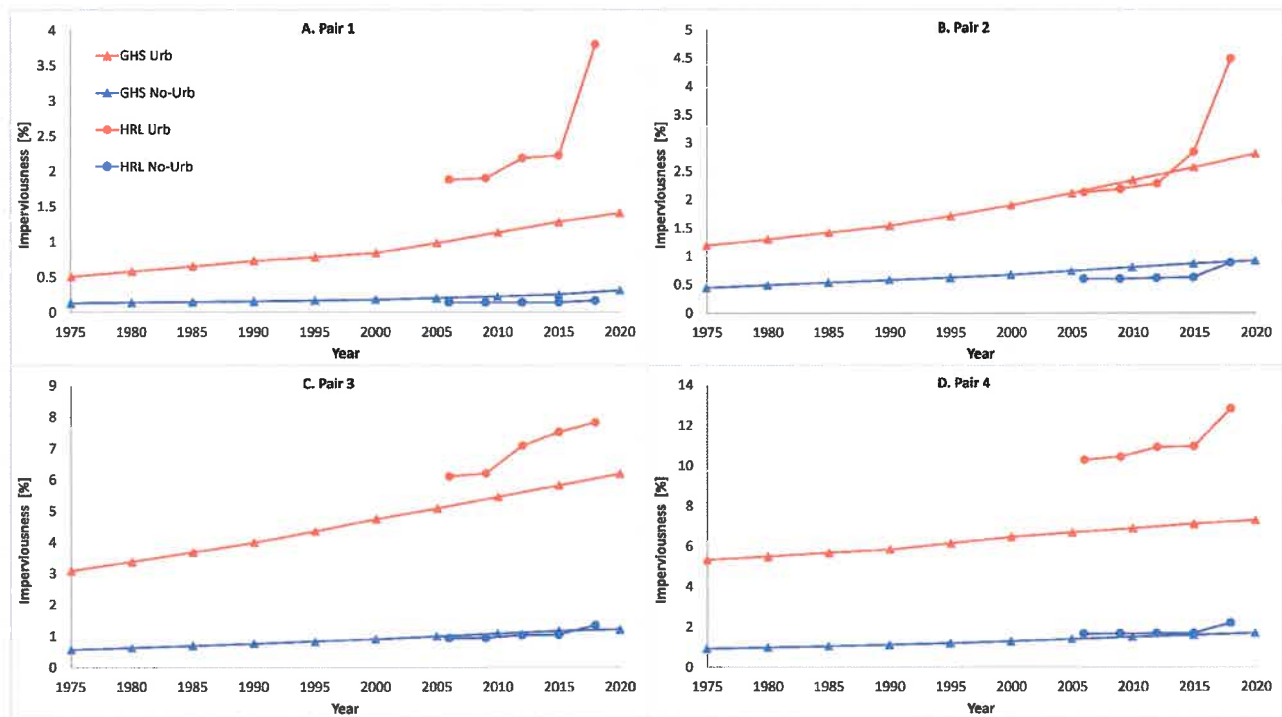


Fig. 3 Changes in imperviousness (%) for all catchment pairs in the period 1975–2020. Red color refers to urban catchments and blue color to non-urban. Circles represent HRL data and triangles GHS

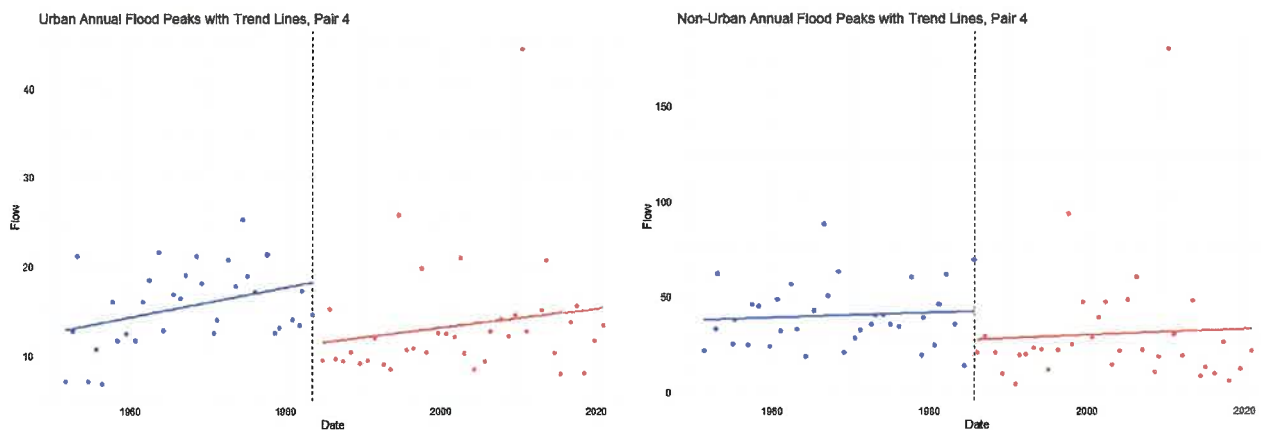


Fig. 4 Change point detection using the Pettitt test for the catchment pair 4. Vertical dashed line represents change point years

3-year intervals is not as stable as for the GHS product. Particularly, high increases reaching 1.7% were revealed for catchments U1 and U2 during the last interval 2015–2018. Pair 3 illustrates a progressive increase in urbanization, with urban values steadily climbing from 1.88% in 2006 to 3.79% in 2018, accompanied by relatively consistent non-urban values hovering around 0.14% throughout the period. Pair 4 presents urban values rising from 6.09% in 2006 to 7.81% in 2018, reflecting a noticeable urban expansion, while the non-urban values show a slight increase from 0.92 to 1.34%.

3.2 Change point detection

The change point analysis for Q_{MAX} time series using the Pettitt test allowed us to detect a change point for both catchments U4 and N4 of the pair 4, while for the remaining three pairs of catchments no change point was detected. The years 1983 and 1985 were the change point years for catchments U4 and N4, respectively (Fig. 4). In both cases an abrupt decrease in Q_{MAX} occurred in mid-1980s. Therefore, we can draw the hypothesis that the change could be caused by climatic factors rather than urbanization. It should be noted

that while pair 4 features the longest record length dating back to 1951, the other pairs have significantly shorter periods which perhaps made it harder to detect the change point in 1980s.

Consequently, in subsequent analysis for pair 4 we split the period into two sub-periods: 1951–1982 and 1984–2020 for U4, and 1951–1984 and 1986–2020 for N4.

3.3 Detection of trends in Q_{MAX}

This section focuses on the detection of monotonic trends for all catchments. The multi-temporal trend analysis results for Q_{MAX} for all paired catchments are shown in Fig. 5. The results confirm the sensitivity of MK test statistics to the

period considered, with clear differences between the urban and non-urban catchments. For catchment U1, a significant increasing trend was detected for most of combinations of starting and ending years. It was particularly strong for starting years in the period 1982–1992 and ending years in the period 2007–2018. In contrast, no significant trends were observed in catchment N1, which belongs to the same pair. This suggests that urbanization may be a plausible factor in explaining the increase in Q_{MAX} in catchment U1 during this period.

The results for pair 2 showed similarities in flood trends between the urban (U2) and non-urban (N2) catchments. In both of them, trends were mostly non-significant, with a few

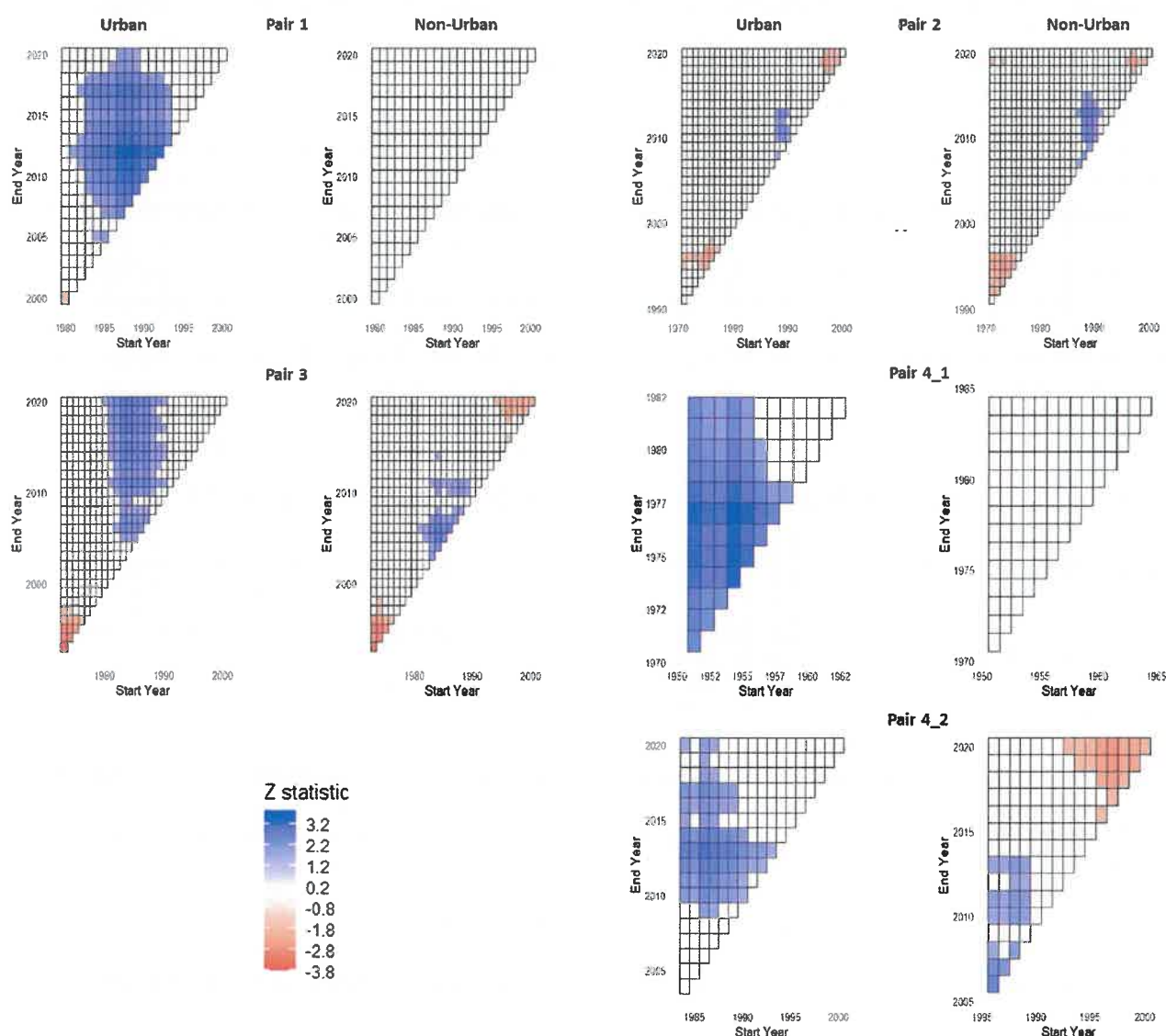


Fig. 5 Multi-temporal trend analysis for Q_{MAX} for all catchment pairs. The x and y axes represent the starting and ending years, respectively. Each pixel is colored according to the resulting Z statistic from the MK

test and the p -value (pixels with $p > 10\%$ are left blank). Red and blue colors represent decreasing and increasing trends, respectively

exceptions that are similar in both catchments. Thus, in this case there is no evidence for the role of urbanization.

For the catchment U3, Q_{MAX} trends are significantly positive across most sub-periods that start in the 1980s. However, trends were mostly non-significant for the same sub-periods for catchment N3 (apart from those ending before 2012). As with the catchment pair 1, it suggests that urbanization could be a factor explaining the differing behavior between the two catchments. Moreover, the difference was more noticeable for sub-periods ending in the years 2015–2020, which were the periods most affected by the urbanization process in catchment U3 (Fig. 3).

Finally, for the catchment pair 4, the catchment U4 showed a predominantly positive trend in Q_{MAX} for almost all possible combinations of start and end years during the sub-period 1 (1951–1982). No significant trends were found for its paired non-urban catchment N4. Therefore, the difference in catchment behaviour could be attributed to urbanization. In the case of the sub-period 2 (1984–2020), the difference between U4 and N4 is not as evident, yet still noticeable. For the urban catchment area U4 in sub-period 2, increasing trends were observed for most of the sub-periods ending in the years 2010–2020. In the case of its non-urban pair N4, the majority of trends were non-significant, although a few significant increasing trends were also detected for the sub-periods ending in years 2005–2013 and decreasing at the end of the years 2016–2020.

3.4 Detection of trends in POT3

Figure 6 shows the results of the multi-temporal trend analysis for the magnitude of POT3 time series in all paired catchments. The results partially support previous findings with Q_{MAX} . The strongest evidence for the impact of urbanization on floods estimated using the POT approach could be found for the catchment pair 4 in the sub-period 2. Some evidence is also observed for catchment pairs 1 and 3, although only for a limited number of combinations of starting and ending years. Quite surprisingly, the non-urban catchment N2 shows an inverse behaviour in comparison with other non-urban catchments, exhibiting a positive trend for the periods starting in years 1980–1985. Therefore, in this case the comparison with its paired catchment U2 leads to a different conclusion regarding the role of imperviousness compared to other pairs.

3.5 Detection of trends in POT frequency

The frequency of flood events is determined using on the POT3F time series. Figure 7 shows the multi-temporal trend changes in the number of annual flood events that exceed a given threshold over time, as determined by the

Poisson regression test. We observed that for the majority of time windows, no statistically significant changes in the flood frequency could be detected. The largest difference between the urban and non-urban catchments was found for the catchment pair 4, for which increases in flood frequency were detected for catchment U4, while no changes were found for catchment N4. For the remaining pairs the differences between urban and non-urban catchments was negligible.

3.6 Multi-temporal correlation

A comprehensive linear correlation analysis was conducted between Q_{MAX} and PCP_{MAX} , SME_{MAX} , and SMN_{MAX} for all possible combinations of starting and ending years within the time windows of data availability of each pair, to have a better insight into the role of climatic factors on flood generation (Fig. 8). It could be expected that non-urban catchments will generally exhibit higher correlation coefficients than their paired urban catchments, as urbanization can be regarded as a confounding factor for the relationship between climate indices and floods. It was the case for catchment pair 1 (particularly strong for the soil moisture excess), pair 3 (precipitation) and pair 4 (precipitation and snow melt). In the case of pair 2, the patterns in correlation plots were largely similar for U2 and N2 catchments for SME and SNM, while for PCP the urban catchment exhibited significantly higher correlations. This result is consistent with previous findings in our study that found no effect of urbanization on this pair (Figs. 5, 6).

3.7 Multiple regression with climate variables

Table 5 presents the results of the multiple regression analysis between Q_{MAX} and climate indices for each pair. The R^2 of the multiple regression model varied considerably between catchments, ranging from 0.07 (U1) to 0.62 (U3 and N3). The coefficients of determination for pairs 1 and 4_2 (sub-period 2) were compared, revealing that non-urban catchments exhibit stronger relationships between floods and climate indices than the urban ones. A detailed analysis of the R^2 values obtained from multiple regression reveals certain patterns. It appears that precipitation is not the dominant explanatory factor in any of the studied catchments. Instead, soil moisture excess and snow melt seem to have higher explanatory power.

In addition, the analysis of residuals did not reveal any significant trends (with an exception of catchment N3 having a statistically significant decreasing trend at $p=0.1$; see Fig. S2-S6 in Electronic Supplementary Material). The absence of statistically significant increasing trends in urban catchments could be interpreted as the lack of an effect of

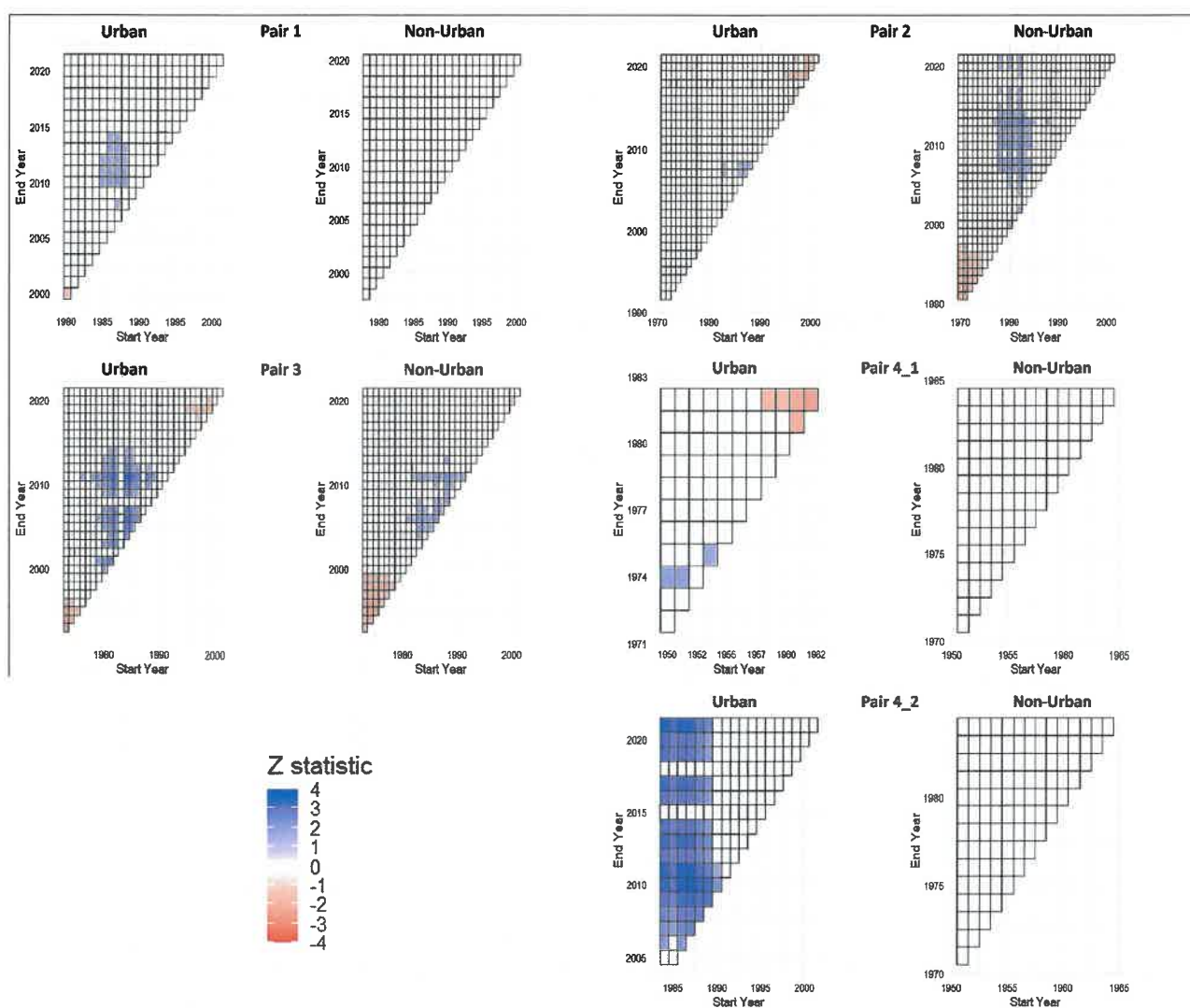


Fig. 6 Multi-temporal trend analysis for the POT3 magnitude time series for all catchment pairs. The x and y axes represent the starting and ending years, respectively. Each pixel is colored according to

the resulting Z statistic from the MK test and the p value (pixels with $p > 10\%$ are left blank). Red and blue colors represent decreasing and increasing trends, respectively

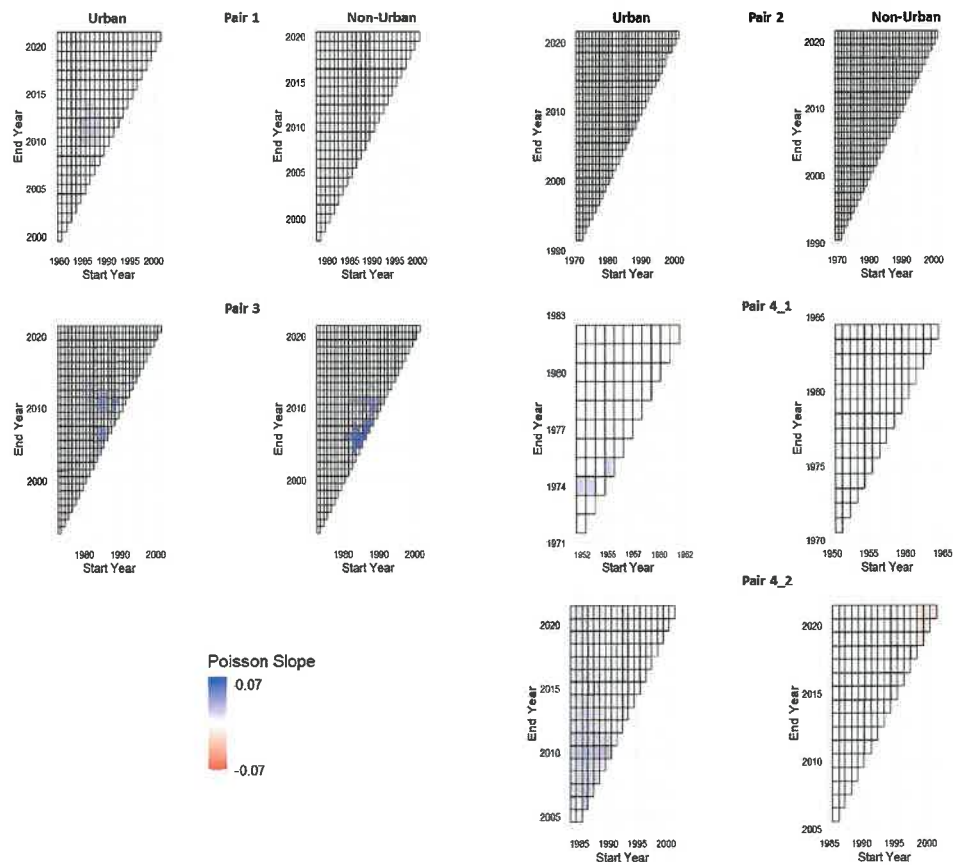
imperviousness in flood changes. However, taking the context of the paired-catchment approach, it makes sense to compare z values of residuals for each pair. The differences in residuals are for all cases quite high and positive except for pair 4 in sub-period 2, thus providing an indirect evidence supporting the hypothesis about the effect of urbanization on floods.

4 Discussion

The rate of imperviousness increase in the studied Polish urban catchments may not have been as high as observed worldwide. For example, Requena et al. (2017) who studied the potential effect of urbanization on the peak flows in

a paired catchment study in the northwest of England, the imperviousness in an urban catchment increased by 7% during 30 years which is much higher than in any of our urban catchments. Prosdocimi et al. (2015) also detected a higher increase (10.1%) over 40 years in an urban catchment in the UK. In Finland, a catchment has rapidly developed from a rural area to urban in 2001–2006, especially for a residential development (Guan et al. 2015). Finally, in the USA, in a historical study, a non-significant increase of annual maximum flows has been detected for a catchment with a higher increase (20%) of imperviousness in around two decades (Brun and Band 2000). However, in our study, the increases of imperviousness between 1975 and 2020 ranged between 0.9 and 3.1% according to the GHS product. It is noteworthy that, with an exception of catchment U4 belonging to

Fig. 7 Multi-temporal trend analysis for the POT3F time series for all catchment pairs. The x and y axes represent the starting and ending years, respectively. Each pixel is colored according to the resulting the Poisson regression test and the p value (pixels with $p > 10\%$ are left blank). Red and blue colors represent decreasing and increasing trends, respectively



Upper Silesian metropolitan area, the identified urban catchments did not intersect with any of the major metropolitan areas in Poland, such as Warsaw, Kraków, Wrocław, Łódź or Poznań. The increase in imperviousness in these areas might have been more pronounced than in catchments used in this study. The reason why several catchments in highly urbanized regions could not be used in our study was that they did not meet our selection criteria outlined in Sect. 2.3, e.g. the flow data had too many gaps or there was no appropriate non-urban catchment in the proximity of 50 km. A small sample size is a limitation of the present study.

In our study, a significant increase in Q_{MAX} was observed for urban catchments in pairs 1, 2 and 4 for some combinations of the starting and ending years. However, non-urban catchments did not generally exhibit any significant trends in Q_{max} , which corroborates well with the study of Venegas-Cordero et al. (2022), who reported that only 18% of 147 flow gauges in Poland exhibit statistically significant trends in the period 1981–2019. Requena et al. (2017) found positive trend in an urban area, similar as our results. Also, they mentioned that the changes in the annual series would be mainly due to changes in summer, where the extreme precipitation events are the main element associated with the summer time (Requena et al. 2017). However, the relationship between extreme precipitation and flooding is more

complex on a larger scale, in non-urban areas, for all but the most extreme precipitation events (Ivancic et al. 2015). Modifications in soil moisture emerge as the prevailing element influencing the identified shifts in flooding dynamics (Wasko and Nathan 2019). In our study the soil moisture excess and snowmelt have a stronger effect than extreme precipitation, which aligns with a recent study that identified these two flood mechanisms as principal ones in Poland (Venegas-Cordero et al. 2023). Nonetheless, a long-term analysis showed that the relative importance of snowmelt as a flood driver was decreasing over large parts of Poland in favour of the soil moisture excess (Venegas-Cordero et al. 2023). This change seems to be influenced by factors such as seasonality and antecedent catchment conditions, which play a crucial role in determining the magnitude and impact of floods (Kochanek et al. 2012; Sivapalan et al. 2005).

It is important to note that the nature of evidence pertaining to the effect of urbanization on floods in our study is, at best, moderate. Floods can exhibit variable patterns across different seasons, influenced by factors such as precipitation, snowmelt, and antecedent catchments conditions (Kochanek et al. 2012; Sivapalan et al. 2005). Hence, conducting seasonal flood analysis could yield stronger relationships. In addition, the distance between urban and non-urban catchments may also play a role. We found

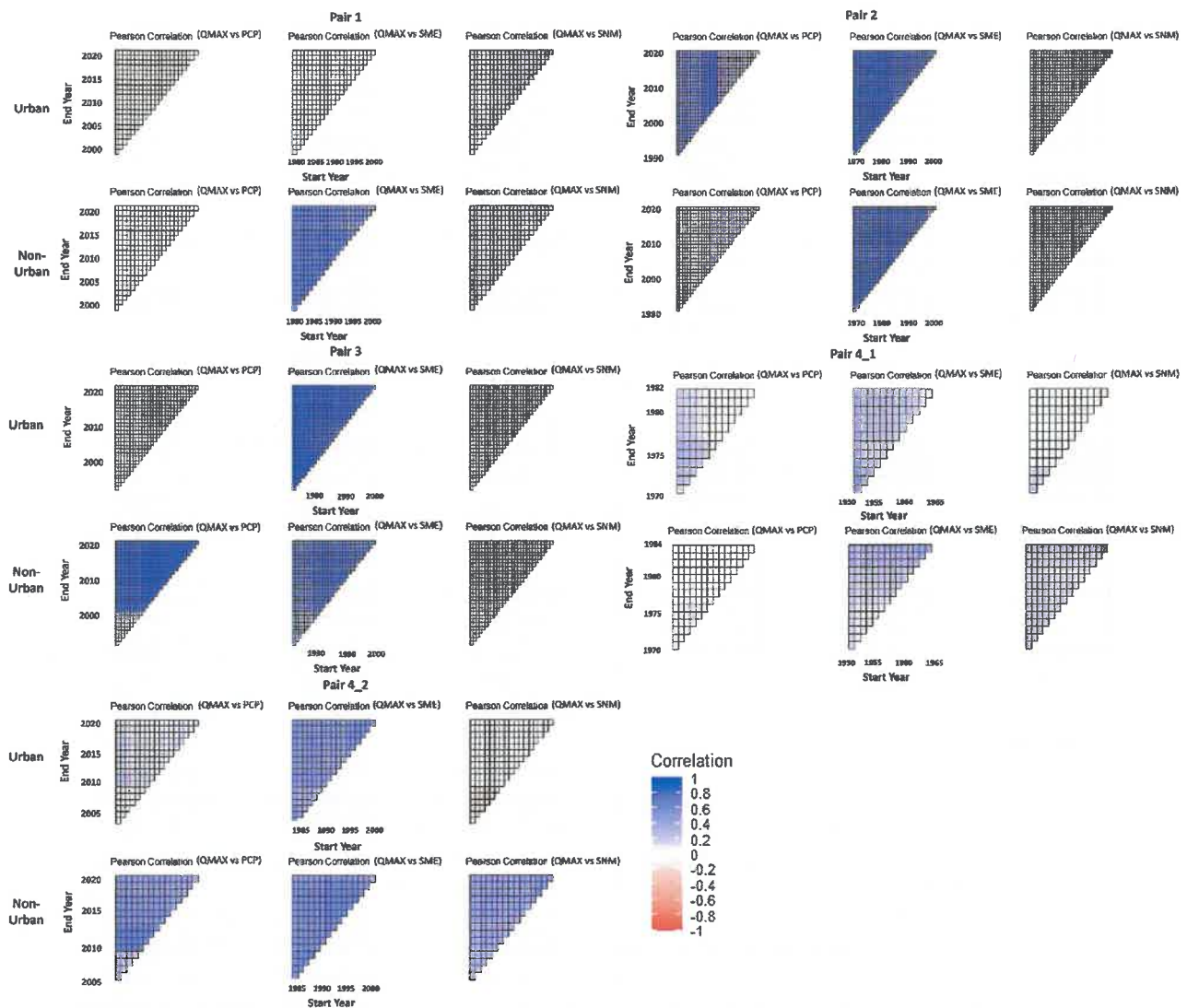


Fig. 8 Multi-temporal Pearson correlation analysis for Q_{MAX} against PCP_{MAX} , SME_{MAX} and SNM_{MAX} for all catchment pairs. The y axis shows the ending year and the x axis represents the starting year. Each

pixel is colored according to the R value. Red and blue colors represent negative and positive correlations, respectively

Table 5 Results of the multiple regression analysis between Q_{MAX} and PCP, SME and SMN climate variables

Pair ID	Catchment	R^2 (multiple)	R^2 (PCP)	R^2 (SME)	R^2 (SMN)	p value (residuals)	z (residuals)
1	U1	0.07	0.02	-0.01	-0.02	0.15	1.44
	N1	0.41	0.01	0.38	0.25	0.71	0.37
2	U2	0.57	0.04	0.31	0.44	0.76	0.30
	N2	0.50	0.14	0.49	0.40	0.40	-0.84
3	U3	0.62	-0.01	0.58	0.58	0.45	-0.75
	N3	0.62	0.35	0.09	0.56	0.09	-1.66
4	U4_1	0.22	-0.01	0.11	0.17	0.11	1.57
	N4_1	0.22	0.01	0.17	0.05	0.83	-0.21
	U4_2	0.31	-0.02	0.24	0.28	0.94	0.06
	N4_2	0.50	0.22	0.23	0.28	0.90	0.11

the most explicit evidence for the role of imperviousness on floods for the catchment pair 4, which was comprised by two adjacent catchments. The distance between catchments in remaining three pairs was between 20 and 40 km, which may have resulted in lower similarity of climatic and physiographic conditions. Therefore, while our study offers valuable insights, the interpretation of the findings should consider these limitations.

Introduction of well-known methodological approaches for future studies, such as hydrological modeling, future climate change scenarios and increasing the catchment sample could expand and improve the analysis of flood attribution and the influence of imperviousness. Indeed, hydrological modeling offers a way to understand how impervious surfaces, climate factors, and floods interact. By simulating these complex processes, researchers can uncover the underlying mechanisms driving flood events (Hu et al. 2021; Ma et al. 2022; Yang and Huang 2023). Additionally, the comparison of more catchment pairs across different regions could give a broader analysis that can reveal regional differences and enable flood management strategies based on specific geographic characteristics.

5 Conclusions

This study examined changes in imperviousness, flood trends, and climate interactions in four catchment pairs in Poland between 1975 and 2020. The findings indicate a consistent upward trajectory in imperviousness in all pairs (much stronger in urban catchments compared to their non-urban counterparts), indicating a significant trend in urbanization dynamics. Change point detection, using the Pettitt test, helped to identify changes in Q_{MAX} time series in both urban and non-urban watersheds for only one catchment pair.

The analysis of Q_{MAX} trends revealed notable variations between urban and non-urban catchments. The pair 2 distinguished itself by showing no discernible evidence of imperviousness influencing changes in flood behavior. The POT approach confirmed the influence of imperviousness on flooding, especially for catchment pair 4 during the later period (1986–2020), with additional evidence observed for catchment pairs 1 and 3.

The analysis of flood frequency (POT3F) showed a significant difference between urban and non-urban catchments for only one catchment pair (number 4). Multitemporal correlation analysis revealed variable relationships between flood magnitude and climatic variables, with non-urban catchments showing higher correlations. Finally, multiple regression analysis highlighted the complex relationships between flooding and climate indices. Non-urban

catchments consistently showed higher coefficients of determination than their urban counterparts. The residual analysis did not show statistically significant increasing trends for most urban catchments, but indicated differences that indirectly supported the hypothesis of the effect of urbanization on flooding. Understanding flood dynamics is essential for developing effective flood risk management strategies in both urban and non-urban environments.

Therefore, we conducted a comprehensive range of statistical methods to investigate the impact of urbanization on fluvial floods in Poland. Although discerning flood trends is a relatively simple task, attributing these trends to urbanization presents a challenge due to the intricate interplay of various factors. In this context, the paired catchments approach offers a valuable advantage by comparing basins with different levels of imperviousness. This allows for the quantification of the impact of urbanization. The method effectively isolates the effects of urbanization within a specific region by assessing observed streamflow, precipitation, soil moisture excess, and snowmelt statistics in paired catchments.

In addition, our study improved previous methodologies by incorporating GIS data on flow gauging stations and catchments across Poland, together with state-of-the-art imperviousness products, which have rarely been used in the context of flood studies. We systematically filtered potential catchment areas based on their size, data availability, and imperviousness characteristics. This rigorous approach ensures the reliability of our findings on the effects of urbanization on flooding and could be easily adapted for flood studies in other regions. In this study, we combined the use of statistical methods and process-based modelling which can be seen as a further methodological improvement. Finally, this study provides useful insights for policymakers, and water resource managers, by demonstrating the relationship between impervious surfaces and flood events.

Supplementary Information The online version contains supplementary material available at <https://doi.org/10.1007/s00477-024-02717-z>.

Acknowledgements This study was supported financially by the National Science Centre (NCN) in Poland under the research project “ATtribution of changes in River FLOODs in Poland (ATRIFLOP)”, grant 2022/45/N/ST10/03551. The authors acknowledge funding from the project PID2019-107027RB-I00 ‘SAFERDAMS: Assessment of the impact of climate change on hydrological dam safety’ of the Spanish Ministry of Science and Innovation (PID2019-107027RB-I00 / AEI / 10.13039/501100011033). We thank the Institute of Meteorology and Water Management-National Research Institute (IMGW-PIB) for providing the river flow data. The comments from two anonymous reviewers helped us to improve the quality of the manuscript.

Author contributions NVC: Conceptualization, Investigation, Methodology, Software, Validation, Formal analysis, Visualization, Writing – original draft, Writing – review & editing. LM: Conceptualization, Writing – original draft, Writing – review & editing. MP: Conceptu-

alization, Investigation, Writing – original draft, Writing – review & editing, Supervision.

Data availability No datasets were generated or analysed during the current study.

Declarations

Competing interests The authors declare no competing interests.

References

- Allan RP, Barlow M, Byrne MP, Cherchi A, Douville H, Fowler HJ, Zolina O (2020) Advances in understanding large-scale responses of the water cycle to climate change. *Ann N Y Acad Sci* 1472(1):49–75
- Aryal YN, Villarini G, Zhang W, Vecchi GA (2018) Long term changes in flooding and heavy rainfall associated with North Atlantic tropical cyclones: roles of the North Atlantic Oscillation and El Niño–Southern Oscillation. *J Hydrol* 559:698–710
- Bayazit Y, Koç C, Bakış R (2021) Urbanization impacts on flash urban floods in Bodrum Province, Turkey. *Hydrol Sci J* 66(1):118–133
- Beckers A, Dewals B, Erpicum S, Dujardin S, Detrembleur S, Teller J, Archambeau P (2013) Contribution of land use changes to future flood damage along the river Meuse in the Walloon region. *Nat Hazards Earth Syst Sci* 13(9):2301–2318
- Berghuijs WR, Harrigan S, Molnar P, Slater LJ, Kirchner JW (2019) The relative importance of different Flood-Generating mechanisms across Europe. *Water Resour Res* 55(6):4582–4593
- Bian G, Du J, Song M, Zhang X, Zhang X, Li R, Xu CY (2020) Detection and attribution of flood responses to precipitation change and urbanization: a case study in Qinhuai River Basin, Southeast China. *Hydrol Res* 51(2):351–365
- Bosch JM, Hewlett J (1982) A review of catchment experiments to determine the effect of vegetation changes on water yield and evapotranspiration. *J Hydrol* 55(1–4):3–23
- Brody S, Blessing R, Sebastian A, Bedient P (2014) Examining the impact of land use/land cover characteristics on flood losses. *J Environ Planning Manage* 57(8):1252–1265
- Brun SE, Band LE (2000) Simulating runoff behavior in an urbanizing watershed. *Comput Environ Urban Syst* 24(1):5–22
- Brunner MI, Swain DL, Wood RR, Willkofer F, Done JM, Gilleland E, Ludwig R (2021) An extremeness threshold determines the regional response of floods to changes in rainfall extremes. *Commun Earth Environ* 2(1):173
- Bulti DT, Abebe BG (2020) A review of flood modeling methods for urban pluvial flood application. *Model Earth Syst Environ* 6:1293–1302
- Davenport FV, Herrera-Estrada JE, Burke M, Diffenbaugh NS (2020) Flood size increases nonlinearly across the western United States in response to lower snow-precipitation ratios. *Water Resources Research*, 56(1): e2019WR025571
- Depietri Y, Renaud FG, Kallis G (2012) Heat waves and floods in urban areas: a policy-oriented review of ecosystem services. *Sustain Sci* 7(1):95–107
- Du S, Van Rompaey A, Shi P, Wang Ja (2015) A dual effect of urban expansion on flood risk in the Pearl River Delta (China) revealed by land-use scenarios and direct runoff simulation. *Nat Hazards* 77:111–128
- Fletcher TD, Andrieu H, Hamel P (2013) Understanding, management and modelling of urban hydrology and its consequences for receiving waters: a state of the art. *Adv Water Resour* 51:261–279
- Francipane A, Pumo D, Sinagra M, La Loggia G, Noto LV (2021) A paradigm of extreme rainfall pluvial floods in complex urban areas: the flood event of 15 July 2020 in Palermo (Italy). *Nat Hazards Earth Syst Sci* 21(8):2563–2580
- Gao Y, Chen J, Luo H, Wang H (2020) Prediction of hydrological responses to land use change. *Sci Total Environ* 708:134998
- Giorgi F, Raffaele F, Coppola E (2019) The response of precipitation characteristics to global warming from climate projections. *Earth Sys Dyn* 10(1):73–89
- Guan M, Sillanpää N, Koivusalo H (2015) Modelling and assessment of hydrological changes in a developing urban catchment. *Hydrol Process* 29(13):2880–2894
- Guerreiro SB, Dawson RJ, Kilsby C, Lewis E, Ford A (2018) Future heat-waves, droughts and floods in 571 European cities. *Environ Res Lett* 13(3):034009
- Hannaford J, Buys G, Stahl K, Tallaksen L (2013) The influence of decadal-scale variability on trends in long European streamflow records. *Hydrol Earth Syst Sci* 17(7):2717–2733
- Hannaford J, Mastrantonas N, Vesuviano G, Turner S (2021) An updated national-scale assessment of trends in UK peak river flow data: how robust are observed increases in flooding? *Hydrol Res* 52(3):699–718
- Hebbert M (2012) Cities and Climate Change (Global Report on Human Settlements 2011). JSTOR
- Hodgkins GA, Whitfield PH, Burn DH, Hannaford J, Renard B, Stahl K, Wilson D (2017) Climate-driven variability in the occurrence of major floods across North America and Europe. *J Hydrol* 552:704–717
- Hoeppe P (2016) Trends in weather related disasters – consequences for insurers and society. *Weather Clim Extremes* 11:70–79
- Hu C, Xia J, She D, Song Z, Zhang Y, Hong S (2021) A new urban hydrological model considering various land covers for flood simulation. *J Hydrol* 603:126833
- Ivancic TJ, Shaw SB (2015) Examining why trends in very heavy precipitation should not be mistaken for trends in very high river discharge. *Clim Change* 133:681–693
- Jiang S, Zheng Y, Wang C, Babovic V (2022) Uncovering Flooding Mechanisms across the Contiguous United States through Interpretive Deep Learning on Representative catchments. *Water Resour Res* 58(1):e2021WR030185
- Jodar-Abellán A, Valdes-Abellán J, Pla C, Gomariz-Castillo F (2019) Impact of land use changes on flash flood prediction using a sub-daily SWAT model in five Mediterranean ungauged watersheds (SE Spain). *Sci Total Environ* 657:1578–1591
- Kendall M (1975) Rank correlation methods, book series, Charles Griffin. Oxford University Press, USA, London
- Kishtawal CM, Niyogi D, Tewari M, Sr P, R. A. and, Shepherd JM (2010) Urbanization signature in the observed heavy rainfall climatology over India. *Int J Climatol* 30(13):1908–1916
- Kochanek K, Strupczewski WG, Bogdanowicz E (2012) On seasonal approach to flood frequency modelling. Part II: flood frequency analysis of Polish rivers. *Hydrol Process* 26(5):717–730
- Kreibich H, Di Baldassarre G, Vorogushyn S, Aerts JC, Apel H, Aronica GT, Merz B (2017) Adaptation to flood risk: results of international paired flood event studies. *Earths Future* 5(10):953–965
- Kundzewicz ZW, Robson AJ (2004) Change detection in hydrological records—a review of the methodology/revue méthodologique de la détection de changements dans les chroniques hydrologiques. *Hydrol Sci J* 49(1):7–19
- Kundzewicz ZW, Kanae S, Seneviratne SI, Handmer J, Nicholls N, Peduzzi P, Sherstyukov B (2014) Flood risk and climate change: global and regional perspectives. *Hydrol Sci J* 59(1):1–28
- Lang M, Ouarda TB, Bobée B (1999) Towards operational guidelines for over-threshold modeling. *J Hydrol* 225(3–4):103–117
- Lin J, Zhang W, Wen Y, Qiu S (2023) Evaluating the association between morphological characteristics of urban land and pluvial

- floods using machine learning methods. *Sustainable Cities Soc* 99:104891
- Ma C, Qi W, Xu H, Zhao K (2022) An integrated quantitative framework to assess the impacts of disaster-inducing factors on causing urban flood. *Nat Hazards* 113(3):1903–1924
- Madsen H, Rasmussen PF, Rosbjerg D (1997) Comparison of annual maximum series and partial duration series methods for modeling extreme hydrologic events: 1. At-site modeling. *Water Resour Res* 33(4):747–757
- Madsen H, Lawrence D, Lang M, Martinkova M, Kjeldsen T (2014) Review of trend analysis and climate change projections of extreme precipitation and floods in Europe. *J Hydrol* 519:3634–3650
- Mallakpour I, Villarini G (2015) The changing nature of flooding across the central United States. *Nat Clim Change* 5(3):250–254
- Mangini W, Viglione A, Hall J, Hundecha Y, Ceola S, Montanari A, Parajka J (2018) Detection of trends in magnitude and frequency of flood peaks across Europe. *Hydrol Sci J* 63(4):493–512
- Mann HB (1945) Nonparametric tests against trend. *Econometrica: J Econometric Soc* : 245–259
- Marcinkowski P, Kardel I, Placzkowska E, Gielczewski M, Osuch P, Okruszko T, Venegas-Cordero., Ignar S, Piniewski M (2021) High-resolution simulated water balance and streamflow data set for 1951–2020 for the territory of Poland. *Geosci Data J* 10(2):195–207
- McGrane SJ (2016) Impacts of urbanisation on hydrological and water quality dynamics, and urban water management: a review. *Hydrol Sci J* 61(13):2295–2311
- Mediero L, Santillán D, Garrote L, Granados A (2014) Detection and attribution of trends in magnitude, frequency and timing of floods in Spain. *J Hydrol* 517:1072–1088
- Mediero L, Soriano E, Oria P, Bagli S, Castellarin A, Garrote L, Schröter K (2022) Pluvial flooding: high-resolution stochastic hazard mapping in urban areas by using fast-processing DEM-based algorithms. *J Hydrol* 608:127649
- Mou Y, Gao X, Yang Z, Xu T, Feng J (2022) Variation characteristics and the impact of urbanization of extreme precipitation in Shanghai. *Sci Rep* 12(1):17618
- Pesaresi M, Politis P, GHS-BUILT-S (2022) R2022A-GHS Built-Up Surface Grid, derived from Sentinel-2 Composite and Landsat, Multitemporal (1975–2030). European Commission, Joint Research Centre (JRC) Sevilla, Spain
- Pettitt AN (1979) A non-parametric approach to the change-point problem. *J Roy Stat Soc: Ser C (Appl Stat)* 28(2):126–135
- Piniewski M, Marcinkowski P, Kundzewicz ZW (2018) Trend detection in river flow indices in Poland. *Acta Geophys* 66(3):347–360
- Piniewski M, Szcześniak M, Kardel I, Chattopadhyay S, Berezowski T (2021) G2DC-PL+: a gridded 2 km daily climate dataset for the union of the Polish territory and the Vistula and Odra basins. *Earth Syst Sci Data* 13(3):1273–1288
- Pińskwar I, Choryński A, Graczyk D (2023) Risk of Flash floods in Urban and Rural municipalities triggered by intense precipitation in Wielkopolska of Poland. *Int J Disaster Risk Sci*, 1–18
- Prein AF, Rasmussen RM, Ikeda K, Liu C, Clark MP, Holland GJ (2017) The future intensification of hourly precipitation extremes. *Nat Clim Change* 7(1):48–52
- Prosdociimi I, Kjeldsen TR, Miller JD (2015) Detection and attribution of urbanization effect on flood extremes using nonstationary flood-frequency models. *Water Resour Res* 51(6):4244–4262
- Requena AI, Prosdociimi I, Kjeldsen TR, Mediero L (2017) A bivariate trend analysis to investigate the effect of increasing urbanisation on flood characteristics. *Hydrol Res* 48(3):802–821
- Ruiz-Villanueva V, Stoffel M, Wyrzyga B, Kundzewicz ZW, Czajka B, Niedzwiedz T (2016) Decadal variability of floods in the northern foreland of the Tatra Mountains. *Reg Environ Chang* 16:603–615
- Salavati B, Oudin L, Furusho-Percot C, Ribstein P (2016) Modeling approaches to detect land-use changes: urbanization analyzed on a set of 43 US catchments. *J Hydrol* 538:138–151
- Sen PK (1968) Estimates of the regression coefficient based on Kendall's tau. *J Am Stat Assoc* 63(324):1379–1389
- Shao M, Zhao G, Kao SC, Cuo L, Rankin C, Gao H (2020) Quantifying the effects of urbanization on floods in a changing environment to promote water security—A case study of two adjacent basins in Texas. *J Hydrol* 589:125154
- Sivapalan M, Blöschl G, Merz R, Gutknecht D (2005) Linking flood frequency to long-term water balance: incorporating effects of seasonality. *Water Resour Res*, 41(6)
- Skougaard Kaspersen P, Høegh Ravn N, Arnbjerg-Nielsen K, Madsen H, Drews M (2017) Comparison of the impacts of urban development and climate change on exposing European cities to pluvial flooding. *Hydrol Earth Syst Sci* 21(8):4131–4147
- Smith A, Tetzlaff D, Marx C, Soulsby C (2023) Enhancing urban runoff modelling using water stable isotopes and ages in complex catchments. *Hydrol Process* 37(2):e14814
- Szeląg B, Suligowski R, Drewnowski J, De Paola F, Fernandez-Morales FJ, Bąk Ł (2021) Simulation of the number of storm overflows considering changes in precipitation dynamics and the urbanisation of the catchment area: a probabilistic approach. *J Hydrol* 598:126275
- Szwagrzyk M, Kaim D, Price B, Wypych A, Grabska E, Kozak J (2018) Impact of forecasted land use changes on flood risk in the Polish carpathians. *Nat Hazards* 94:227–240
- Tabari H (2020) Climate change impact on flood and extreme precipitation increases with water availability. *Sci Rep* 10(1):1–10
- Tramblay Y, Mimeau L, Neppel L, Vinet F, Sauquet E (2019) Detection and attribution of flood trends in Mediterranean basins. *Hydrol Earth Syst Sci* 23(11):4419–4431
- Van Loon AF, Rangecroft S, Coxon G, Breaña Naranjo JA, Van Ogtrop F, Van Lanen HA (2019) Using paired catchments to quantify the human influence on hydrological droughts. *Hydrol Earth Syst Sci* 23(3):1725–1739
- Venegas-Cordero N, Kundzewicz ZW, Jamro S, Piniewski M (2022) Detection of trends in observed river floods in Poland. *J Hydrology: Reg Stud* 41:101098
- Venegas-Cordero N, Cherrat C, Kundzewicz ZW, Singh J, Piniewski M (2023) Model-based assessment of flood generation mechanisms over Poland: the roles of precipitation, snowmelt, and soil moisture excess. *Sci Total Environ* : 164626
- Vicente-Serrano SM, Peña-Gallardo M, Hannaford J, Murphy C, Lorenzo-Lacruz J, Dominguez-Castro F, Vidal JP (2019) Climate, irrigation, and land cover change explain streamflow trends in countries bordering the northeast Atlantic. *Geophys Res Lett* 46(19):10821–10833
- Villarini G, Serinaldi F, Smith JA, Krajewski WF (2009) On the stationarity of annual flood peaks in the continental United States during the 20th century. *Water Resour Res*, 45(8)
- Villarini G, Smith JA, Ntelekos AA, Schwarz U (2011) Annual maximum and peaks-over-threshold analyses of daily rainfall accumulations for Austria. *J Geophys Research: Atmos* 116:D5
- Vormoor K, Lawrence D, Schlichting L, Wilson D, Wong WK (2016) Evidence for changes in the magnitude and frequency of observed rainfall vs. snowmelt driven floods in Norway. *J Hydrol* 538:33–48
- Wang X, Kinsland G, Poudel D, Fenech A (2019) Urban flood prediction under heavy precipitation. *J Hydrol* 577:123984
- Wasko C, Nathan R (2019) Influence of changes in rainfall and soil moisture on trends in flooding. *J Hydrol* 575:432–441
- Wu C, Huang G (2015) Changes in heavy precipitation and floods in the upstream of the Beiji River basin, South China. *Int J Climatol* 35(10):2978–2992

Yang X, Huang S (2023) Attribution assessment of hydrological trends and extremes to climate change for Northern high latitude catchments in Norway. *Clim Change* 176(10):139

Zhang H, Wang B, Li Liu D, Zhang M, Leslie LM, Yu Q (2020) Using an improved SWAT model to simulate hydrological responses to land use change: a case study of a catchment in tropical Australia. *J Hydrol* 585:124822

Springer Nature or its licensor (e.g. a society or other partner) holds exclusive rights to this article under a publishing agreement with the author(s) or other rightsholder(s); author self-archiving of the accepted manuscript version of this article is solely governed by the terms of such publishing agreement and applicable law.

Publisher's Note Springer Nature remains neutral with regard to jurisdictional claims in published maps and institutional affiliations.

Co-author statements - Article 3

Appendix no. 2 – co-authorship statement

Warsaw, 01-04-2024

Nelson Enrique Venegas Cordero
nelson_venegas@sggw.edu.pl

**Department of Hydrology, Meteorology
and Water Management, Warsaw
University of Life Sciences**

Co-authorship statement

I hereby represent that in the article: Urbanization vs climate drivers: investigating changes in fluvial floods in Poland. Authors: Authors: Nelson Venegas-Cordero, Luis Mediero, and Mikołaj Piniewski. Journal Stochastic Environmental Research and Risk Assessment, 2024, my individual contribution in the development thereof involved: Conceptualization, Investigation, Methodology, Software, Validation, Formal analysis, Visualization, Writing – original draft, Writing – review & editing.



Nelson Enrique Venegas Cordero

Appendix no. 2 – co-authorship statement

Madrid, 01-04-2024

Luis Mediero
luis.mediero@upm.es

**Department of Civil Engineering:
Hydraulics, Energy and
Environment, Universidad
Politécnica de Madrid, 28040
Madrid, Spain.**

Co-authorship statement

I hereby represent that in the article: Urbanization vs climate drivers: investigating changes in fluvial floods in Poland. Authors: Authors: Nelson Venegas-Cordero, Luis Mediero, and Mikołaj Piniewski. Journal Stochastic Environmental Research and Risk Assessment, 2024, my individual contribution in the development thereof involved: Conceptualization, Writing – original draft, Writing – review & editing.



Luis Mediero

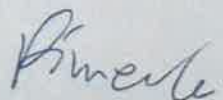
Appendix no. 2 – co-authorship statement

Warsaw, 01-04-2024

Mikołaj Piniewski
Department of Hydrology, Meteorology and Water Management,
Warsaw University of Life Sciences
mikolaj_piniewski@sggw.edu.pl

Co-authorship statement

I hereby represent that in the article: Urbanization vs climate drivers: investigating changes in fluvial floods in Poland. Authors: Nelson Venegas-Cordero, Luis Mediero, and Mikołaj Piniewski. Journal: Stochastic Environmental Research and Risk Assessment, 2024, my individual contribution in the development thereof involved: Conceptualization, Investigation, Writing – original draft, Writing – review & editing, Supervision.



Mikołaj Piniewski

